1993

Criteria for collected data in least squares circle fitting

Jyh-jeng Deng
Iowa State University

Order Number 9413968

Criteria for collected data in least squares circle fitting

Deng, Jyh-jeng, Ph.D.

Iowa State University, 1993

U·M·I
300 N. Zeeb Rd.
Ann Arbor, MI 48106

Criteria for collected data in least squares circle fitting

by

Jyh-jeng Deng

A Dissertation Submitted to the

Graduate Faculty in Partial Fulfillment of the

Requirements for the Degree of

DOCTOR OF PHILOSOPHY

Department: Industrial and Manufacturing Systems Engineering
Major: Industrial Engineering

Approved:

Signature was redacted for privacy.

In Charge of Major Work

Signature was redacted for privacy.

For the Major Department

Signature was redacted for privacy.

For the Graduate College

Members of the Committee:

Signature was redacted for privacy.

Iowa State University
Ames, Iowa
1993

A Dedication

.

Thanks, Mom & Dad.

.

TABLE OF CONTENTS

LIST OF TABLES

LIST OF FIGURES

ACKNOWLEDGMENTS

I am especially grateful to Dr. John Jackman and Dr. Way Kuo for their guidance, patience, and encouragement throughout the course of this research. For helpful criticism and advice on the manuscript and serving as research committee, I express my appreciation to Dr. Herbert A. David, Dr. David A. Harville, and Dr. Douglas D. Gemmill. In particular, Dr. Herbert A. David suggested the proof of Appendix C. I also thank the National Science Foundation, Deere & Company, and the Engineering Research Institute at Iowa State University for supporting the research project, Functionality and Cost Engineering (FACE), on which I have been working during the course of my doctoral program. Special thanks are given to Dr. Richard H. Sprague in the Mathematics Department for providing the proof of Lemma 3 in Appendix A.1.

CHAPTER 1. INTRODUCTION

Circularity is a measure of the extent to which a physical surface matches the ideal geometry of a circle. Departure from circularity is given by the width of the smallest annulus that contains all elements of the surface [1],[2]. As the width of the annulus decreases, the circularity improves. Figure 1.1 illustrates this measure with a profile of a surface and the enclosing annulus as the shaded region.

In practice, existing standards [3] suggest that using a set of discrete data points, circularity be evaluated as follows. First, a least squares center is calculated from a set of measured points. The distance from the center to each data point is calculated to determine the minimum and maximum distances. The difference between these is the departure from circularity.

For a given set of data points, the least squares center and best fitted circle is obtained by finding the minimum sum of the squares of the distances of measured points to their fitted circle [3],[4]. Given that there are n data points (x_i, y_i), $\forall\ i = 1, 2, \ldots, n$, we want to find a circle with center (x_c, y_c) and radius r_c that minimizes

$$f(x, y, r) = \sum_{i=1}^{n} (\sqrt{(x_i - x)^2 + (y_i - y)^2} - r)^2. \tag{1.1}$$

In order to satisfy this minimum condition, we take the first partial derivative

of (1.1) with respect to r and equate it to zero, obtaining

$$r = \frac{1}{n}\sum_{i=1}^{n}\sqrt{(x_i - x)^2 + (y_i - y)^2}. \tag{1.2}$$

Substituting for r in (1.1), our goal is to find the point (x, y) that gives a minimum for

$$f(x,y) = \sum_{i=1}^{n}\left(\sqrt{(x_i - x)^2 + (y_i - y)^2} - \frac{1}{n}\sum_{j=1}^{n}\sqrt{(x_j - x)^2 + (y_j - y)^2}\right)^2. \tag{1.3}$$

This type of problem has also been investigated in the contexts of archaeology [5] and microwave engineering [6]. The problem was studied by Cox, [7] who proposed the algorithm in section 1.2.

1.1 Motivation

Coordinate Measurement Machines (CMMs) and the least squares method are a popular measurement tool and analysis method used in circularity evaluation. Much literature has focused on the "methods divergence" problem [9], however, no investigation has been done on the nature of this analysis method. Our goal in this research is to examine $f(x, y)$ carefully and determine under what conditions it will render a unique measure of the departure from circularity.

1.2 Cox's Iterative Approach

Suppose that (x, y) is the Cartesian coordinate of the estimated center and r the estimated radius of the best fitted circle. In order to minimize (1.3), (x, y, r) has to satisfy

$$x = \overline{x} - \frac{r}{n}\sum_{i=1}^{n}\frac{x_i - x}{r_i}, \tag{1.4}$$

$$y = \overline{y} - \frac{r}{n}\sum_{i=1}^{n}\frac{y_i - y}{r_i}, \quad \text{and} \tag{1.5}$$

$$r = \frac{1}{n}\sum_{i=1}^{n} r_i. \tag{1.6}$$

Here r_i is the distance between the i^{th} point (x_i, y_i) and (x, y). Although an explicit solution of (1.4), (1.5), and (1.6) cannot be obtained due to the coupling between equations, a solution can be obtained through successive iteration. We start with an initial guess for the center and use this to calculate the set of r_i's and hence a first approximation of r using (1.6). This is then inserted into (1.4) and (1.5) to give us improved estimates of x and y. We repeat the process until we have satisfied some convergence criteria.

1.3 $LS1$ Estimation Problem

Berman and Culpin [13] have pointed out that Cox's procedure is not trouble-free and indicated that this was as an $LS1$ estimation problem. They have shown empirically that for some sets of data $f(x, y)$ has no minimum, but has a saddle point, while for others it has several local minima. They have also shown that when data points lie close to the circumference of a circle and are sufficiently dispersed around it, (1.4), (1.5) and (1.6) have a unique solution which is at the minimum of $f(x, y)$. However, their work was limited to empirical data. No mathematical proof is provided that shows the general behavior of $f(x, y)$. Also, there was no investigation of the conditions under which a unique solution can be obtained.

Here we use three sets of data points to illustrate three specific cases, i.e., a unique global minimum of $f(x, y)$, multiple local minima of $f(x, y)$, and no minimum, but only saddle points of $f(x, y)$. In Figure 1.2, we are given a set of four data points

with Cartesian coordinates of $(1.1, 0)$, $(0, 1)$, $(-1.1, 0)$, and $(0, -1)$. Then we draw a three-dimensional graph of $-f(x, y)$ with respect to x and y as shown in Figure 1.3 to show the surface profile. It is clear that there is a unique global minimum of $f(x, y)$. In Figure 1.4, we look from the top of the (x, y) axes. The darker shaded areas correspond to the lower value of $-f(x, y)$. The square white area indicates the unique global minimum. In Figure 1.5, we are given a set of data points of $(4, 0)$, $(0, 1)$, $(-4, 0)$, and $(0, -1)$ representing an elliptical surface. Figures 1.6 and 1.7 are the corresponding three-dimensional graph and contour graph of Figure 1.5. They indicate that there exist two local minima of $f(x, y)$. In Figure 1.8, we distend the circle further to obtain a set of data points of $(6, 0)$, $(0, 1)$, $(-6, 0)$, and $(0, -1)$. Figures 1.9 and 1.10 are the corresponding three-dimensional graph and contour graph of $-f(x, y)$ for Figure 1.8. They indicate that there exist three saddle points of $f(x, y)$, none of them is a local minimum.

1.4 Generalized Circle Fitting Method

The metric presented in (1.1) is the L_2 metric [14]. For the general case of any L_p metric, our objective function in (1.1) becomes

$$f(x, y, r) = \sum_{i=1}^{n} \left((|x_i - x|^p + |y_i - y|^p)^{\frac{1}{p}} - r \right)^2. \tag{1.7}$$

Taking the first partial derivative of (1.7) with respect to r and equating it to zero, we can solve for r and substitute its value into (1.7). Our goal is to find the point (x, y) that gives a minimum for

$$f(x, y) = \sum_{i=1}^{n} \left((|x_i - x|^p + |y_i - y|^p)^{\frac{1}{p}} - \frac{1}{n} \sum_{j=1}^{n} (|x_j - x|^p + |y_j - y|^p)^{\frac{1}{p}} \right)^2. \tag{1.8}$$

We can generalize the problem further from the least square estimation to the the L_q norm estimation [15]. In the L_q norm estimation, our objective function (1.7) becomes

$$f(x,y,r) = \sum_{i=1}^{n} \left| (|x_i - x|^p + |y_i - y|^p)^{\frac{1}{p}} - r \right|^q, \tag{1.9}$$

with $p, q \geq 1$. We have constrained our investigation to $p = q = 2$ due to common practice of circularity evaluation. We have not discussed the statistical model of the observed data points and its implication. The choice of an optimal p and q with respect to the statistical (asymptotic) efficiencies [16] of the estimators of (x, y, r) is not considered. The effect of the distribution of points is considered to be a separate issue and is outside the scope of this discussion.

1.5 Significance of the Research

The significance of the research is that for the first time, we can provide criteria for the arrangement of data points obtained from surface of a cylindrical part with a CMM such that it will render a unique measure of the departure from circularity. We use this measure of departure from circularity to characterize cylindrical surfaces. The criteria will cover the majority of data sets encountered with these types of measurement.

Using the criteria, practitioners can avoid making major errors when evaluating the measure of departure from circularity for cylindrical precision parts. If the measure of departure from circularity is no larger than its corresponding circularity tolerance, then the part is regarded as satisfying the design specifications.

1.6 Research Objectives

If $f(x, y)$ is quasiconvex, (a sufficient condition to ensure the existence of a unique local minimum in the entire domain for $f(x, y)$ (except for special cases)) [11], then we can use any of the standard optimization procedures (such as found in Matlab [10]) to solve this problem. Under this condition, if we find the local minimum, we also find the global minimum.

However, we have found that $f(x, y)$ is not quasiconvex. Thus, we need to determine under what conditions $f(x, y)$ will have a unique global minimum. The proof of nonquasiconvexity of $f(x, y)$ is valid for $n \geq 4$ points with arbitrary Cartesian coordinates.

We develop specific criteria for the data points such that there is a unique global minimum of $f(x, y)$. The criteria have to be consistent with the modern measurement technology (such as a CMM), and applicable to the majority of data sets encountered with these types of measurements.

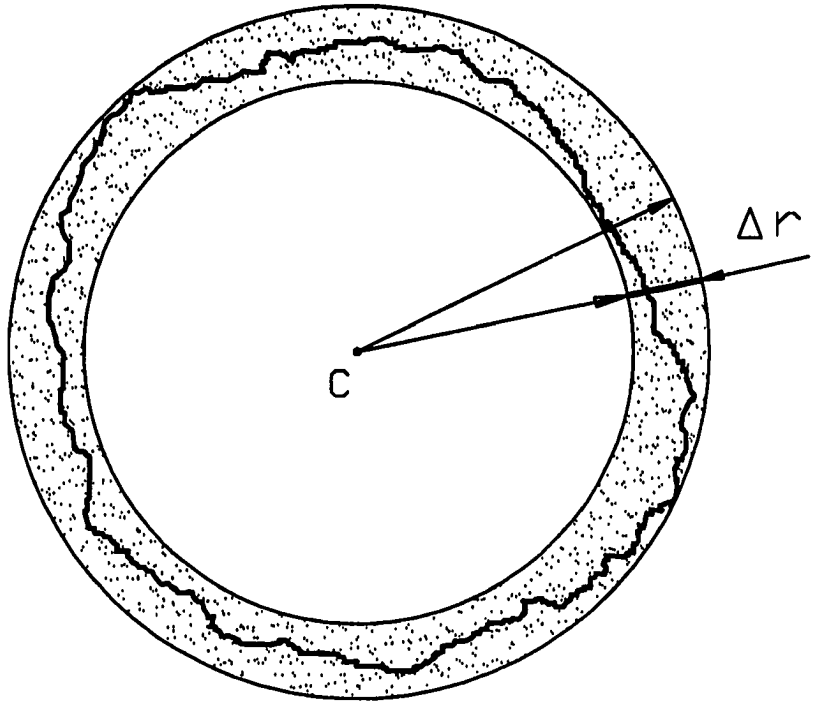

Figure 1.1: An Illustration of Departure of Circularity.

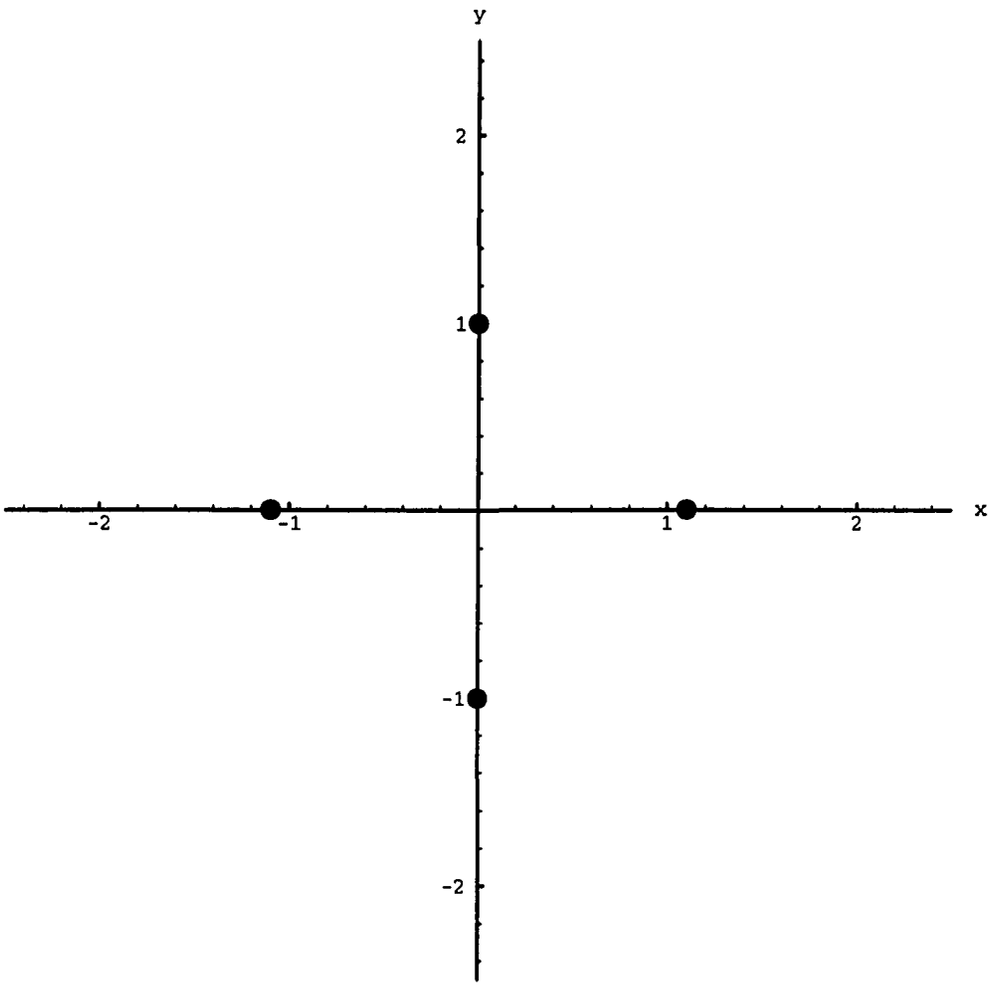

Figure 1.2: Layout of Four Data Points – Example 1.

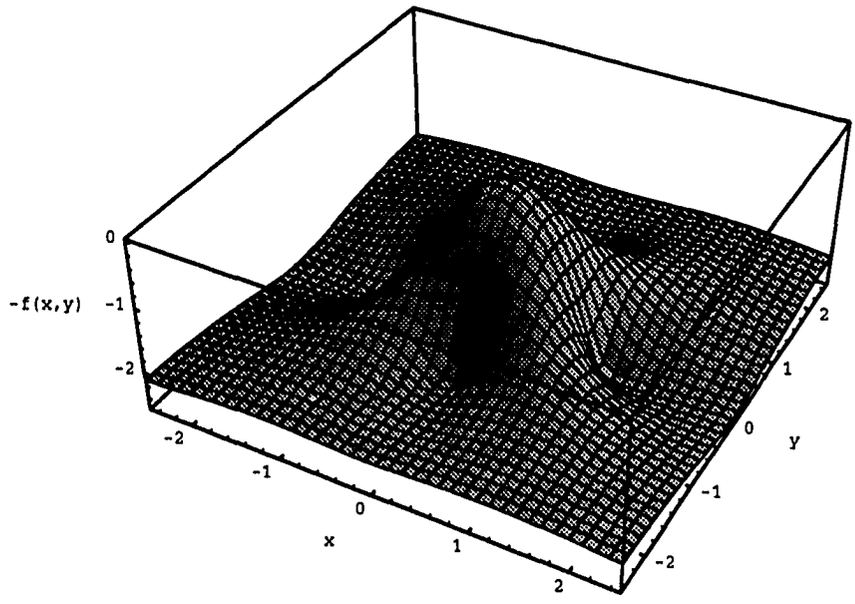

Figure 1.3: Three-Dimensional Graph for Example 1.

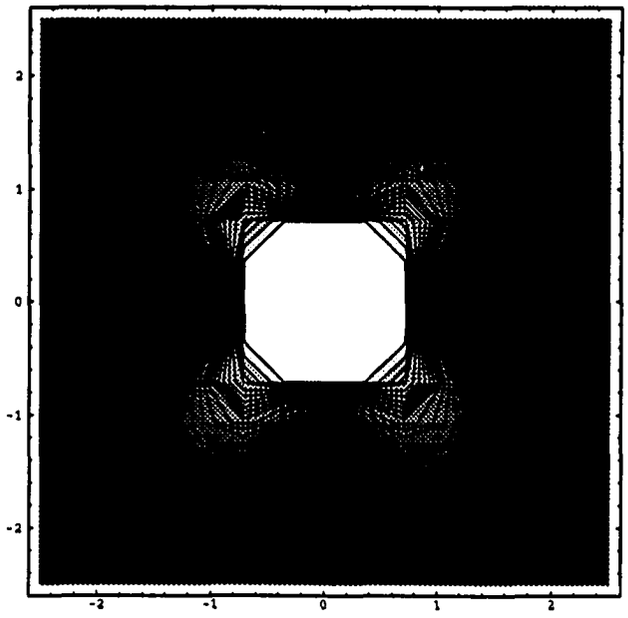

Figure 1.4: A Contour Plot for Example 1.

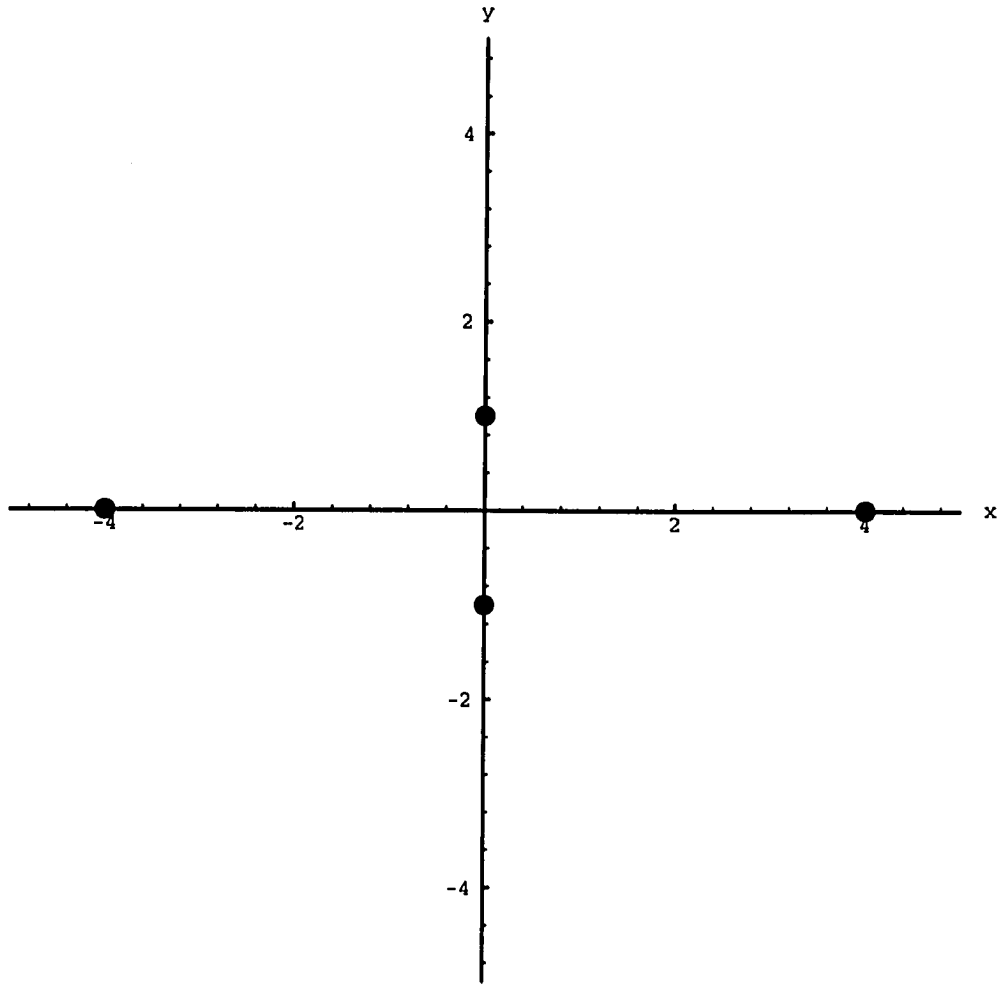

Figure 1.5: Layout of Four Data Points – Example 2.

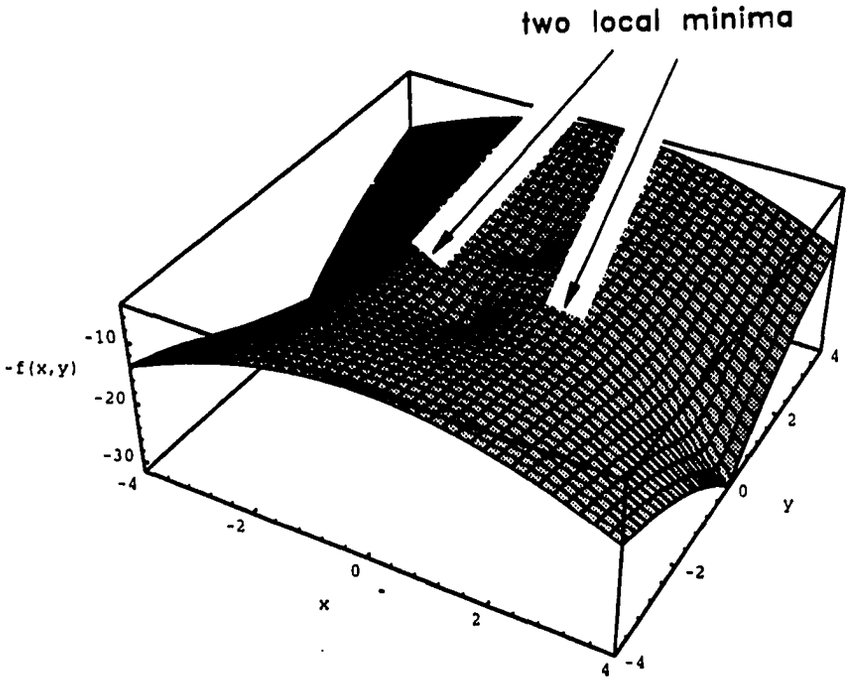

Figure 1.6: Three-Dimensional Graph for Example 2.

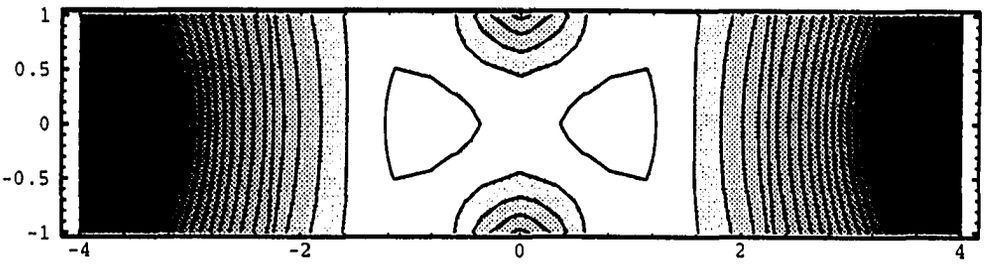

Figure 1.7: A Contour Plot for Example 2.

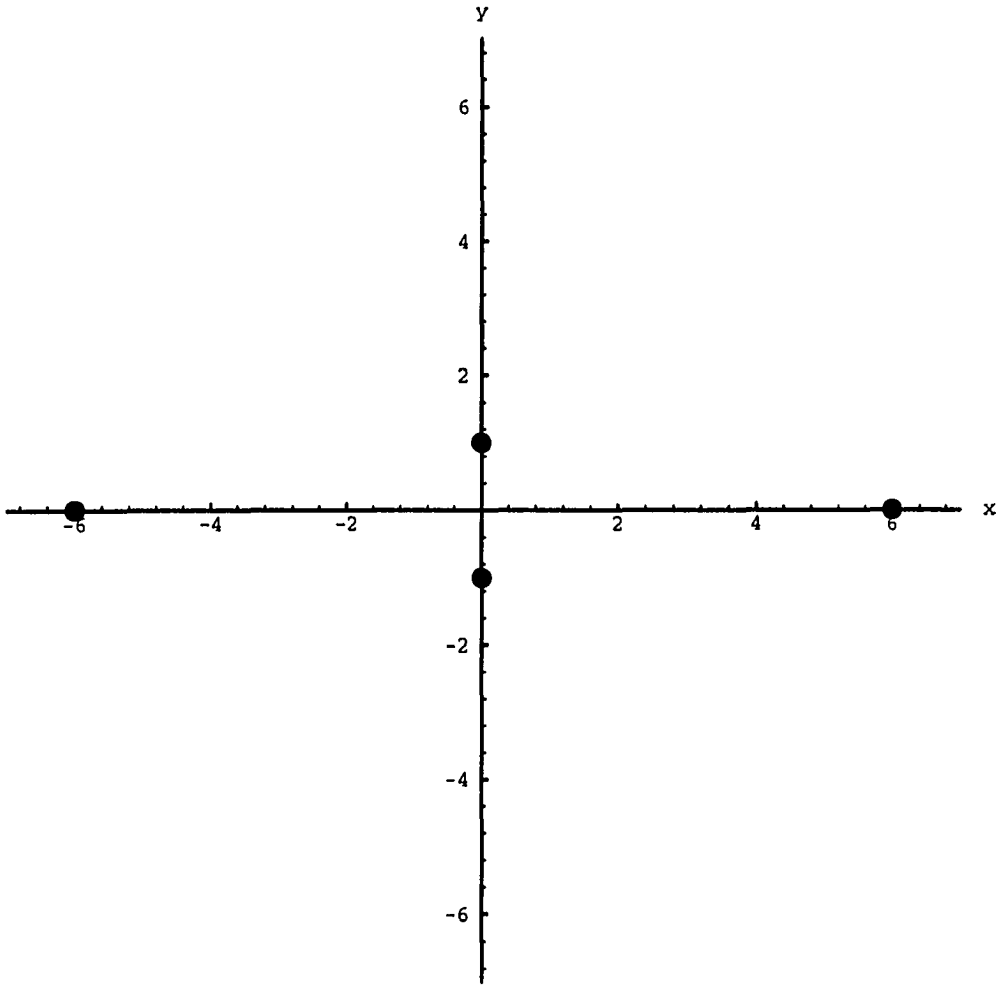

Figure 1.8: Layout of Four Data Points – Example 3.

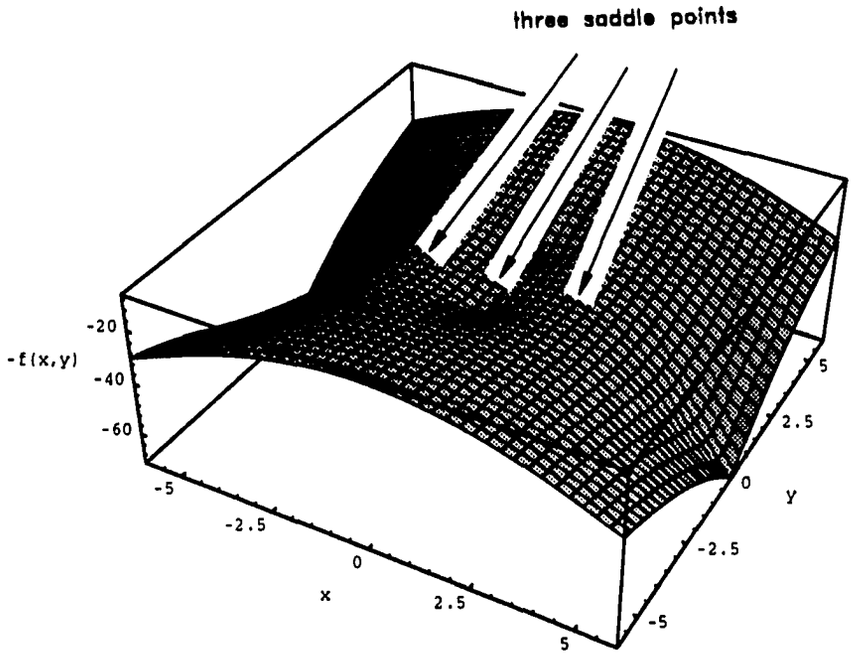

Figure 1.9: Three-Dimensional Graph for Example 3.

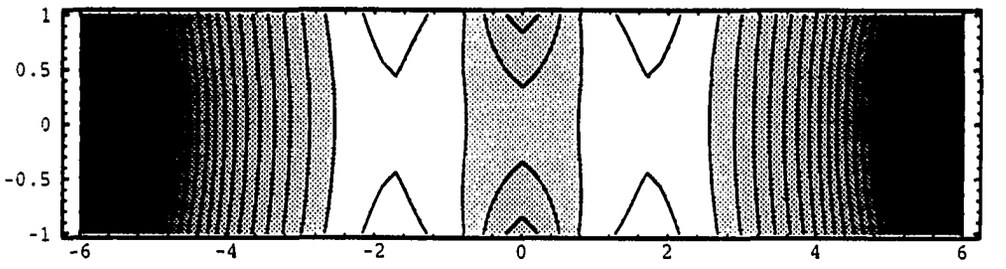

Figure 1.10: A Contour Plot for Example 3.

CHAPTER 2. The Nature of $f(x,y)$

We start by showing that $f(x,y)$ is a continuous function $\forall\ x,y$.

Proposition 1 Function $f(x,y)$ is continuous.

Before doing the proof, we need the following corollary.

Corollary 3.7 of chapter 2 in Mendelson[12]: Let (X,d), (Y,d'), (Z,d'') be metric spaces. Let $f: X \to Y$ and $g: Y \to Z$ be continuous. Then $gf: X \to Z$ is continuous.

Proof:

1. Let

$$p_i(x,y) \;=\; (x_i - x)^2 + (y_i - y)^2. \tag{2.1}$$

Being a polynomial, $p_i(x,y)$ is continuous. Furthermore let

$$q(x) \;=\; \sqrt{x} \quad \text{for } x \geq 0.$$

It is clear that $q(x)$ is continuous for $x \geq 0$. So we obtain

$$p_i : (R,R) \to R^+ \quad \text{is continuous, and} \tag{2.2}$$
$$q : R^+ \to R^+ \quad \text{is continuous.} \tag{2.3}$$

Therefore by (2.2), (2.3) and corollary 3.7 of chapter 2 in Mendelson [12], we obtain

$$q \circ p_i : (R,R) \to R^+ \quad \text{is continuous}$$

where

$$q \circ p_i(x,y) \;=\; \sqrt{(x_i - x)^2 + (y_i - y)^2}.$$

2. Given that $q \circ p_i(x,y)$ is continuous $\forall\, i$ as we have shown, we obtain that

$$h_i(x,y) \;=\; \sqrt{(x_i - x)^2 + (y_i - y)^2} - \frac{1}{n}\sum_{j=1}^{n}\sqrt{(x_j - x)^2 + (y_j - y)^2}$$

is a continuous function. Let

$$k(x) \;=\; x^2.$$

It is clear that $k(x)$ is continuous. So we obtain

$$h_i : (R,R) \to R \quad \text{is continuous, and} \tag{2.4}$$
$$k : R \to R^+ \quad \text{is continuous.} \tag{2.5}$$

Therefore by (2.4), (2.5) and corollary 3.7 of chapter 2 in Mendelson [12], we obtain

$$k \circ h_i : (R,R) \to R^+ \quad \text{is continuous}$$

$\forall\, i$, where

$$k \circ h_i(x,y) \;=\; \left(\sqrt{(x_i - x)^2 + (y_i - y)^2} - \frac{1}{n}\sum_{j=1}^{n}\sqrt{(x_j - x)^2 + (y_j - y)^2}\right)^2.$$

3. Since $k \circ h_i(x,y)$ is continuous $\forall\, i$, so $\sum_{i=1}^{n} k \circ h_i(x,y)$ is continuous. i.e.,

$$\begin{aligned} f(x,y) \;&=\; \sum_{i=1}^{n} k \circ h_i(x,y) \\ &=\; \sum_{i=1}^{n}\left(\sqrt{(x_i - x)^2 + (y_i - y)^2} - \frac{1}{n}\sum_{j=1}^{n}\sqrt{(x_j - x)^2 + (y_j - y)^2}\right)^2 \end{aligned}$$

is continuous.

This concludes the proof.

Proposition 2 Function $f(x, y)$ is not a quasiconvex function.

The key to proving Proposition 2 is to find at least one point at which the function $f(x, y)$ is not quasiconvex. To find this point, it is sufficient to find a cutting plane perpendicular to the x, y plane such that the graph function on the cutting plane is not quasiconvex. We will show that there exists at least one such cutting plane for $f(x, y)$. The proofs are shown in two parts: general cases and trivial cases. Before doing the proof, we need the following definition and lemma.

Quasiconvexity at $\overline{\mathbf{x}}$ of definition 3.5.13 in Bazaraa [11]: Let S be a nonempty convex set in E_n, and $f : S \to E_1$. The function f is said to be quasiconvex at $\overline{\mathbf{x}} \in S$ if

$$f[\lambda\overline{\mathbf{x}} + (1-\lambda)\mathbf{x}] \leq maximum\{f(\mathbf{x}), f(\overline{\mathbf{x}})\}$$

for each $\lambda \in (0, 1)$ and for each $\mathbf{x} \in S$.

Lemma 1 Given n data points, $\{A_1, A_2, A_3, \ldots, A_n\}$, with A_1 as origin and point $Q(r\cos\theta, r\sin\theta)$ a point on the boundary of an arbitrarily small disc that surrounds point A_1, it is possible to find a point Q such that the difference between the $f(A_1)$ and $f(Q)$ will be a maximum (except for trivial cases).

Lemma 1 is proved as follows.

Proof:

Using A_1 as the origin we obtain, $A_1(0,0)$, A_2 $(R_1\cos\alpha_1, R_1\sin\alpha_1)$, A_3 $(R_2\cos\alpha_2, R_2\sin\alpha_2)$, ..., and $A_n(\ R_{n-1}\cos\alpha_{n-1}, R_{n-1}\sin\alpha_{n-1})$, where R_i is the distance between points A_1 and A_{i+1} and α_i is the polar angle of A_{i+1} with respect to A_1. Let

point $Q(r\cos\theta, r\sin\theta)$ be a point on the boundary of an arbitrarily small disc that surrounds point A_1 (see Figure 2.1). If we let m_i be the ratio between R_i and r, $\frac{R_i}{r}$, the value of $f(x,y)$ at A_1 is given by

$$f(0,0) = r^2[\frac{n-1}{n}\sum_{i=1}^{n-1} m_i^2 - \frac{2}{n}\sum_{1\le j<k\le n} m_{j-1}m_{k-1}]. \tag{2.6}$$

Note that $R_0 = m_0 r$ and R_0 can be regarded as distance from point A_1 to itself, which results in $m_0 = 0$. The function value at Q is evaluated as

$$\begin{aligned} f(r\cos\theta, r\sin\theta) &= \frac{n-1}{n}r^2[n + \sum_{i=1}^{n-1} m_i^2 - 2\sum_{i=1}^{n-1} m_i\cos(\theta-\alpha_i)] \\ &\quad -\frac{2}{n}r^2 \sum_{1\le j<k\le n} \sqrt{1+m_{j-1}^2 - 2m_{j-1}\cos(\theta-\alpha_{j-1})}\, * \\ &\quad \sqrt{1+m_{k-1}^2 - 2m_{k-1}\cos(\theta-\alpha_{k-1})}. \end{aligned} \tag{2.7}$$

Let $g(\theta)$ be the difference between $f(A_1)$ and $f(Q)$. By subtracting (2.7) from (2.6), we find that

$$\begin{aligned} g(\theta) = -\frac{2}{n}r^2 \sum_{1\le j<k\le n} m_{j-1}m_{k-1} - \\ \frac{n-1}{n}r^2[n - 2\sum_{i=1}^{n-1} m_i\cos(\theta-\alpha_i)] + \\ \frac{2}{n}r^2 \sum_{1\le j<k\le n} \sqrt{1+m_{j-1}^2 - 2m_{j-1}\cos(\theta-\alpha_{j-1})}\, * \\ \sqrt{1+m_{k-1}^2 - 2m_{k-1}\cos(\theta-\alpha_{k-1})}. \end{aligned}$$

Since we can put an arbitrarily small disc around point A_1, the values of m_i can be made arbitrarily large. At the limits as $m_i \to \infty\ \forall\ i$, the function $g(\theta)$ can be approximated by

$$\hat{g}(\theta) = \frac{2}{n}r^2[(n-1)\sum_{i=1}^{n-1} m_i\cos(\theta-\alpha_i) -$$

$$\sum_{2\le j<k\le n}[m_{k-1}\cos(\theta-\alpha_{j-1})+m_{j-1}\cos(\theta-\alpha_{k-1})]+\sum_{i=1}^{n-1}m_i]$$

$$\begin{aligned}
= \frac{2}{n}r^2[&\cos(\theta-\alpha_1)((n-1)m_1-m_2-m_3-\ldots-m_{n-1})\\
&+\cos(\theta-\alpha_2)((n-1)m_2-m_1-m_3-\ldots-m_{n-1})\\
&+\cos(\theta-\alpha_3)((n-1)m_3-m_1-m_2-\ldots-m_{n-1})\\
&+\ldots\\
&+\cos(\theta-\alpha_{n-1})((n-1)m_{n-1}-m_1-m_2-\ldots-m_{n-2})\\
&+\sum_{i=1}^{n-1}m_i]. \qquad (2.8)
\end{aligned}$$

In order to find the maximum value of $\hat{g}(\theta)$ (and therefore the maximum difference between $f(A_1)$ and $f(Q)$) with respect to θ, it is necessary to find the first and second derivatives of $\hat{g}(\theta)$. Equating $\hat{g}'(\theta)$ to zero, we obtain

$$\tan(\theta)=\frac{B_1}{B_2}. \qquad (2.9)$$

Here,

$$\begin{aligned}
B_1 = &\sin\alpha_1((n-1)m_1-m_2-m_3-\ldots-m_{n-1})\\
&+\sin\alpha_2((n-1)m_2-m_1-m_3-\ldots-m_{n-1})\\
&+\ldots\\
&+\sin\alpha_{n-1}((n-1)m_{n-1}-m_1-m_2-\ldots-m_{n-2})
\end{aligned}$$

and,

$$\begin{aligned}
B_2 = &\cos\alpha_1((n-1)m_1-m_2-m_3-\ldots-m_{n-1})\\
&+\cos\alpha_2((n-1)m_2-m_1-m_3-\ldots-m_{n-1})\\
&+\ldots\\
&+\cos\alpha_{n-1}((n-1)m_{n-1}-m_1-m_2-\ldots-m_{n-2}).
\end{aligned}$$

There are two possible solutions for θ, therefore, to find the correct solution we take the second derivative of $\hat{g}(\theta)$ with respect to θ and obtain

$$\begin{aligned}\hat{g}''(\theta) &= \frac{2}{n}r^2[\cos(\theta-\alpha_1)(-(n-1)m_1+m_2+m_3+\ldots+m_{n-1}) \\ &+\cos(\theta-\alpha_2)(-(n-1)m_2+m_1+m_3+\ldots+m_{n-1}) \\ &+\cos(\theta-\alpha_3)(-(n-1)m_3+m_1+m_2+\ldots+m_{n-1}) \\ &+\ldots \\ &+\cos(\theta-\alpha_{n-1})(-(n-1)m_{n-1}+m_1+m_2+\ldots+m_{n-2})]. \quad (2.10)\end{aligned}$$

We know that for $\hat{g}''(\theta) < 0$ we can find a maximum. Therefore, we choose θ such that $\hat{g}''(\theta) < 0$. Both the $\sin\theta$ and $\cos\theta$ are necessary to uniquely specify θ. Using (2.9) and the value of θ for which $\hat{g}''(\theta) < 0$, we obtain

$$\sin\theta = \frac{B_1}{B}$$

and

$$\cos\theta = \frac{B_2}{B}$$

where,

$$B = \sqrt{B_1^2+B_2^2}. \quad (2.11)$$

In testing for a maximum we obtain $\hat{g}''(\theta) = -\frac{2}{n}r^2B$. Since B is always greater than zero (except for trivial cases), $\hat{g}''(\theta) < 0$. This concludes the proof. Now we proceed to prove Proposition 2 in the next two sections.

2.1 Proof for General Cases (i.e., when $B \neq 0$)

Proof:

Given n data points $A_1, A_2, \ldots, A_n$, we can define a coordinate system with its origin at any one of the points and then express the other data points in polar coordinates with respect to this origin. Let A_1 be the origin. Then from Lemma 1, we can find a point Q on the boundary of an arbitrarily small disc that surrounds point A_1, such that the $\hat{g}(\theta)$ will be a maximum. If we choose the cutting plane such that its angle in the x, y plane with respect to A_1, is $\frac{\pi}{2}$ radians from θ (see Figure 2.1), then by quasiconvexity at $\overline{\mathbf{x}}$ of definition 3.5.13 in Bazaraa [11] we are able to show $f(x, y)$ at A_1 is not quasiconvex on the cutting plane by showing that a local maximum exists on the cutting plane. This can be shown by using the difference between $f(A_1)$ and $f(x, y)$ where (x, y) is both in the cutting plane and in the neighborhood of A_1 (i.e., $\hat{g}(\theta)$). Since the angle of the cutting plane deviates from θ by $\frac{\pi}{2}$ radians, we find the difference between $f(A_1)$ and $f(x, y)$ by finding values of the function $\hat{g}(\theta)$ with θ equal to the cutting angle (i.e., $\theta - \frac{\pi}{2}$) and π plus the cutting angle (i.e., $\theta + \frac{\pi}{2}$). If both function values are greater than zero, then $f(A_1)$ is greater than $f(Q')$ and $f(Q'')$. Here Q' has polar coordinate of $(r, \theta - \frac{\pi}{2})$ and Q'' has polar coordinate of $(r, \theta + \frac{\pi}{2})$. The two points are both on the cutting plane and in the neighborhood of A_1 (see Figure 2.1). This means point A_1 is a local maximum on the cutting plane.

Let β_1 and β_2 be the angles for the cutting plane (see Figure 2.1). Substituting $\beta_1 = \theta - \frac{\pi}{2}$ and $\beta_2 = \theta + \frac{\pi}{2}$ into (2.8), we obtain

$$\hat{g}(\beta_1) = \frac{2}{n} r^2 \sum_{i=1}^{n-1} m_i \tag{2.12}$$

and

$$\hat{g}(\beta_2) = \frac{2}{n} r^2 \sum_{i=1}^{n-1} m_i. \tag{2.13}$$

Both $\hat{g}(\beta_1)$ and $\hat{g}(\beta_2) > 0$. This indicates that if we use a plane $y = \tan(\beta_1)x$ to cut through the three-dimensional graph defined for $f(x, y)$, then on the cutting plane, the point A_1 will be local maximum point. Therefore, on the cutting plane, $f(x, y)$ is not quasiconvex at the origin point. This concludes the proof for general cases.

2.2 Proof for Trivial Cases (i.e., when $B = 0$)

Proof:

From (2.11) we know when $B = 0$, it implies that $B_1 = 0$ and $B_2 = 0$. In order to equate $\hat{g}'(\theta)$ to zero, $\tan(\theta)$ must be zero, $+\infty$, or $-\infty$ based on (2.9). As a result of that, the possible solutions for θ are 0, or $\frac{\pi}{2}$, or π, or $\frac{3}{2}\pi$. We can show that (2.12) and (2.13) are true for the cases of $\theta = 0$, and $\frac{\pi}{2}$, and π, and $\theta = \frac{3}{2}\pi$. By the argument in section 2.1, we conclude that, on the cutting plane, $f(x, y)$ is not quasiconvex at the origin point. This concludes the proof for trivial cases.

Therefore, as $m_i > 0$ for at least one value of i (i.e., at least one data point is different from the others), then both $\hat{g}(\beta_1)$ and $\hat{g}(\beta_2) > 0$. This indicates that if we use a plane $y = \tan(\beta_1)x$ to cut through the three-dimensional graph defined for $f(x, y)$, then on the cutting plane, the point A_1 will be a local maximum point. Therefore, on the cutting plane, $f(x, y)$ is not quasiconvex at the origin point. This conclude the proof of Proposition 2.

One interesting feature in the proof is worth noting. Regardless of the arrangement of the data points, the magnitude of slope at the origin point on the cutting

plane is always $\frac{2}{n}\sum_{i=1}^{n-1} R_i$.

2.3 Illustration

Given ten data points in Table 2.1, which are depicted in Figure 2.2, we want to illustrate that the function defined by (1.3) is not quasiconvex at data point A_7(-0.849468,-0.617175). The three-dimensional graph of $-f(x,y)$ vs. x and y and point A_7 are shown in Figure 2.3. First, we convert all the Cartesian coordinates into polar coordinates with the origin at data point A_7. For these data points mentioned above, we obtain R_i and α_i $\forall$ $i = 1,2,\ldots,9$ as shown in Table 2.2. Here R_i is the distance from point A_7 to point A_i for $i = 1,\ldots,6$ and the distance from point A_7 to point A_{i+1} for $i = 7,8,9$. The α_i is the corresponding polar angle for R_i with respect to point A_7. Using (2.9), we can get $\theta = 0.628319$.

Using a perpendicular plane through the line $y = \tan(2.19911)x$ to cut through the three-dimensional surface, a cutting plane as shown in Figures 2.4, 2.5, and 2.6 is obtained. In Figure 2.4 we show the relationship between the data points and the cutting plane. In Figure 2.5 we show the relationship between the contour of $f(x,y)$ and the cutting plane. Note that the y' axis in Figures 2.4 and 2.6 are identical and is the intersection between the cutting plane and the x,y plane. The z axis in Figure 2.6 represents the function value of $f(x,y)$ with respect to the y' axis. The intersection between the axes y' and z is the point A_7. The magnitude of the slope on both sides of the point A_7 is 2.65178, which is equal to $\frac{1}{5}\sum_{i=1}^{9} R_i$.

Table 2.1: Cartesian Coordinates of Ten Points.

Point	x	y
A_1	1.05	0
A_2	0.849468	0.617175
A_3	0.324468	0.998609
A_4	-0.324468	0.998609
A_5	-0.849468	0.617175
A_6	-1.05	0
A_7	-0.849468	-0.617175
A_8	-0.324468	-0.998609
A_9	0.324468	-0.998609
A_{10}	0.849468	-0.617175

Table 2.2: Transformed Polar Coordinates of Nine Points With the Origin at Data Point A_7.

n	R_n	α_n (in radians)
1	1.99722	0.314159
2	2.1	0.628319
3	1.99722	0.942478
4	1.23435	1.25664
5	1.23435	1.5708
6	0.648936	1.88496
7	0.648936	5.65487
8	1.23435	5.96903
9	1.69894	6.28319

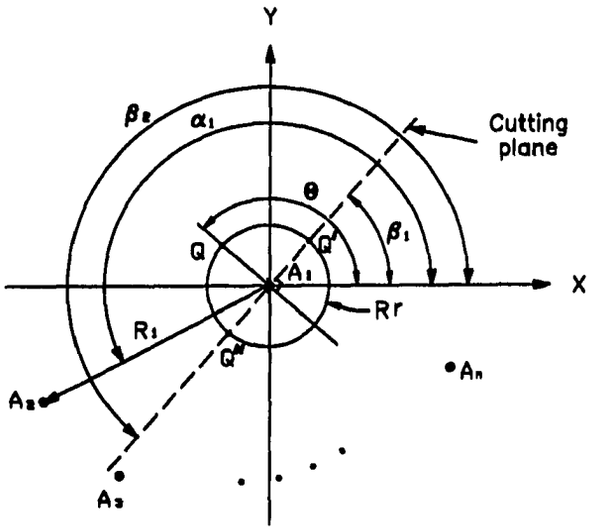

Figure 2.1: Arrangements of Points $A_1, A_2, \ldots, A_n$, and Q.

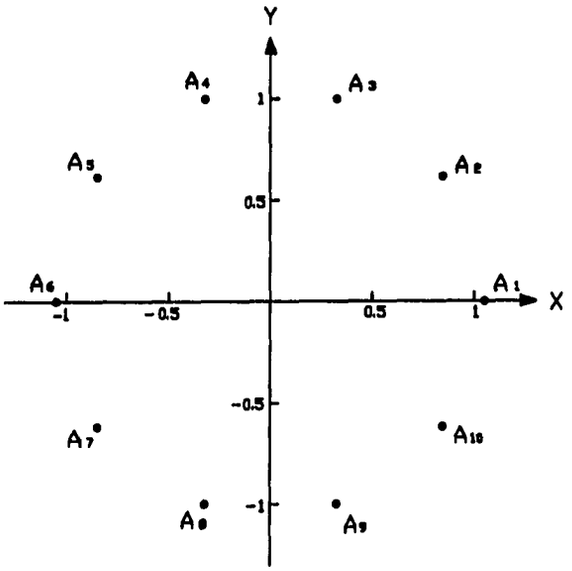

Figure 2.2: Arrangements of Ten Points $A_1, A_2, \ldots$, and A_{10}.

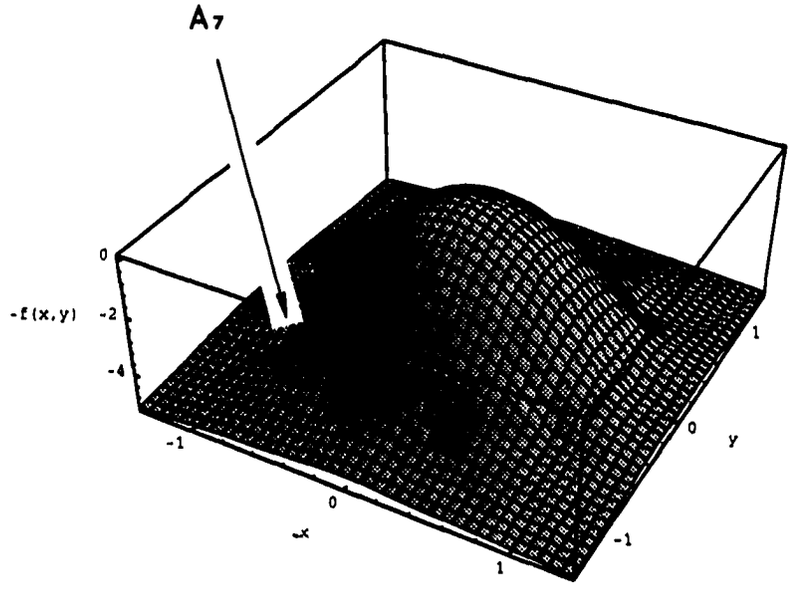

Figure 2.3: Three-Dimensional Plot of Ten Data Points and Point A_7.

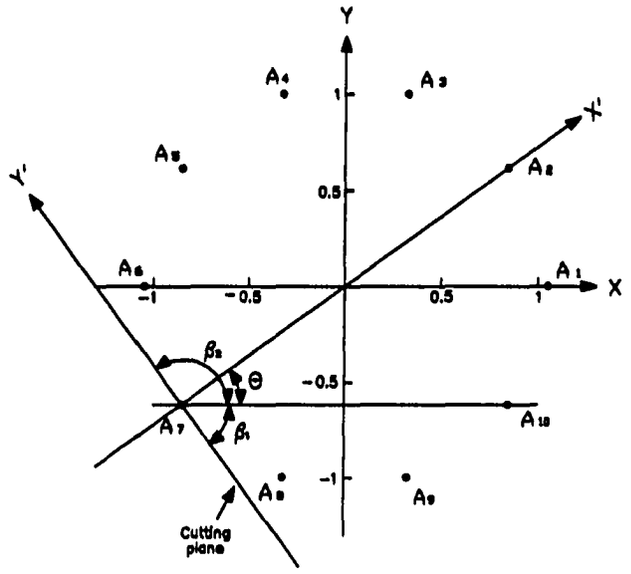

Figure 2.4: Relationship Between the Cutting Plane and Ten Data Points.

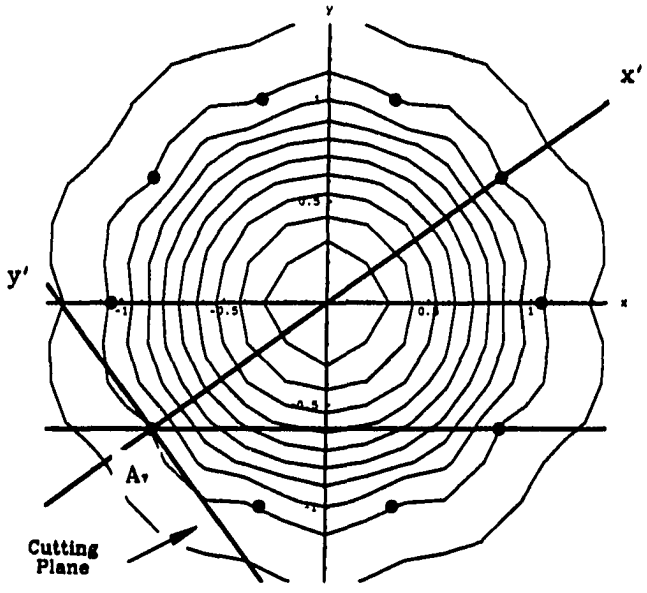

Figure 2.5: A Relationship Between the Contour of $f(x, y)$ and its Cutting Plane at the Point A_7.

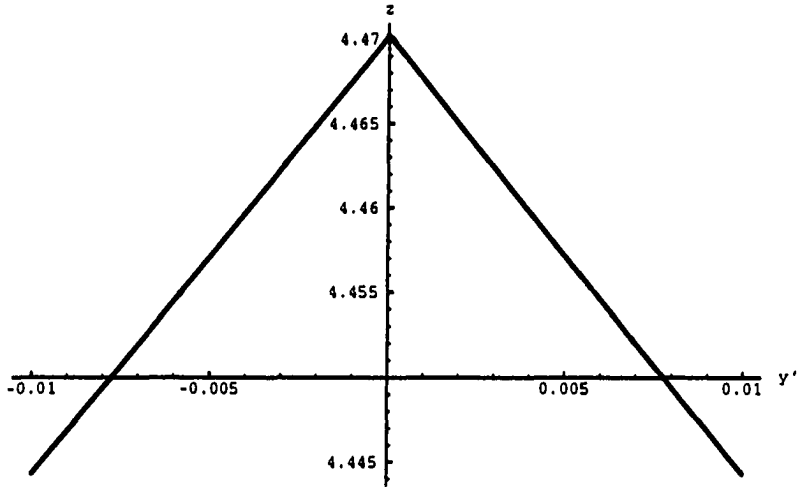

Figure 2.6: A Cutting Plane at the Point A_7.

CHAPTER 3. MEASUREMENT OF A CYLINDRICAL FEATURE

Consider a hole (created through some manufacturing process) that is fairly circular. Initial measurements are used to give an estimate (O) of the center and the diameter [8]. We assume the hole has satisfied the specification of the size tolerance before we measure the departure from circularity. Using a discrete measurement device (such as a CMM), we can obtain a set of observed data points (using polar coordinates) that are separated by a constant angle θ and have a distance $1+\epsilon_i$ from O. Here we assume an ideal measuring device such that no error is introduced during measurement. In the case of n points, $\theta = \frac{2\pi}{n}$, as shown in Figure 3.1. Note that in Figure 3.1 the coordinates of data points are expressed in polar coordinates.

Using this arrangement of data points, we can simplify the problem of finding a least squares center. Thus, the condition that the set of observed data points be separated by a constant θ is a necessary condition to determine the fundamental criteria for one global minimum.

Without loss of generality, we arbitrarily indicate that the radius of the inner circle is 1 as shown in Figure 3.1. This inner radius can be no smaller than the radius of the hole when the hole is at its maximum material condition (MMC)[17]. The width of the annulus is defined as κ.

To find a solution for (1.3), we narrow the search to a bounded area where

the center should be located. We present an approximation method using Taylor's theorem to show that if κ is small enough, then there exists one and only one circle (whose center lies in the bounded area) which best fits the observed data points. Conversely, if κ is too large, multiple solutions exist. Typical values for κ from the ISO standard [17] show that regardless of hole diameter, κ is almost always less than 0.05 for any design specification. Therefore, we limit our derivation to sets of points that satisfy the criterion of $\kappa \leq 0.05$.

3.1 Search Region

The ith point in a data set of n points has Cartesian coordinate of (x_i, y_i) and polar coordinate of $(1+\epsilon_i, (i-1)\frac{2\pi}{n})$, where $0 \leq \epsilon_i \leq \kappa$ and $\kappa \leq 0.05$. Here ϵ_i is the distance from point (x_i, y_i) to the inner circle of the annulus. Let D be a disc with center of $(0,0)$ and radius of 1, and $Int(D)$ be the interior of D. Thus, in our particular case, we can rephrase the least squares circle fitting problem in (1.3) as the global minimum searching problem as follows:

$$\begin{aligned} Minimize\ f(x,y) \ = \ & \sum_{i=1}^{n} \left(\sqrt{(x_i - x)^2 + (y_i - y)^2} - \right. \\ & \left. \frac{1}{n} \sum_{j=1}^{n} \sqrt{(x_j - x)^2 + (y_j - y)^2} \right)^2 \end{aligned} \tag{3.1}$$

$$\begin{aligned} \text{subject to} \quad & x_i = (1+\epsilon_i)\cos((i-1)\tfrac{2\pi}{n}), \\ & y_i = (1+\epsilon_i)\sin((i-1)\tfrac{2\pi}{n}), \text{ and} \\ & (x,y) \in Int(D). \end{aligned}$$

The reason we restricted our search region to be in $Int(D)$ is as follows. When a cylindrical part satisfies the size tolerance specification, the profile of the surface of

the cylindrical part should be confined to the annulus of Figure 3.1 after we normalize the profile of the surface by transforming the minimum radius of the size specification to 1. Let r_i be the distance from point A_i to the origin of the coordinate system and r_{min} be the minimum radius of the size specification. Then we obtain a normalized polar coordinate of A_i with new radius of A_i of $1 + \epsilon_i$. Here ϵ_i is defined as follows

$$\epsilon_i = \frac{r_i - r_{min}}{r_{min}}.$$

The center of the best fitted circle for a given set of discrete data points from the surface profile should be in the interior region, $Int(D)$.

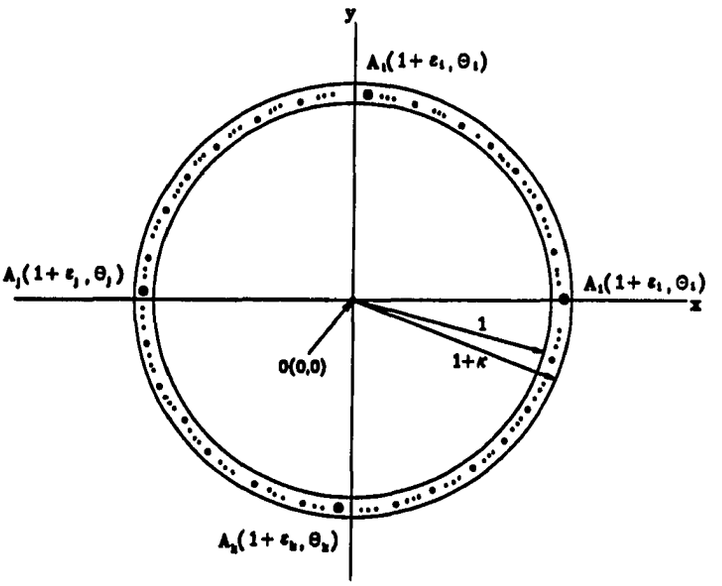

Figure 3.1: Layout of n Data Points in an Annulus.

CHAPTER 4. POSSIBLE REGION OF THE CENTER OF BEST FITTED CIRCLE

Searching for a possible region of the center of best fitted circle can be divided into two parts. Let $O'(x_c, y_c)$ be the center of the best fitted circle. First, we search for a conservative region of the center based on the fact that $O'(x_c, y_c)$ will be fairly close to point $O(0,0)$ in Figure 4.1 when κ is small. By definition in (3.1), (x_c, y_c) is a global minimum of $f(x,y)$, therefore, we can find a square conservative region, i.e., G_n, for (x_c, y_c) by using an inequality constraint, $f(x,y) \leq f(0,0)$. G_n is conservative because we have chosen a point $O(0,0)$ in close proximity to $O'(x_c, , y_c)$ as a basis to construct the region of $O'(x_c, y_c)$.

Given the difficulty of solving the first order necessary conditions (FONCs) of minimization [18] for $f(x,y)$, we use a Taylor approximation, $\hat{f}(x,y)$, for $f(x,y)$. The accuracy of this approximation is limited to a square region, A^*, centered at $(0,0)$ with width 2κ. We can show that both G_n is much larger than A^* and $A^* \subset G_n$ when $n \geq 4$. Therefore, we need to refine G_n so that it will be contained in A^*.

In the second step we accomplish this using an iterative algorithm. In this method, we apply the FONCs of $f(x,y)$ to G_n to obtain a refined region of $O'(x_c, y_c)$. We continue this process until the boundary of the refined region of $O'(x_c, y_c)$ has satisfied some convergence criteria. The final refined region of $O'(x_c, y_c)$ is G_n^*. We

can show that if n is a multiple of 4 and it is limited to $4 \leq n \leq 200$, then

$$O'(x_c, y_c) \in G_n^* \quad \text{and}$$
$$G_n^* \subset A^*.$$

The size of G_n^* depends on n.

4.1 Determination of G_n

The determination of G_n is divided into two parts. First we find a region, say G_n', which satisfies the constraint, $f(x,y) \leq f(0,0)$. The size of G_n' depends on ϵ_i $\forall$ i. Second, we find the largest circumscribed square region of G_n', i.e., G_n, to simplify the search of the conservative region for the center $O'(x_c, y_c)$. We show that G_n is independent of ϵ_i $\forall$ i.

4.1.1 Determination of G_n'

Let us consider the case of finding the center for a set of n points where $n \geq 4$. The observed points have polar coordinates of $(1+\epsilon_i, (i-1)\frac{2\pi}{n})$ and Cartesian coordinates of (x_i, y_i) (see Figure 4.1). The distance $\overline{O'A_i}$ can be represented as $1+\epsilon_i+\delta_i$, where δ_i can be regarded as the difference between $\overline{O'A_i}$ and $\overline{OA_i}$ as O' deviates from O (see Figure 4.2). Therefore, from (3.1) the value of $f(x,y)$ at (x_c, y_c) becomes

$$\begin{aligned} f(x_c, y_c) &= \sum_{i=1}^{n} \left(1+\epsilon_i+\delta_i-(1+\bar{\epsilon}+\bar{\delta})\right)^2 \\ &= \sum_{i=1}^{n} \left((\epsilon_i-\bar{\epsilon})^2 + 2(\epsilon_i-\bar{\epsilon})(\delta_i-\bar{\delta}) + (\delta_i-\bar{\delta})^2\right) \end{aligned} \tag{4.1}$$

where $\overline{\epsilon} = \frac{1}{n}\sum_{i=1}^{n}\epsilon_i$ and $\overline{\delta} = \frac{1}{n}\sum_{i=1}^{n}\delta_i$. By definition in (3.1) we know that (x_c, y_c) is a global minimum of $f(x, y)$, therefore we obtain

$$f(x_c, y_c) \leq f(0, 0). \tag{4.2}$$

Substituting (4.1) into (4.2) and simplifying, we obtain

$$\sum_{i=1}^{n}\left(2(\epsilon_i - \overline{\epsilon})(\delta_i - \overline{\delta}) + (\delta_i - \overline{\delta})^2\right) \leq 0. \tag{4.3}$$

According to Cauchy's inequality[12], we have the relationship

$$-\sqrt{\sum_{i=1}^{n}(\epsilon_i - \overline{\epsilon})^2 \sum_{i=1}^{n}(\delta_i - \overline{\delta})^2} \leq \sum_{i=1}^{n}(\epsilon_i - \overline{\epsilon})(\delta_i - \overline{\delta}). \tag{4.4}$$

Substituting the left side of (4.4) into (4.3) we obtain

$$-2\sqrt{\sum_{i=1}^{n}(\epsilon_i - \overline{\epsilon})^2 \sum_{i=1}^{n}(\delta_i - \overline{\delta})^2} + \sum_{i=1}^{n}(\delta_i - \overline{\delta})^2 \leq 0. \tag{4.5}$$

Rearranging the terms in (4.5), we obtain

$$\sum_{i=1}^{n}(\delta_i - \overline{\delta})^2 \leq 2\sqrt{\sum_{i=1}^{n}(\epsilon_i - \overline{\epsilon})^2 \sum_{i=1}^{n}(\delta_i - \overline{\delta})^2}. \tag{4.6}$$

Squaring both sides of (4.6) and simplifying give

$$\sum_{i=1}^{n}(\delta_i - \overline{\delta})^2 \leq 4\sum_{i=1}^{n}(\epsilon_i - \overline{\epsilon})^2. \tag{4.7}$$

We observe from (4.7) that the sample variance of δ is at most 4 times the sample variance of ϵ. G_n' is given by the minimum of $\delta_i's$, which we define as δ_*. If we change our frame of reference by looking at $\overline{O'A_i}$ from A_i, we would define a disc, say D_i, with radius of $1 + \epsilon_i + \delta_*$. Let $Int(D_i)$ be the interior of D_i. In this way, we can construct G_n' by finding the intersection of the $Int(D_i)$ $\forall$ i as shown in Figure 4.3. We claim that $O'(x_c, y_c)$ has to be in G_n'. The argument is as follows.

4.1.1.1 $O'(x_c, y_c)$ **is in** G'_n Suppose that (x_c, y_c) falls outside G'_n, then (x_c, y_c) has to fall into one of the $Int(D_i)$, say $Int(D_l)$. By definition the distance between A_l and $O'(x_c, y_c)$, which is $\overline{O'A_l}$, is $1 + \epsilon_l + \delta_l$. Since $O'(x_c, y_c)$ falls into disc D_l, thus we know that $\overline{O'A_l}$ is less than the radius of D_l, which is $1 + \epsilon_l + \delta_*$. Thus we obtain

$$\begin{aligned} \overline{O'A_l} &< 1 + \epsilon_l + \delta_*, \\ \Longleftrightarrow 1 + \epsilon_l + \delta_l &< 1 + \epsilon_l + \delta_*, \\ \Longleftrightarrow \delta_l &< \delta_*. \end{aligned} \tag{4.8}$$

We observe from (4.8) that it contradicts the fact that δ_* is the minimum of $\delta'_i s$. Thus we conclude that $O'(x_c, y_c)$ has to be in G'_n.

4.1.1.2 Determination of δ_* In order to find δ_*, we rely on the following facts.

1. Region condition in (4.7).
2. When $n \geq 4$, $\sum_{i=1}^{n} \delta_i > 0$ if $(x_c, y_c) \neq (0, 0)$ (see Appendix A).
3. When $n \geq 4$, if $(x_c, y_c) \neq (0, 0)$, then at least one of $\delta'_i s < 0$ (see Appendix B).
4. When $(x_c, y_c) = (0, 0)$, then $\delta_i = 0 \; \forall \; i$.

After relabeling $\delta_i \; \forall \; i$, we obtain a set of new labels $\Delta'_i s$ such that Δ_n is the minimum of $\Delta_i \; \forall \; i$. It is clear that δ_* can be obtained by solving the following nonlinear programming problem.

$$\text{Minimize} \quad \Delta_n$$

$$\begin{aligned} \text{subject to} \quad & 4\sum_{i=1}^{n}(\epsilon_i - \overline{\epsilon})^2 \geq \sum_{i=1}^{n}(\Delta_i - \overline{\Delta})^2. \\ & \sum_{i=1}^{n}\Delta_i \geq 0. \\ & \text{at least one of } \Delta_i's \leq 0. \end{aligned}$$

This minimum deviation, i.e., δ_*, defines G_n' shown in Figure 4.3 as the bounded region not contained in $Int(D_i)\ \forall\ i$.

We can show that the global minimum of Δ_n occurs, i.e., $\Delta_n = \delta_*$, when the arrangement of $\Delta_i's$ is given in Figure 4.4. In this special arrangement $\sum_{i=1}^{n}\Delta_i = 0$, and $\Delta_1 = \Delta_2 = \ldots = \Delta_{n-1} = -\frac{1}{n-1}\Delta_n$, where $\Delta_n < 0$ (see Appendix C). Therefore, in this special arrangement

$$\begin{aligned} \sum_{i=1}^{n}(\delta_i - \overline{\delta})^2 &= \sum_{i=1}^{n}(\Delta_i - \overline{\Delta})^2 \\ &= \sum_{i=1}^{n}\Delta_i^2 \\ &= \Delta_n^2 + (n-1)(-\frac{\Delta_n}{n-1})^2 \\ &= \frac{n}{n-1}\Delta_n^2 \\ &= \frac{n}{n-1}\delta_*^2. \end{aligned} \tag{4.9}$$

Substituting (4.9) into (4.7) we obtain

$$\begin{aligned} \frac{n}{n-1}\delta_*^2 &\leq 4\sum_{i=1}^{n}(\epsilon_i - \overline{\epsilon})^2 \\ \Longrightarrow \quad \delta_*^2 &\leq \frac{4(n-1)}{n}\sum_{i=1}^{n}(\epsilon_i - \overline{\epsilon})^2 \\ \Longrightarrow \quad \delta_* &\geq -\sqrt{\frac{4(n-1)}{n}\sum_{i=1}^{n}(\epsilon_i - \overline{\epsilon})^2}. \end{aligned} \tag{4.10}$$

We can show that (see Appendix D)

$$\sum_{i=1}^{n}(\epsilon_i - \overline{\epsilon})^2 \leq \frac{n}{4}\kappa^2. \tag{4.11}$$

Substituting (4.11) into (4.10), we obtain

$$\delta_* \geq -\sqrt{n-1}\kappa. \tag{4.12}$$

From Figure 4.3, it is clear that the size of G'_n is dependent on $\epsilon_i \ \forall \ i$, and δ_*.

4.1.2 Derive G_n from G'_n

We can easily show that with ϵ_i, $\forall \ i$ and δ_* as variables, the largest G'_n occurs when $\epsilon_i = 0 \ \forall \ i$ and $\delta_* = -\kappa\sqrt{n-1}$ as shown in Figure 4.5 (see Appendix E).

To simplify the discussion, we define the circumscribed square for G'_n in Figure 4.5 as G_n. The width of the G_n is $2s_n$ (see Figure 4.6). When n is a multiple of 4, s_n is the x coordinate of the intersection of two circles with centers of polar coordinates of $(1,0)$ and $(1, \frac{2\pi}{n})$ and common radius of $1-\kappa\sqrt{n-1}$. i.e.,

$$\begin{aligned} s_n &= \{x : (x-1)^2 + y^2 = (1-\kappa\sqrt{n-1})^2, \\ &\quad (x - \cos\frac{2\pi}{n})^2 + (y - \sin\frac{2\pi}{n})^2 = (1-\kappa\sqrt{n-1})^2, \text{ and } x < 1\} \\ &= \frac{1 - \sqrt{1 - \frac{2-2\cos\frac{2\pi}{n}}{\sin^2\frac{2\pi}{n}}(2\kappa\sqrt{n-1} - (n-1)\kappa^2)}}{\frac{2-2\cos\frac{2\pi}{n}}{\sin^2\frac{2\pi}{n}}}. \end{aligned}$$

When $n \geq 4$ and n is not a multiple of 4, s_n is $\sqrt{x^2+y^2}$ where (x,y) is the Cartesian coordinate of the intersection of two circles with centers of polar coordinates of $(1,0)$ and $(1, \frac{2\pi}{n})$ and common radius of $1-\sqrt{n-1}\kappa$. i.e.,

$$\begin{aligned} s_n &= \{\sqrt{x^2+y^2} : (x-1)^2 + y^2 = (1-\sqrt{n-1}\kappa)^2, \\ &\quad (x - \cos\frac{2\pi}{n})^2 + (y - \sin\frac{2\pi}{n})^2 = (1-\sqrt{n-1}\kappa)^2, \text{ and } x < 1\}. \end{aligned}$$

Assigning a number to n and κ, we are able to use Maple [24] to solve for s_n numerically. G_n in Figure 4.6 contains the center $O'(x_c, y_c)$ regardless of the values of $\epsilon_i \ \forall \ i$.

4.2 Iterative Procedure for Finding G_n^*.

We can obtain a smaller possible region, which is closer to $O(0,0)$, of the center $O'(x_c, y_c)$ by calculating a new boundary of the center $O'(x_c, y_c)$ based on putting constraints, i.e., the FONCs of $f(x,y)$, to the boundary of G_n. We then use this new boundary as an input to the next iteration. We continue this process until the boundary of the center $O'(x_c, y_c)$ has satisfied some convergence criteria. Let G_n^i be the refined region after applying the FONCs of $f(x,y)$ to G_n^{i-1}. Note that G_n^0 equals G_n. We define the final refined region as G_n^*. In this way we can obtain a smaller G_n^* by contracting G_n in Figure 4.6 towards point $O(0,0)$.

4.2.1 Determination of G_n^1

We obtain G_n^1 by finding boundaries for x and y. Taking the first partial derivatives of $f(x,y)$ with respect to x and y, we obtain

$$\frac{\partial f(x,y)}{\partial x} = 2\sum_{i=1}^{n}\left(\sqrt{(x-x_i)^2+(y-y_i)^2} - \frac{1}{n}\sum_{j=1}^{n}\sqrt{(x-x_j)^2+(y-y_j)^2}\right) * \left(\frac{x-x_i}{\sqrt{(x-x_i)^2+(y-y_i)^2}} - \frac{1}{n}\sum_{j=1}^{n}\frac{x-x_j}{\sqrt{(x-x_j)^2+(y-y_j)^2}}\right) \quad (4.13)$$

and

$$\frac{\partial f(x,y)}{\partial y} = 2\sum_{i=1}^{n}\left(\sqrt{(x-x_i)^2+(y-y_i)^2} - \frac{1}{n}\sum_{j=1}^{n}\sqrt{(x-x_j)^2+(y-y_j)^2}\right) * \left(\frac{y-y_i}{\sqrt{(x-x_i)^2+(y-y_i)^2}} - \frac{1}{n}\sum_{j=1}^{n}\frac{y-y_j}{\sqrt{(x-x_j)^2+(y-y_j)^2}}\right). \quad (4.14)$$

In order to satisfy the FONCs of $f(x,y)$, we equate (4.13) and (4.14) to zero.

Simplifying, we obtain

$$n(\sum_{i=1}^{n} A_i) = (\sum_{i=1}^{n} \sqrt{A_i^2 + B_i^2})(\sum_{i=1}^{n} \frac{A_i}{\sqrt{A_i^2 + B_i^2}}) \quad (4.15)$$

and

$$n(\sum_{i=1}^{n} B_i) = (\sum_{i=1}^{n} \sqrt{A_i^2 + B_i^2})(\sum_{i=1}^{n} \frac{B_i}{\sqrt{A_i^2 + B_i^2}}), \quad (4.16)$$

where $A_i = x_i - x$, $B_i = y_i - y$. Substituting $r_i = \sqrt{A_i^2 + B_i^2}$, $\cos\theta_i' = \frac{A_i}{\sqrt{A_i^2+B_i^2}}$ and $\sin\theta_i' = \frac{B_i}{\sqrt{A_i^2+B_i^2}}$, we can rephrase (4.15) and (4.16) as

$$n\left(\sum_{i=1}^{n} \epsilon_i \cos((i-1)\frac{2\pi}{n}) - nx\right) = \left(\sum_{i=1}^{n} r_i\right)\left(\sum_{i=1}^{n} \cos\theta_i'\right) \quad (4.17)$$

and

$$n\left(\sum_{i=1}^{n} \epsilon_i \sin((i-1)\frac{2\pi}{n}) - ny\right) = \left(\sum_{i=1}^{n} r_i\right)\left(\sum_{i=1}^{n} \sin\theta_i'\right). \quad (4.18)$$

4.2.1.1 Upper bound of x for G_n^1 We can find the upper bound of x for G_n^1 by applying (4.17) to G_n as follows. Let L_{nl} be the lower bound of the left side of (4.17), so that

$$L_{nl} \leq n\left(\sum_{i=1}^{n} \epsilon_i \cos((i-1)\frac{2\pi}{n}) - nx\right).$$

Isolating x, we obtain the upper bound

$$x \leq \frac{1}{n^2}\left(n\sum_{i=1}^{n} \epsilon_i \cos((i-1)\frac{2\pi}{n}) - L_{nl}\right). \quad (4.19)$$

One way to find L_{nl} is to find a lower bound of the right side of (4.17). A lower bound of the right side of (4.17) can be obtained by finding the most negative value for $\sum_{i=1}^{n} \cos\theta_i'$, $L_{nc\theta'}$, and the largest value for $\sum_{i=1}^{n} r_i$, U_{nr}. Since $U_{nr} > 0$ and $L_{nc\theta'} < 0$, $U_{nr}L_{nc\theta'}$ will be the lower bound of the right side of (4.17).

U_{nr} is the global maximum value of $\sum_{i=1}^{n} r_i \ \forall \ (x,y) \in G_n$ and $\epsilon_i \ \forall \ i$. Similarly, $L_{nc\theta'}$ is the global minimum value of $\sum_{i=1}^{n} \cos\theta_i' \ \forall \ (x,y) \in G_n$ and $\epsilon_i \ \forall \ i$. By setting $L_{nl} = U_{nr} L_{nc\theta'}$, we can solve for upper bound of x in (4.19) as

$$x \ \leq \ \frac{1}{n^2}\left(n\sum_{i=1}^{n}\epsilon_i \cos((i-1)\frac{2\pi}{n}) - U_{nr}L_{nc\theta'}\right). \tag{4.20}$$

Let $t_1 = \lfloor \frac{n}{4} \rfloor$ stand for the largest integer not greater than $\frac{n}{4}$. Knowing $n \geq 4$, we can show that

$$\sum_{i=1}^{n}\epsilon_i \cos\left((i-1)\frac{2\pi}{n}\right) \ \leq \ U_{n\kappa c} \tag{4.21}$$

where

$$U_{n\kappa c} \ = \ \kappa + 2\kappa \sum_{i=2}^{t_1+1} \cos\left((i-1)\frac{2\pi}{n}\right). \tag{4.22}$$

Substituting (4.21) into (4.20), we obtain an upper bound of x of G_n^1, say x_n^{1*}, as

$$\begin{aligned} x \ &\leq \ \frac{1}{n^2}(nU_{n\kappa c} - U_{nr}L_{nc\theta'}) \\ \text{or} \quad x \ &\leq \ x_n^{1*}. \end{aligned} \tag{4.23}$$

4.2.1.2 Lower bound of x for G_n^1 The lower bound of x can be determined in a similar manner. Let U_{nl} be the upper bound of the left side of (4.17), so that

$$n\left(\sum_{i=1}^{n}\epsilon_i \cos((i-1)\frac{2\pi}{n}) - nx\right) \ \leq \ U_{nl}.$$

Again, isolating x we obtain

$$\frac{1}{n^2}\left(n\sum_{i=1}^{n}\epsilon_i \cos((i-1)\frac{2\pi}{n}) - U_{nl}\right) \ \leq \ x. \tag{4.24}$$

To find U_{nl}, we use the right side of (4.17) and find an upper bound of $\sum_{i=1}^{n} r_i$, U_{nr}, and an upper bound of $\sum_{i=1}^{n} \cos\theta_i'$, $U_{nc\theta'}$. Since $U_{nr} > 0$ and $U_{nc\theta'} > 0$, $U_{nr}U_{nc\theta'}$ will

be the upper bound of the right side of (4.17). Here $U_{nc\theta'}$ is a global maximum value of $\sum_{i=1}^{n} \cos\theta_i'$. By setting $U_{nl} = U_{nr}U_{nc\theta'}$, we can find the lower bound for x as

$$\frac{1}{n^2}\left(n\sum_{i=1}^{n}\epsilon_i \cos((i-1)\frac{2\pi}{n}) - U_{nr}U_{nc\theta'}\right) \leq \quad x. \tag{4.25}$$

Applying the similar procedure of finding the upper bound of $\sum_{i=1}^{n}\epsilon_i \cos\left((i-1)\frac{2\pi}{n}\right)$ as shown in (4.21), we can find its lower bound as follows:

$$\sum_{i=1}^{n}\epsilon_i \cos\left((i-1)\frac{2\pi}{n}\right) \quad \geq \quad L_{n\kappa c} \tag{4.26}$$

where

$$L_{n\kappa c} \quad = \quad \kappa \sum_{i=t_1+2}^{n-t_1} \cos\left((i-1)\frac{2\pi}{n}\right). \tag{4.27}$$

Substituting (4.26) into (4.25), we obtain a lower bound of x of G_n^1, say x_{n*}^1, as follows:

$$\begin{aligned} \frac{1}{n^2}(nL_{n\kappa c} - U_{nr}U_{nc\theta'}) \quad &\leq \quad x \\ \text{or} \quad x_{n*}^1 \quad &\leq \quad x. \end{aligned} \tag{4.28}$$

4.2.1.3 Relationship between x_{n*}^1 and x_n^{1*} If $n \geq 4$, n is even and $(x, y) \in G_n$ where $G_n \subset Int(D)$, then we can show that (see Appendices F and G)

$$L_{nc\theta'} = -U_{nc\theta'} \tag{4.29}$$

and

$$L_{n\kappa c} = -U_{n\kappa c}. \tag{4.30}$$

Thus (4.28) becomes

$$\begin{aligned} x_{n*}^1 \quad &= \quad -\frac{1}{n^2}(nU_{n\kappa c} - U_{nr}L_{nc\theta'}) \\ &\leq \quad x. \end{aligned} \tag{4.31}$$

Note that $x_n^{1*} = -x_{n*}^1$ (i.e., G_n^1 is symmetric in x).

4.2.1.4 Upper and lower bounds of y for G_n^1 Repeating the same process for y, we define $L_{ns\theta'}$ as the global minimum value of $\sum_{i=1}^n \sin\theta_i'$, $U_{ns\theta'}$ be the global maximum value of $\sum_{i=1}^n \sin\theta_i'$, $L_{n\kappa s}$ be the global minimum value of $\sum_{i=1}^n \epsilon_i \sin\left((i-1)\frac{2\pi}{n}\right)$, and $U_{n\kappa s}$ be the global maximum value of $\sum_{i=1}^n \epsilon_i \sin\left((i-1)\frac{2\pi}{n}\right)$. Note that

$$U_{n\kappa s} = \kappa \sum_{i=1}^{t_2+1} \sin\left((i-1)\frac{2\pi}{n}\right), \quad \text{and} \tag{4.32}$$

$$L_{n\kappa s} = \kappa \sum_{i=t_2+2}^{n} \sin\left((i-1)\frac{2\pi}{n}\right), \tag{4.33}$$

where $t_2 = \lfloor \frac{n}{2} \rfloor$. We can show that the upper and lower bounds of y of G_n^1, say y_n^{1*} and y_{n*}^1, as

$$\begin{aligned} y &\leq \frac{1}{n^2}(nU_{n\kappa s} - U_{nr}L_{ns\theta'}) \\ &= y_n^{1*} \end{aligned} \tag{4.34}$$

and

$$\begin{aligned} y_{n*}^1 &= \frac{1}{n^2}(nL_{n\kappa s} - U_{nr}U_{ns\theta'}) \\ &\leq y. \end{aligned} \tag{4.35}$$

Applying the similar proofs in Appendices F and G, we can show that if $n \geq 4$, n is even, and $(x, y) \in G_n$ where $G_n \subset Int(D)$, then

$$L_{ns\theta'} = -U_{ns\theta'}, \quad \text{and} \tag{4.36}$$

$$L_{n\kappa s} = -U_{n\kappa s}. \tag{4.37}$$

Substituting (4.36) and (4.37) into (4.35), we obtain

$$\begin{aligned} y^1_{n*} &= -\frac{1}{n^2}(nU_{n\kappa s} - U_{nr}L_{ns\theta'}) \\ &\leq y. \end{aligned} \tag{4.38}$$

Note that $y^{1*}_n = -y^1_{n*}$ (i.e., G^1_n is symmetric in y).

4.2.1.5 Relationship among x^1_{n*}, x^{1*}_n, y^1_{n*} and y^{1*}_n We can show that if n is a multiple of 4 and $(x, y) \in G_n$ where $G_n \subset Int(D)$, then (see Appendices H and I)

$$U_{nc\theta'} = U_{ns\theta'} \tag{4.39}$$

and

$$U_{n\kappa c} = U_{n\kappa s}. \tag{4.40}$$

Combining (4.29), (4.36) and (4.39), we obtain

$$U_{nc\theta'} = U_{ns\theta'} = -L_{nc\theta'} = -L_{ns\theta'}. \tag{4.41}$$

Furthermore, combining (4.30), (4.37), and (4.40), we obtain

$$U_{n\kappa c} = U_{n\kappa s} = -L_{n\kappa c} = -L_{n\kappa s}. \tag{4.42}$$

Substituting (4.41) and (4.42) into (4.23), (4.28), (4.34), and (4.35), we find that

$$x^{1*}_n = y^{1*}_n = -x^1_{n*} = -y^1_{n*}. \tag{4.43}$$

Therefore, G^1_n is also a square. Squareness of G^1_n is desirable, because it simplifies the determination of $x^{1*}_n, y^{1*}_n, x^1_{n*}$ and y^1_{n*}. The dimensions of G^1_n can be found by solving for one of the boundaries, say x^{1*}_n. Thus in the case of $n = 4m$, the problem reduces to finding the global maximum of $\sum_{i=1}^n r_i$ (i.e., U_{nr}) and the global minimum of $\sum_{i=1}^n \cos\theta'_i$ (i.e., $L_{nc\theta'}$).

4.2.2 Determination of U_{nr}

We can find U_{nr} as follows. Let $g_n(x, y, \epsilon_1, \epsilon_2, \ldots, \epsilon_n) = \sum_{i=1}^{n} r_i$, then based on the definition of r_i

$$g_n(x, y, \epsilon_1, \epsilon_2, \ldots, \epsilon_n) = \sum_{i=1}^{n} \sqrt{(x_i - x)^2 + (y_i - y)^2}. \tag{4.44}$$

From Propositions 3 and 4 in Appendix A, we know that given values of $\epsilon_i \; \forall \, i$, $\sum_{i=1}^{n} r_i$ is a continuous and strictly convex function of x and y with the global minimum at $(0,0)$. It is clear that G_n is a nonempty compact polyhedral set in E_2. Therefore, by Theorem 2 in Appendix J, the maximum of $\sum_{i=1}^{n} r_i$ must occur at an extreme point of G_n (i.e., one of the four vertices in G_n). Recall that U_{nr} is the global maximum value of $g_n(x, y, \epsilon_1, \epsilon_2, \ldots, \epsilon_n)$. Therefore, we obtain that U_{nr} corresponds to one of the four vertices in G_n.

We can show that the global maximum values of $g_n(x, y, \epsilon_1, \epsilon_2, \ldots, \epsilon_n)$ is invariant when (x, y) is at any one of the vertices of G_n (see Appendix K). Recall that s_n is one half the length of a side of G_n. Thus the upper right vertex of G_n has coordinate of (s_n, s_n). Therefore without loss of generality, we we can find U_{nr} by choosing $(x, y) = (s_n, s_n)$ first. Then with $\epsilon_i's$ as variables, we can find U_{nr} by finding the global maximum of $g_n(s_n, s_n, \epsilon_1, \epsilon_2, \ldots, \epsilon_n)$. It is summarized as follows.

$$\begin{aligned} U_{nr} &= MAX\{g_n(s_n, s_n, \epsilon_1, \epsilon_2, \ldots, \epsilon_n) : \epsilon_i \; \forall \; i.\} \\ &= MAX\{\sum_{i=1}^{n} \sqrt{(x_i - s_n)^2 + (y_i - s_n)^2} : \epsilon_i \; \forall \; i.\} \end{aligned}$$

We can show that, with $\epsilon_i's$ as variables, a maximum value for $g_n(s_n, s_n, \epsilon_1, \epsilon_2, \ldots, \epsilon_n)$, occurs when $\epsilon_i = \kappa \; \forall \; i$ (see Appendix L). Thus, we obtain

$$U_{nr} = MAX\{g_n(s_n, s_n, \epsilon_1, \epsilon_2, \ldots, \epsilon_n) : \epsilon_i \; \forall \; i.\}$$

$$= \sum_{i=1}^{n} \sqrt{((1+\kappa)\cos\theta_i - s_n)^2 + ((1+\kappa)\sin\theta_i - s_n)^2}. \qquad (4.45)$$

4.2.3 Determination of $L_{nc\theta'}$

Now we proceed to find $L_{nc\theta'}$ as follows. Let $h_n(x, y, \epsilon_1, \epsilon_2, \ldots, \epsilon_n)$ be $\sum_{i=1}^{n} \cos\theta_i'$, then based on the definition of $\cos\theta_i'$

$$h_n(x, y, \epsilon_1, \epsilon_2, \ldots, \epsilon_n) = \sum_{i=1}^{n} \frac{x_i - x}{\sqrt{(x_i - x)^2 + (y_i - y)^2}}. \qquad (4.46)$$

Then we take the first partial derivative of $h_n(x, y, \epsilon_1, \epsilon_2, \ldots, \epsilon_n)$ with respect to x and obtain

$$\begin{aligned} \frac{\partial h_n(x, y, \epsilon_1, \epsilon_2, \ldots, \epsilon_n)}{\partial x} &= \sum_{i=1}^{n} \frac{-(y_i - y)^2}{((x_i - x)^2 + (y_i - y)^2)^{1.5}} \\ &< 0. \end{aligned} \qquad (4.47)$$

By (4.47) we know that $h_n(x, y, \epsilon_1, \epsilon_2, \ldots, \epsilon_n)$ is a decreasing function of x given y. Therefore, we know that when $(x, y) \in G_n$, the global minimum of $h_n(x, y, \epsilon_1, \epsilon_2, \ldots, \epsilon_n)$ occurs when (x, y) is located at its rightmost boundary of G_n (in this special case, $x = s_n$ and $-s_n \leq y \leq s_n$). If we can show that given $\epsilon_i \; \forall \; i$, $h_n(x, y, \epsilon_1, \epsilon_2, \ldots, \epsilon_n)$ is a strictly concave function of y when x is at the maximum value of G_n, then it is clear that the global minimum of $h_n(x, y, \epsilon_1, \epsilon_2, \ldots, \epsilon_n)$ occurs when (x, y) is at one of its extreme points (i.e., P_1 or P_2 in Figure 4.6).

In order to show that $h_n(x, y, \epsilon_1, \epsilon_2, \ldots, \epsilon_n)$ is a strictly concave function of y when x is at its maximum value of G_n, we take the second partial derivative of $h_n(x, y, \epsilon_1, \epsilon_2, \ldots, \epsilon_n)$ with respect to y and obtain

$$\frac{\partial^2 h_n(x, y, \epsilon_1, \epsilon_2, \ldots, \epsilon_n)}{\partial y^2} = \sum_{i=1}^{n} (x_i - x) \frac{-(x_i - x)^2 + 2(y_i - y)^2}{((x_i - x)^2 + (y_i - y)^2)^{2.5}}.$$

If we can show that given $\frac{\partial^2 h_n(x,y,\epsilon_1,\epsilon_2,\ldots,\epsilon_n)}{\partial y^2} < 0$ when $x = s_n$ and $-s_n \leq y \leq s_n$, then $h_n(x, y, \epsilon_1, \epsilon_2, \ldots, \epsilon_n)$ is a strictly concave function of y.

Mathematically, it is very difficult to show this, however, by assigning a number to n such that $4 \leq n \leq 200$, and n is a multiple of 4, we can use optimization software, such as simulated annealing [22] [23], to find the global maximum of $\frac{\partial^2 h_n(x,y,\epsilon_1,\epsilon_2,\ldots,\epsilon_n)}{\partial y^2}$ numerically. If the global maximum of $\frac{\partial^2 h_n(x,y,\epsilon_1,\epsilon_2,\ldots,\epsilon_n)}{\partial y^2} < 0$, then we conclude that $\frac{\partial^2 h_n(x,y,\epsilon_1,\epsilon_2,\ldots,\epsilon_n)}{\partial y^2} < 0$. Indeed, if $4 \leq n \leq 200$ and n is a multiple of 4, we can show that $\frac{\partial^2 h_n(x,y,\epsilon_1,\epsilon_2,\ldots,\epsilon_n)}{\partial y^2} < 0 \; \forall \; x = s_n$, $-s_n \leq y \leq s_n$, and $\epsilon_i \; \forall \; i$ numerically by simulated annealing. Therefore, by the previous argument, the global minimum of $h_n(x, y, \epsilon_1, \epsilon_2, \ldots, \epsilon_n)$ occurs when the (x, y) is at point $\mathrm{P_1}$ or $\mathrm{P_2}$ (see Figure 4.6). Recall that $L_{nc\theta'}$ is a global minimum value of $h_n(x, y, \epsilon_1, \epsilon_2, \ldots, \epsilon_n)$. Therefore, we obtain that $L_{nc\theta'}$ occurs when (x, y) is at point $\mathrm{P_1}$ or $\mathrm{P_2}$.

We can show that when $(x, y) \in G_n$ where $G_n \subset Int(D)$, and n is a multiple of 4, the global minimum value of $h_n(x, y, \epsilon_1, \epsilon_2, \ldots, \epsilon_n)$ with (x, y) being of the Cartesian coordinates of $\mathrm{P_1}(s_n, s_n)$ is equal to the global minimum value of $h_n(x, y, \epsilon_1, \epsilon_2, \ldots, \epsilon_n)$ with (x, y) being of the Cartesian coordinates of $\mathrm{P_2}(s_n, -s_n)$ (see Appendix M). Thus, without loss of generality, we arbitrarily choose (x, y) to be the Cartesian coordinate of $\mathrm{P_1}$ to search $L_{nc\theta'}$. Note that

$$h_n(s_n, s_n, \epsilon_1, \epsilon_2, \ldots, \epsilon_n) \;=\; \sum_{i=1}^{n} \cos\theta_i', \tag{4.48}$$

where

$$\cos\theta_i' \;=\; \frac{x_i - s_n}{\sqrt{(x_i - s_n)^2 + (y_i - s_n)^2}} \tag{4.49}$$

$\forall \; i$. If we can find ϵ_i such as to minimize $\cos\theta_i' \; \forall \; i$, then by (4.48) we know that it minimizes $h_n(s_n, s_n, \epsilon_1, \epsilon_2, \ldots, \epsilon_n)$ as well.

4.2.3.1 Conditions of minimization of $\cos\theta_i'$ Using lines $y - s_n = 0$ and $x - y = 0$, we divide the annulus into four areas as shown in Figure 4.7. We can show geometrically that, with ϵ_i as a variable, when (x, y) is at point P_1 (s_n, s_n), a global minimum value of $\cos\theta_i'$ occurs when ϵ_i satisfies one of the following conditions.

1. If (x_i, y_i) falls into region I $\forall$ ϵ_i, then we choose the corresponding ϵ_i to be κ. See Figure 4.8. The argument is as follows.

   When (x_i, y_i) falls into region I, it is clear that $\theta_i' \leq \frac{\pi}{4}$. Since $\cos\theta_i'$ is a strictly decreasing function of θ_i' when $0 \leq \theta_i' \leq \frac{\pi}{4}$, thus we know that $\cos\theta_i'$ is smaller when θ_i' becomes larger. We observe that for a given θ_i, with ϵ_i as a variable, θ_i' is larger as ϵ_i becomes larger. Therefore, we obtain that $\cos\theta_i'$ is smaller when ϵ_i becomes larger. Thus, when (x_i, y_i) falls into region I, in order to obtain the minimum value of $\cos\theta_i'$, we choose $\epsilon_i = \kappa$.

2. If (x_i, y_i) falls into region II or III or IV $\forall$ ϵ_i, then we choose the corresponding ϵ_i to be 0 or κ or 0 correspondingly. See Figure 4.9, 4.10 and 4.11. The argument is similar to condition 1.

3. If (x_i, y_i) falls into both regions I & IV $\forall$ ϵ_i, then we choose the corresponding $\cos\theta_i'$ to be the minimum of $\left\{ \frac{(1+\kappa)\cos\theta_i - s_n}{\sqrt{((1+\kappa)\cos\theta_i - s_n)^2 + ((1+\kappa)\sin\theta_i - s_n)^2}}, \frac{\cos\theta_i - s_n}{\sqrt{(\cos\theta_i - s_n)^2 + (\sin\theta_i - s_n)^2}} \right\}$. See Figure 4.12. The argument is as follows.

   By condition 1, we can show that if (x_i, y_i) falls into region I for some ϵ_i, say $z \leq \epsilon_i \leq \kappa$, then, in order to obtain the minimum value of $\cos\theta_i'$, we choose $\epsilon_i = \kappa$. Here z is the distance from the point SP, which is the intersection point of lines $y = \tan\theta_i\, x$ and $y = s_n$, to the inner circle of the annulus (see

Figure 4.12). i.e.,

$$\begin{aligned} & MIN\ \{\cos\theta_i' : z \le \epsilon_i \le \kappa\} \\ = & \frac{(1+\kappa)\cos\theta_i - s_n}{\sqrt{((1+\kappa)\cos\theta_i - s_n)^2 + ((1+\kappa)\sin\theta_i - s_n)^2}}. \end{aligned} \tag{4.50}$$

By condition 2, we can show that if (x_i, y_i) falls into region IV for some ϵ_i, say $0 \le \epsilon_i \le z$, then the minimum value of $\cos\theta_i'$ occurs when $\epsilon_i = 0$. i.e.,

$$MIN\ \{\cos\theta_i' : 0 \le \epsilon_i \le z\} = \frac{\cos\theta_i - s_n}{\sqrt{(\cos\theta_i - s_n)^2 + (\sin\theta_i - s_n)^2}}. \tag{4.51}$$

Thus by (4.50) and (4.51), we obtain

$$\begin{aligned} MIN\ \{\cos\theta_i' : 0 \le \epsilon_i \le \kappa\} = MIN \Bigg\{ & \frac{\cos\theta_i - s_n}{\sqrt{(\cos\theta_i - s_n)^2 + (\sin\theta_i - s_n)^2}}, \\ & \frac{(1+\kappa)\cos\theta_i - s_n}{\sqrt{((1+\kappa)\cos\theta_i - s_n)^2 + ((1+\kappa)\sin\theta_i - s_n)^2}} \Bigg\}. \end{aligned} \tag{4.52}$$

4. If (x_i, y_i) falls into both regions II & III $\forall\ \epsilon_i$, then we choose the corresponding $\cos\theta_i'$ to be -1. See Figure 4.13. The argument is similar to condition 3.

5. If (x_i, y_i) falls into the boundaries between regions I & II or between regions III & IV $\forall\ \epsilon_i$, then the choice of ϵ_i does not make any difference to $\cos\theta_i'$. i.e., when (x_i, y_i) falls into the boundary between regions I & II, (See Figure 4.14)

$$\begin{aligned} \cos\theta_i' &= \cos\theta_i \\ &= \cos\frac{\pi}{4} \\ &= \frac{1}{\sqrt{2}} \quad \forall\ \epsilon_i, \end{aligned} \tag{4.53}$$

and when (x_i, y_i) falls into the boundary between regions III & IV, (See Figure 4.15)

$$\cos\theta_i' = \cos\theta_i$$

$$= \cos\frac{5}{4}\pi$$
$$= -\frac{1}{\sqrt{2}} \quad \forall\ \epsilon_i. \tag{4.54}$$

The conditions above are coded in subroutine LCTHETA $(s_n, n, L_{nc\theta'})$ (see Appendix N) to find the $L_{nc\theta'}$ given s_n and n.

4.2.4 Iterative algorithm of searching the upper bound of x of G_n^*

Let x_n^{i*} be the upper bound of x of G_n^i and x_n^* be the upper bound of x of G_n^*. Since $\kappa \leq 0.05$, we choose κ to be 0.05 in the iterative algorithm to cover all situations of κ. The iterative algorithm, which is to find x_n^* for $4 \leq n \leq 200$ and n is a multiple of 4, is summarized as follows:

$\kappa = 0.05$;

$\theta_i = (i-1)\frac{2\pi}{n}$;

for n from 4 by 4 to 200 do

$t_1 = \frac{n}{4}$;

$s_n = \frac{1-\sqrt{1-\frac{2-2\cos\frac{2\pi}{n}}{\sin^2\frac{2\pi}{n}}(2\sqrt{n-1}\kappa-(n-1)\kappa^2)}}{\frac{2-2\cos\frac{2\pi}{n}}{\sin^2\frac{2\pi}{n}}}$;

$U_{nr} = \sum_{i=1}^{n}\sqrt{((1+\kappa)\cos\theta_i - s_n)^2 + ((1+\kappa)\sin\theta_i - s_n)^2}$;

$U_{n\kappa c} = \kappa + 2\kappa\sum_{i=2}^{t_1+1}\cos\left((i-1)\frac{2\pi}{n}\right)$;

Call LCTHETA$(s_n, n, L_{nc\theta'})$;

$x_n^{1*} = \frac{1}{n^2}(nU_{n\kappa c} - U_{nr}L_{nc\theta'})$;

test $= \frac{s_n - x_n^{1*}}{\kappa}100$;

$j = 1$;

while test > 0.0001 do

$s_n = x_n^{j*}$;

$j = j + 1$;

$U_{nr} = \sum_{i=1}^{n} \sqrt{((1+\kappa)\cos\theta_i - s_n)^2 + ((1+\kappa)\sin\theta_i - s_n)^2}$;

Call LCTHETA$(s_n, n, L_{nc\theta'})$;

$x_n^{j*} = \frac{1}{n^2}(nU_{n\kappa c} - U_{nr}L_{nc\theta'})$;

test $= \frac{s_n - x_n^{j*}}{\kappa} 100$;

enddo;

$x_n^* = x_n^{j*}$;

print x_n^*;

enddo;

Numerically we can show that x_n^* of G_n^* can be expressed as $x_n^* = a(n)\kappa$ where $a(n)$ is a function of n and $a(n) < 1$ (see Appendix O). We also can show that $\frac{\partial^2 h_n(x,y,\epsilon_1,\epsilon_2,\ldots,\epsilon_n)}{\partial y^2} < 0$ for $a(n)\kappa \leq x \leq s_n$, $-x \leq y \leq x$, and $\epsilon_i \ \forall \ i$, numerically by simulated annealing (see Appendix P). This ensures us to use subroutine LCTHETA$(s_n, n, L_{nc\theta'})$ in the iterative algorithm validly when we use the value $x_n^{(i-1)*}$ as the input to s_n to find the value $L_{nc\theta'}$, which, in turn, is used to find x_n^{i*}.

Note that the program stops when the difference between $x_n^{(i-1)*}$ and x_n^{i*} is less than 0.000001κ. By (4.43) we have shown that G_n^1 is a square. Applying the same manner to search G_n^i, we obtain that G_n^i is a square as well. Therefore we obtain that G_n^* is a square and $|x| < a(n)\kappa$ and $|y| < a(n)\kappa$ for $(x,y) \in G_n^*$, $4 \leq n \leq 200$ and n is a multiple of 4. Recall that in section 4.1, the G_n is such that $|x| \leq s_n$ and $|y| \leq s_n$. It is clear that $a(n)\kappa < s_n$ (see Appendix O). Thus, we know that G_n^* is closer to $(0,0)$ than G_n is. Recall that A^* is the square region centered at $O(0,0)$

with width of 2κ. From Appendix O we obtain that $G_n^* \subset A^*$. Thus we can use Taylor's theorem to approximate $f(x, y)$ where $(x, y) \in G_n^*$.

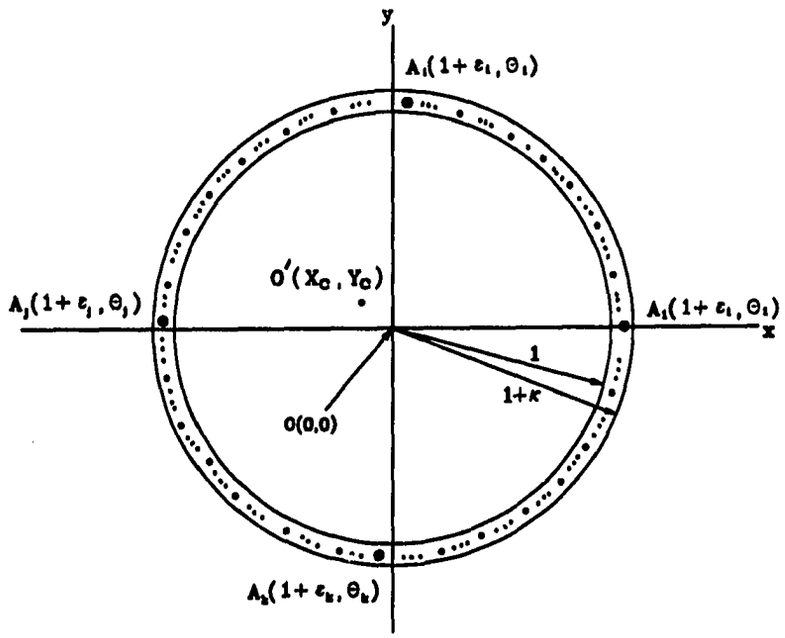

Figure 4.1: A Possible Arrangement of n Data Points and the Center $O'(x_c, y_c)$.

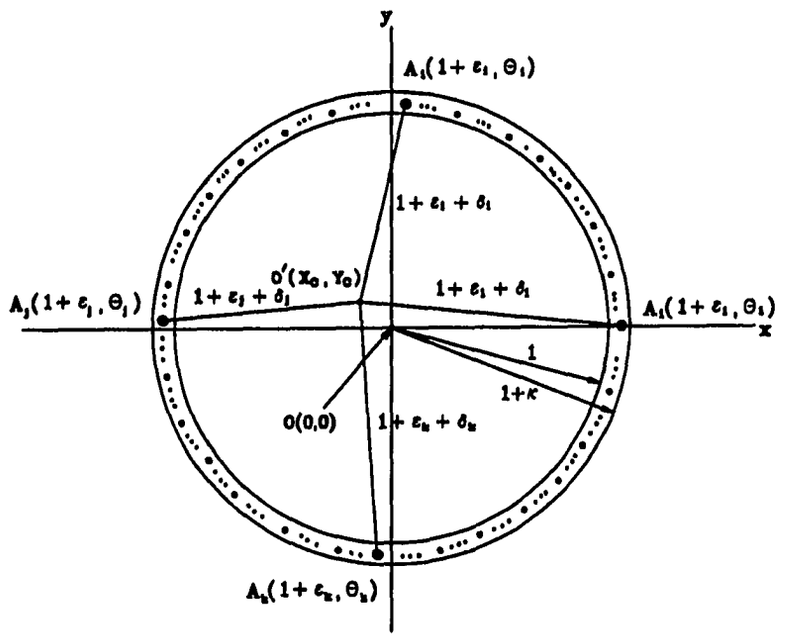

Figure 4.2: A Relationship Between $\overline{O'A_i}$ and $1+\epsilon_i+\delta_i$.

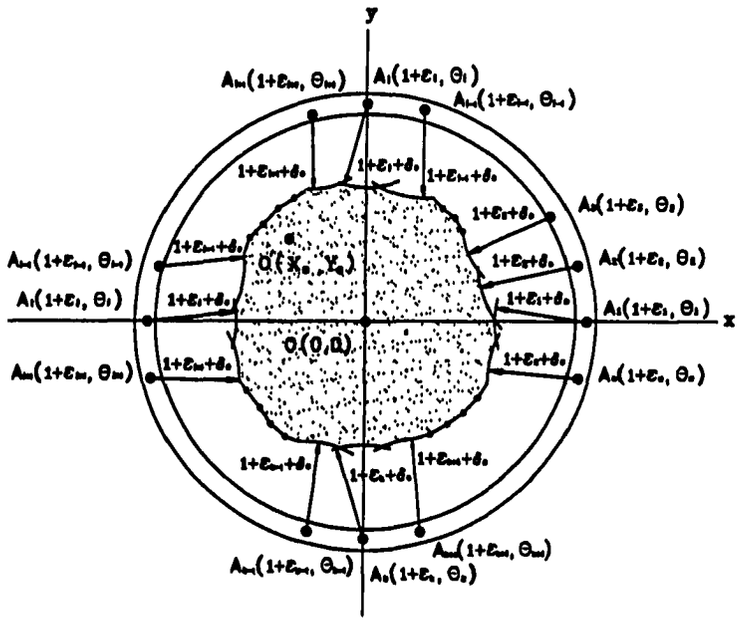

Figure 4.3: The G'_n.

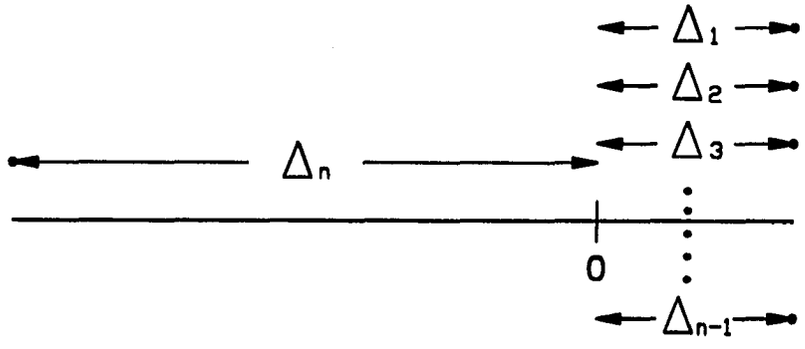

Figure 4.4: A Configuration for Searching δ_*.

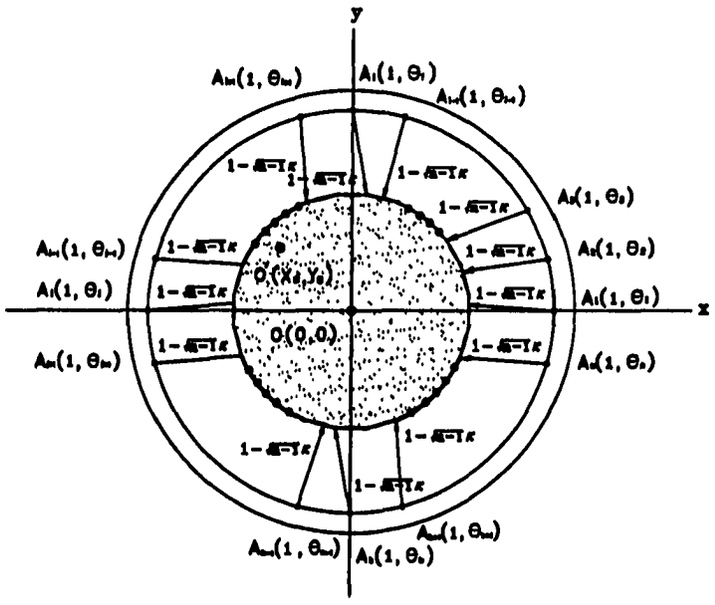

Figure 4.5: The Largest G_n'.

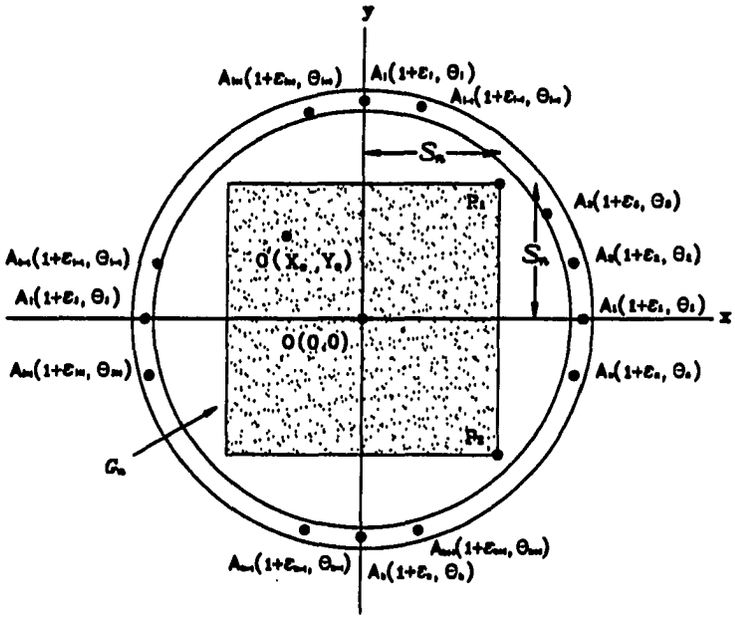

Figure 4.6: The G_n.

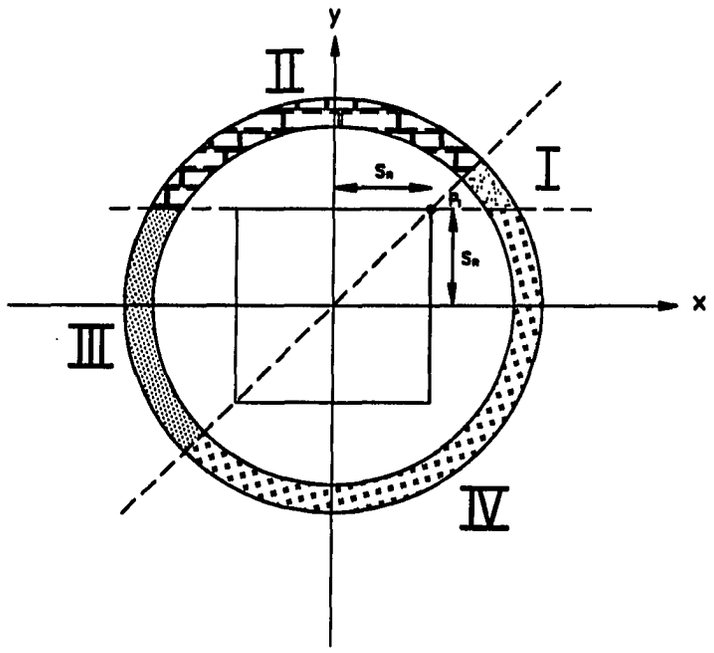

Figure 4.7: Four Divisions of Annulus.

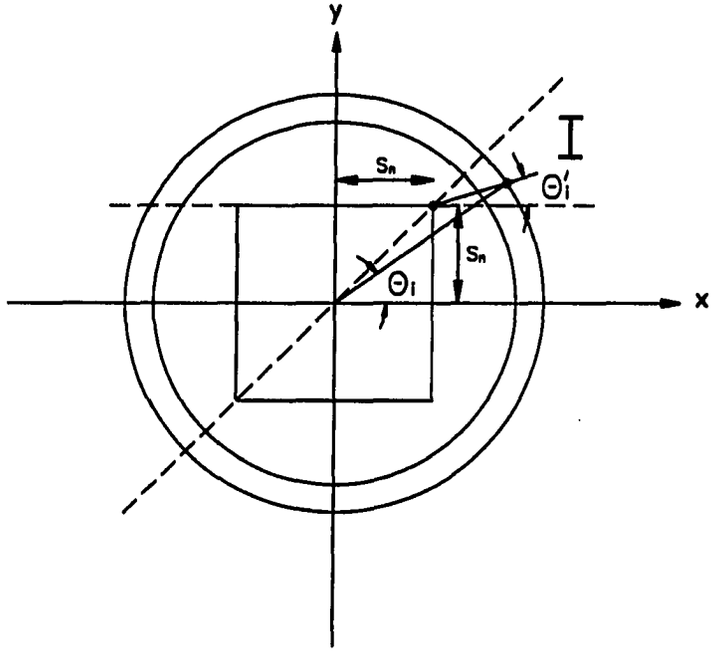

Figure 4.8: Illustration of ϵ_i in Region I Which Minimizes $\cos\theta_i'$.

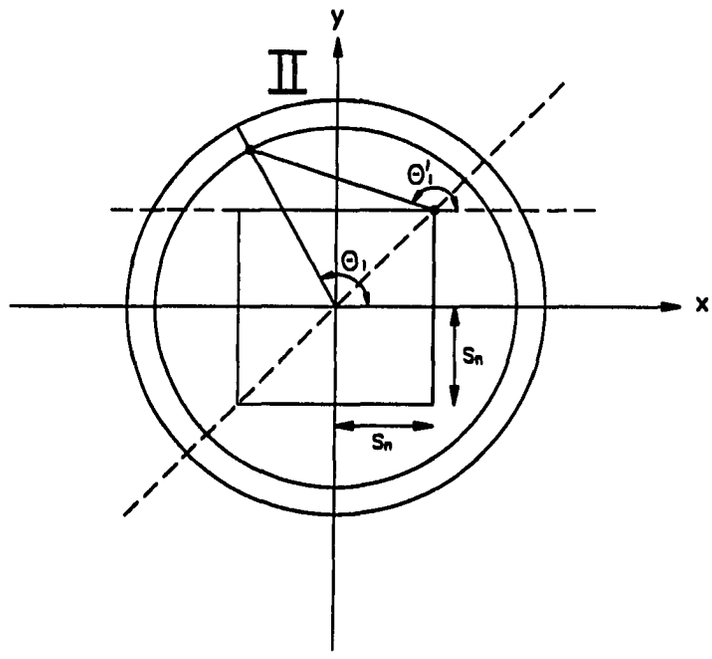

Figure 4.9: Example of ϵ_i in Region II Which Minimizes $\cos\theta_i'$.

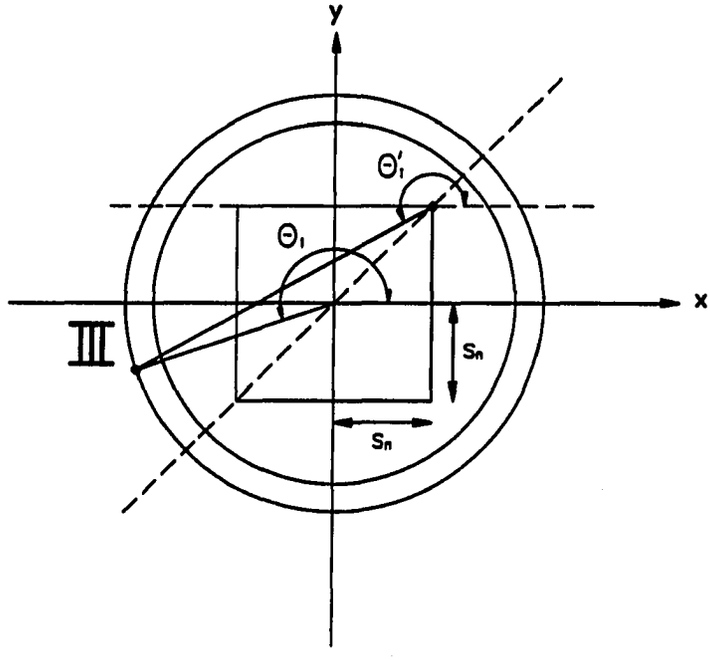

Figure 4.10: Picture of ϵ_i in Region III Which Minimizes $\cos\theta_i'$.

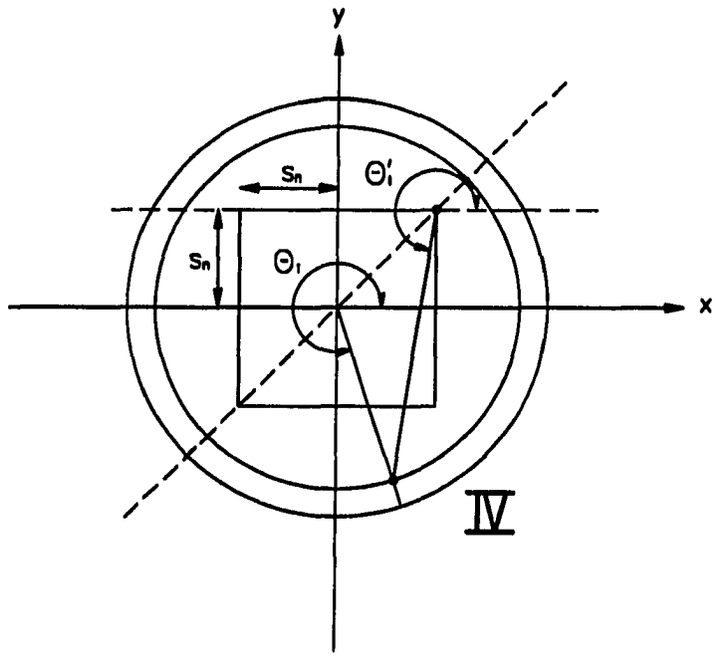

Figure 4.11: Diagram of ϵ_i in Region IV Which Minimizes $\cos\theta_i'$.

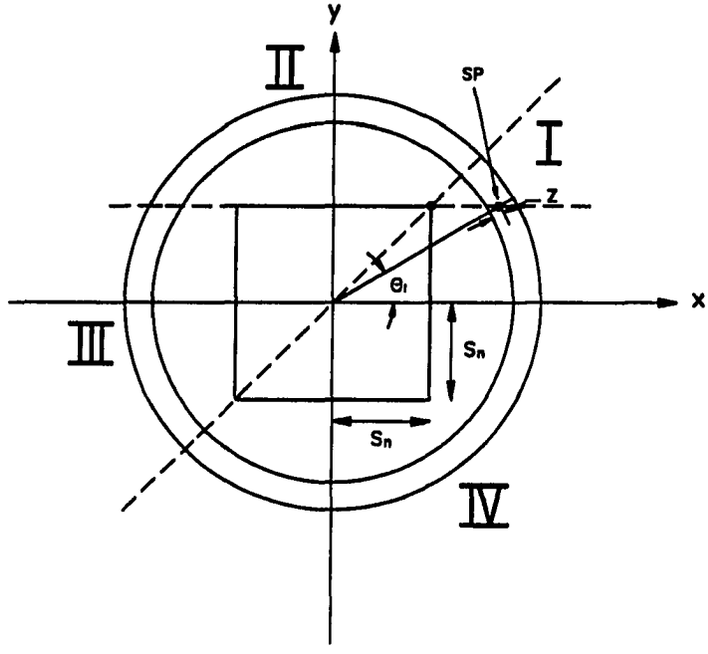

Figure 4.12: Instance of ϵ_i When (x_i, y_i) is Between Regions I & IV.

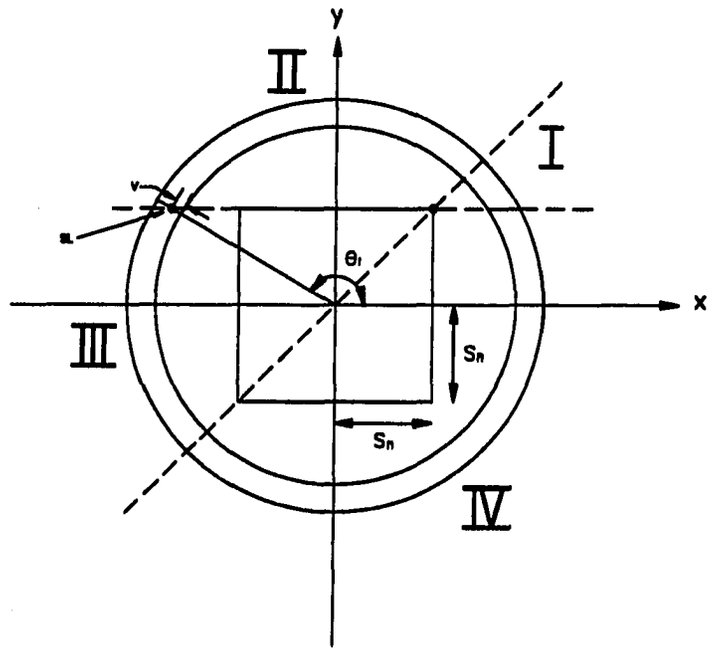

Figure 4.13: Drawing of ϵ_i When (x_i, y_i) is Between Regions II & III.

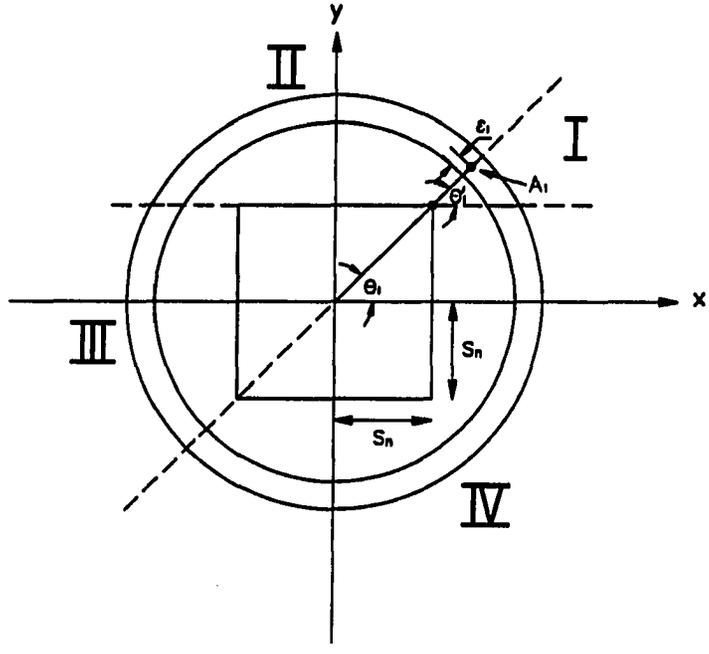

Figure 4.14: Sketch of ϵ_i When (x_i, y_i) is Between Regions I & II.

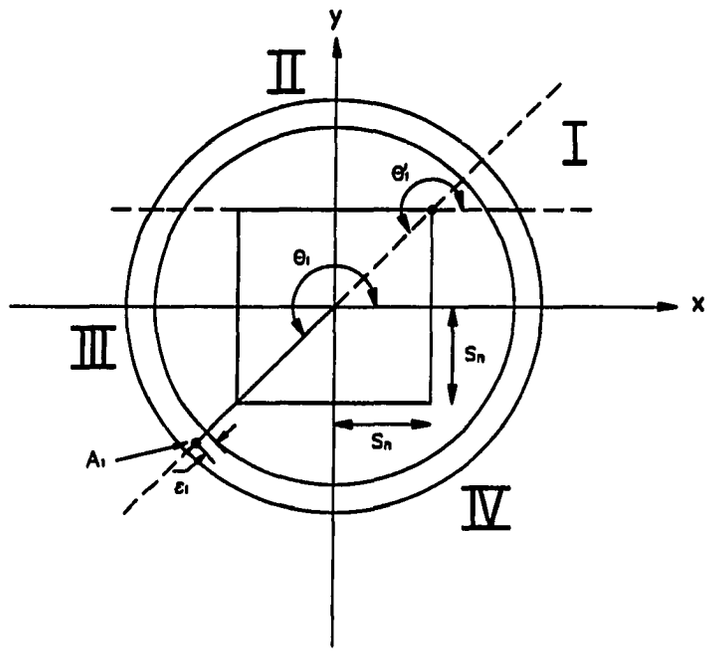

Figure 4.15: Representation of ϵ_i When (x_i, y_i) is Between Regions III & IV.

CHAPTER 5. GLOBAL MINIMUM OF $f(x,y)$

The theme of this chapter is to show that there exists a unique circle within $Int(D)$ to satisfy (3.1) when $4 \leq n \leq 200$ and n is a multiple of 4. This can be done by showing that there exists a unique center (x_c, y_c) which is both the only local minimum and the only global minimum of $f(x,y)$.

This chapter is divided into three parts. First, we will derive an approximation of $f(x,y)$ by $\hat{f}(x,y)$ by Taylor's theorem when $(x,y) \in G_n^*$ and show that there is only one point, say $(\hat{x}_c, \hat{y}_c)$, which satisfies the FONCs of $\hat{f}(x,y)$. Second, we will show that $\hat{f}(x,y)$ is a strictly convex function in G_n^*. Third, we will show that $(\hat{x}_c, \hat{y}_c)$ is both the only local minimum and the only global minimum of $f(x,y)$ for (x,y) $\in Int(D)$. Note that $(\hat{x}_c, \hat{y}_c)$ is an approximation of the unique center (x_c, y_c). The details are as follows.

5.1 Taylor Approximation of $f(x,y)$

In section 4.2.4 we have shown that for $4 \leq n \leq 200$ and n is a multiple of 4, the final refined region of $O'(x_c, y_c)$ should be confined in a region (x,y), i.e. G_n^*, such that $|x| < 0.05$ and $|y| < 0.05$. It is clear that $G_n^* \subset A^*$. Therefore we can approximate the function $f(x,y)$ fairly with a linear polynomial, $\hat{f}(x,y)$, by the Taylor's theorem. Indeed, we can generalize the approximation of $f(x,y)$ as follows.

For the n data points case, if $O'(x_c, y_c)$ is within A^*, then we can use Taylor theorem to approximate $\overline{O'A_i}$ by $\overline{Q_iA_i}$. Here $\overline{Q_iA_i}$ is the projection of $\overline{O'A_i}$ over line $\overleftrightarrow{OA_i}$ (see Figure 5.1). As a result, we can show that the general formula of $\hat{f}(x, y)$ is given by (see Appendix Q):

$$\hat{f}(x,y) = \sum_{i=1}^{n}\left(\epsilon_i - x\cos\theta_i - y\sin\theta_i - \frac{1}{n}\sum_{j=1}^{n}\epsilon_j\right)^2 \tag{5.1}$$

where $\theta_i = (i-1)\frac{2\pi}{n}\ \forall\ i$.

5.1.1 Point which satisfies FONCs

Taking the first partial derivatives of $\hat{f}(x, y)$ in (5.1) with respect to x and y, we obtain

$$\frac{\partial\hat{f}(x,y)}{\partial x} = 2\sum_{i=1}^{n}(\epsilon_i - x\cos\theta_i - y\sin\theta_i - \frac{1}{n}\sum_{j=1}^{n}\epsilon_j)(-\cos\theta_i) \tag{5.2}$$

and

$$\frac{\partial\hat{f}(x,y)}{\partial y} = 2\sum_{i=1}^{n}(\epsilon_i - x\cos\theta_i - y\sin\theta_i - \frac{1}{n}\sum_{j=1}^{n}\epsilon_j)(-\sin\theta_i). \tag{5.3}$$

Solving for $(\hat{x}_c, \hat{y}_c)$ at $\frac{\partial\hat{f}(x,y)}{\partial x} = 0$ and $\frac{\partial\hat{f}(x,y)}{\partial y} = 0$, we get

$$\hat{x}_c = \frac{\sum_{i=1}^{n}\epsilon_i\cos\theta_i\sum_{i=1}^{n}\sin^2\theta_i - \sum_{i=1}^{n}\epsilon_i\sin\theta_i\sum_{i=1}^{n}\sin\theta_i\cos\theta_i}{\sum_{i=1}^{n}\cos^2\theta_i\sum_{i=1}^{n}\sin^2\theta_i - (\sum_{i=1}^{n}\sin\theta_i\cos\theta_i)^2} \tag{5.4}$$

and

$$\hat{y}_c = \frac{\sum_{i=1}^{n}\epsilon_i\sin\theta_i\sum_{i=1}^{n}\cos^2\theta_i - \sum_{i=1}^{n}\epsilon_i\cos\theta_i\sum_{i=1}^{n}\sin\theta_i\cos\theta_i}{\sum_{i=1}^{n}\cos^2\theta_i\sum_{i=1}^{n}\sin^2\theta_i - (\sum_{i=1}^{n}\sin\theta_i\cos\theta_i)^2}. \tag{5.5}$$

Applying the proof of Lemma 3 in Appendix A, we can show that when $n \geq 4$

$$\sum_{i=1}^{n}\cos\left((i-1)\frac{4\pi}{n}\right) = 0, \text{ and} \tag{5.6}$$

$$\sum_{i=1}^{n}\sin\left((i-1)\frac{4\pi}{n}\right) = 0. \tag{5.7}$$

Thus it is clear that

$$\begin{aligned}
\sum_{i=1}^{n} \cos^2\theta_i &= \sum_{i=1}^{n} \left(\frac{1}{2}(1+\cos 2\theta_i)\right) \\
&= \frac{n}{2} + \frac{1}{2}\sum_{i=1}^{n} \cos 2\theta_i \\
&= \frac{n}{2} + \frac{1}{2}\sum_{i=1}^{n} \cos\left((i-1)\frac{4\pi}{n}\right) \\
&= \frac{n}{2}, \qquad (\because (5.6)) \qquad (5.8) \\
\sum_{i=1}^{n} \sin^2\theta_i &= \sum_{i=1}^{n} (1-\cos^2\theta_i) \\
&= n - \sum_{i=1}^{n} \cos^2\theta_i \\
&= n - \frac{n}{2} \\
&= \frac{n}{2}, \text{ and} \qquad (5.9) \\
\sum_{i=1}^{n} \sin\theta_i \cos\theta_i &= \frac{1}{2}\sum_{i=1}^{n} \sin(2\theta_i) \\
&= \frac{1}{2}\sum_{i=1}^{n} \sin\left((i-1)\frac{4\pi}{n}\right) \\
&= 0. \qquad (\because (5.7)) \qquad (5.10)
\end{aligned}$$

Substituting (5.8), (5.9), and (5.10) into (5.4) and (5.5), we acquire

$$\hat{x}_c = \frac{2}{n}\sum_{i=1}^{n} \epsilon_i \cos\theta_i \qquad (5.11)$$

and

$$\hat{y}_c = \frac{2}{n}\sum_{i=1}^{n} \epsilon_i \sin\theta_i. \qquad (5.12)$$

5.1.2 Accuracy of Approximation

The accuracy of our approximation of $f(x,y)$ by $\hat{f}(x,y)$ can be measured by the accuracy of the approximation of $\overline{O'A_i}$ by $\overline{Q_iA_i}$ $\forall\, i$. An error function $E_i(\kappa)$ $\forall\, i$ gives

the accuracy relative to the length of $\overline{O'A_i}$ and is specified by

$$\begin{aligned} E_i(\kappa) &= \frac{\overline{O'A_i} - \overline{Q_iA_i}}{\overline{O'A_i}} \\ &= 1 - \cos\alpha_i. \end{aligned} \tag{5.13}$$

Here α_i is the angle formed by lines $\overline{O'A_i}$ and $\overline{OA_i}$ (see Figure 5.1). Thus the smaller the $\cos\alpha_i$ is, the bigger the error $E_i(\kappa)$ will be. We can show that the global minimum of $\cos\alpha_i \ \forall\ 0 \le \epsilon_i \le \kappa$, $(x_c, y_c) \in A^*$ and $0 \le \theta_i \le 2\pi$ occurs when (see Appendix R)

$$\begin{aligned} \epsilon_i &= 0, \\ \cos\theta_i &= \frac{-2\kappa + \sqrt{2 - 4\kappa^2}}{2}, \\ \sin\theta_i &= \frac{2\kappa + \sqrt{2 - 4\kappa^2}}{2}, \text{ and} \\ (x_c, y_c) &= (-\kappa, \kappa). \end{aligned}$$

This is illustrated in the triangle of Figure 5.2, from which we obtain the minimum value of $\cos\alpha_i$, $\cos\alpha^*$, as

$$\begin{aligned} \cos\alpha^* &= \frac{1 + \overline{O'A_i}^2 - 2\kappa^2}{2\overline{O'A_i}} \\ &= \frac{1 + \kappa\cos\theta_i - \kappa\sin\theta_i}{\sqrt{(\cos\theta_i + \kappa)^2 + (\sin\theta_i - \kappa)^2}} \\ &= \sqrt{1 - 2\kappa^2}. \end{aligned}$$

Since $\{\theta_i : \theta_i = (i-1)\frac{2\pi}{n},\ \forall\ i\}$ is a subset of $\{\theta_i : 0 \le \theta_i \le 2\pi\}$, thus we know that

$$\cos\alpha_i \ \ge\ \cos\alpha^* \ \forall\ i.$$

Thus an upper bound of $E_i(\kappa)\ \forall\ i$, $E(\kappa)^*$ would be

$$E(\kappa)^* = 1 - \sqrt{1 - 2\kappa^2}. \tag{5.14}$$

As we would expect, (5.14) demonstrates that $E(\kappa)^*$ is proportional to κ.

5.2 $\hat{f}(x,y)$ is a Strictly Convex Function in G_n^*

Before doing the proof, we need the following lemma, definitions and theorems.

Lemma 1 of chapter 2 in Searle [19]: The symmetric matrix **A** is positive definite if and only if all its principal leading minors have positive determinants.

Definition 3.3.5 in Bazaraa [11]: Let S be a nonempty set in E_n, and let $f : S \to E_1$. Then f is said to be *twice differentiable* at $\overline{\mathbf{x}} \in \text{int } S$ if there exist a vector $\nabla f(\overline{\mathbf{x}})$, and nxn symmetric matrix $\mathbf{H}(\overline{\mathbf{x}})$, called the *Hessian* matrix, and a function $\alpha : E_n \to E_1$ such that

$$\begin{aligned} f(\mathbf{x}) &= f(\overline{\mathbf{x}}) + \nabla f(\overline{\mathbf{x}})^t(\mathbf{x}-\overline{\mathbf{x}}) + \frac{1}{2}(\mathbf{x}-\overline{\mathbf{x}})^t\mathbf{H}(\overline{\mathbf{x}})(\mathbf{x}-\overline{\mathbf{x}}) + \\ &\quad \|\mathbf{x}-\overline{\mathbf{x}}\|^2\alpha(\overline{\mathbf{x}};\mathbf{x}-\overline{\mathbf{x}}) \end{aligned}$$

for each $\mathbf{x} \in S$, where $\lim_{\mathbf{x}\to\overline{\mathbf{x}}} \alpha(\overline{\mathbf{x}};\mathbf{x}-\overline{\mathbf{x}}) = 0$. The function f is said to be twice differentiable on the open set $S' \subset S$ if it is twice differentiable at each point in S'.

Theorem 14 of chapter 10 in DePree [35]: (Taylor's Theorem for $N = 2$). Suppose D is an open convex subset of R^n, $f : D \to R$, and $\mathbf{x}_0, \mathbf{x}_0 + \mathbf{h} \in D$. If f has continuous third order partial derivatives in D,

$$\begin{aligned} f(\mathbf{x}_0+\mathbf{h}) &= f(\mathbf{x}_0) + \nabla f(\mathbf{x}_0)\cdot\mathbf{h} + \frac{1}{2}\sum_{j=1}^{n}\sum_{i=1}^{n} D_{ij}f(\mathbf{x}_0)h_ih_j + \\ &\quad \frac{1}{3!}\sum_{k=1}^{n}\sum_{j=1}^{n}\sum_{i=1}^{n} D_{ijk}f(\zeta)h_ih_jh_k, \text{ where } \zeta \in [\mathbf{x}_0, \mathbf{x}_0+\mathbf{h}]. \quad (5.15) \end{aligned}$$

Let

$$R_2(\mathbf{x}_0,\mathbf{h}) = \frac{1}{3!}\sum_{k=1}^{n}\sum_{j=1}^{n}\sum_{i=1}^{n} D_{ijk}f(\zeta)h_ih_jh_k. \quad (5.16)$$

Note that the continuity of the partial derivatives of f implies $|R_2(\mathbf{x}_0,\mathbf{h})| \leq M_2\|\mathbf{h}\|^3$, where M_2 is independent of $\mathbf{h}$; consequently,

$$\lim_{\|\mathbf{h}\|\to 0} R_2(\mathbf{x}_0,\mathbf{h})/\|\mathbf{h}\|^2 = 0. \quad (5.17)$$

Definition 15 of chapter 10 in DePree [35]: If D is an open subset of R^n and $f : D \rightarrow R$ has continuous second order partial derivatives at $\mathbf{x}_0 \in D$, the *Hessian* of f at $\mathbf{x}_0$ is the nxn (symmetric) matrix

$$[D_{ij}f(\mathbf{x}_0)]_{i,j=1,\ldots,n} = \nabla^2 f(\mathbf{x}_0).$$

Using the Hessian, we can write the formula in (5.15) as

$$f(\mathbf{x}_0 + \mathbf{h}) = f(\mathbf{x}_0) + \nabla f(\mathbf{x}_0) \cdot \mathbf{h} + \frac{1}{2}(\nabla^2 f(\mathbf{x}_0)\mathbf{h}^t)^t \cdot \mathbf{h} + R_2(\mathbf{x}_0, \mathbf{h}).$$

In these expressions, $\mathbf{h}^t$ is the transpose of the row matrix $\mathbf{h}$.

Theorem 3.3.8 in Bazaraa [11]: Let S be a nonempty open convex set in E_n, and let $f : S \rightarrow E_1$ be twice differentiable on S. If the Hessian matrix is positive definite at each point in S, then f is strictly convex.

Proof:

1. Using (5.2) and (5.3), we take the second partial derivatives of $\hat{f}(x, y)$ with respect to x and y, obtaining

$$\frac{\partial^2 \hat{f}(x,y)}{\partial x^2} = 2\sum_{i=1}^{n} \cos^2 \theta_i = n, \tag{5.18}$$

$$\frac{\partial^2 \hat{f}(x,y)}{\partial x \partial y} = 2\sum_{i=1}^{n} \cos \theta_i \sin \theta_i = 0, \quad \text{and} \tag{5.19}$$

$$\frac{\partial^2 \hat{f}(x,y)}{\partial y^2} = 2\sum_{i=1}^{n} \sin^2 \theta_i = n. \tag{5.20}$$

We construct the Hessian matrix of $\hat{f}(x, y)$ as follows:

$$\hat{\mathbf{H}} = \begin{bmatrix} \frac{\partial^2 \hat{f}(x,y)}{\partial x^2} & \frac{\partial^2 \hat{f}(x,y)}{\partial x \partial y} \\ \frac{\partial^2 \hat{f}(x,y)}{\partial x \partial y} & \frac{\partial^2 \hat{f}(x,y)}{\partial y^2} \end{bmatrix} = \begin{bmatrix} n & 0 \\ 0 & n \end{bmatrix}.$$

The determinants of the principal leading minors of $\hat{\mathbf{H}}$ are $\det(\hat{\mathbf{H}}[1,1])$ and $\det(\hat{\mathbf{H}})$. Seeing that $\det(\hat{\mathbf{H}}[1,1]) = n$ and $\det(\hat{\mathbf{H}}) = n^2$ with $n > 0$, by lemma 1 of chapter 2 in Searle [19], we know that Hessian matrix $\hat{\mathbf{H}}$ is positive definite.

2. Taking the third partial derivatives of $\hat{f}(x,y)$ with respect to x and y, we have

$$\frac{\partial^3 \hat{f}(x,y)}{\partial x^3} = 0, \tag{5.21}$$

$$\frac{\partial^3 \hat{f}(x,y)}{\partial x^2 \partial y} = 0, \tag{5.22}$$

$$\frac{\partial^3 \hat{f}(x,y)}{\partial x \partial y^2} = 0, \quad \text{and} \tag{5.23}$$

$$\frac{\partial^3 \hat{f}(x,y)}{\partial y^3} = 0. \tag{5.24}$$

By (5.21), (5.22), (5.23) and (5.24) we know that the third partial derivatives of $\hat{f}(x,y)$ exist and are continuous, thus by definition 3.3.5 in Bazaraa [11], theorem 14 of chapter 10 in DePree [35] and definition 15 of chapter 10 in DePree [35], we obtain that $\hat{f}(x,y)$ is twice differentiable. It is clear that G_n^* is a nonempty open convex set.

3. By proof statements 1 and 2 and theorem 3.3.8 in Bazaraa [11] we conclude that $\hat{f}(x,y)$ is strictly convex when $(x,y) \in G_n^*$.

This concludes the proof.

5.3 $(\hat{x}_c, \hat{y}_c)$ is Both the Only Local Minimum and the Only Global Minimum of $f(x,y)$

In this section we devise two steps to show that $(\hat{x}_c, \hat{y}_c)$ in (5.11) and (5.12) is both the only local minimum and the only global minimum of $f(x,y)$ for $(x,y) \in Int(D)$.

First, we will show that $(\hat{x}_c, \hat{y}_c)$ is both the only local minimum and the only global minimum of $f(x,y)$ in G_n^*. Second, we will show that $(\hat{x}_c, \hat{y}_c)$ is both the only local minimum and the only global minimum of $f(x,y)$ in $Int(D)$. Now we proceed to proof of the first step as follows.

5.3.1 Local Minimum and Global Minimum in G_n^*

First, we will show that $(\hat{x}_c, \hat{y}_c)$ is the only local minimum of $f(x,y)$. Before doing the proof, we need the following theorems.

Theorem 4.1.4 in Bazaraa [11]: Suppose that $f : E_n \rightarrow E_1$ is twice differentiable at $\overline{\mathbf{x}}$. If all the first partial derivatives of f are zero at $\overline{\mathbf{x}}$ and the Hessian matrix value at $\overline{\mathbf{x}}$ is positive definite, then $\overline{\mathbf{x}}$ is a local minimum.

Theorem 15.40 in Faires [25]: If a function f has a local minimum at (x_0, y_0), then (x_0, y_0) is a critical point of f. Here the critical point is a point in E_2 such that either its first partial derivatives of f are zero, or at least one of the first partial derivatives fail to exist.

Proof A:

1. Given that $\hat{f}(x,y)$ is a good approximation of $f(x,y)$ and $\hat{f}(x,y)$ is differentiable as we have shown, by theorem 15.40 in Faires [25] we know that if there is a local minimum of $\hat{f}(x,y)$ in G_n^*, then the local minimum can only occur at critical point where its first partial derivatives of $\hat{f}(x,y)$ are zero (i.e., critical point which satisfies FONCs).

2. Given $(\hat{x}_c, \hat{y}_c)$ which satisfies the FONCs of $\hat{f}(x,y)$ as we have shown, we know that if there is a local minimum of $\hat{f}(x,y)$ in G_n^*, then the local minimum can only occur at $(\hat{x}_c, \hat{y}_c)$.

3. Given that $\hat{f}(x,y)$ is twice differentiable and the Hessian matrix value of $\hat{f}(x,y)$ at $(\hat{x}_c, \hat{y}_c)$ is positive definite as we have shown, by theorem 4.1.4 in Bazaraa [11] we conclude that $(\hat{x}_c, \hat{y}_c)$ is the only local minimum of $\hat{f}(x,y)$ in G_n^*, which in turn, is the only local minimum of $f(x,y)$ in G_n^*.

Second, we will show that $(\hat{x}_c, \hat{y}_c)$ is the only global minimum of $f(x,y)$ in G_n^*. Before doing the proof, we need the following theorem.

Theorem 3.4.2 in Bazaraa [11]: Let S be a nonempty convex set in E_n, and $f : S \rightarrow E_1$. Consider the problem to minimize $f(\mathbf{x})$ subject to $\mathbf{x} \in$ S. Suppose that $\overline{\mathbf{x}} \in S$ is a local minimum solution to the problem. If f is strictly convex, then $\overline{\mathbf{x}}$ is the unique global minimum solution.

Proof B:

1. Given that $(\hat{x}_c, \hat{y}_c)$ is the only local minimum of $\hat{f}(x,y)$ in G_n^*, G_n^* is a nonempty convex set in E_2, and $\hat{f}(x,y)$ is strictly convex in G_n^* as we have shown, by theorem 3.4.2 in Bazaraa we conclude that $(\hat{x}_c, \hat{y}_c)$ is the only global minimum of $\hat{f}(x,y)$ in G_n^*, which in turn, is the only global minimum of $f(x,y)$ in G_n^*.

This concludes proof of the first step. Now we proceed to proof of the second step.

5.3.2 Local Minimum and Global Minimum in $Int(D)$

First, we will show that $(\hat{x}_c, \hat{y}_c)$ is the only local minimum of $f(x,y)$ for $(x,y) \in Int(D)$.

Proof A:

1. Given that $f(x,y)$ is continuous and differentiable for $(x,y) \in Int(D)$, no point outside G_n^* satisfies the FONCs of $f(x,y)$ as we have shown, by theorem 15.40 in Faires [25] we know that if there is a local minimum for $(x,y) \in Int(D)$, then the local minimum occurs only at the point in G_n^* which satisfies the FONCs.

2. Since $(\hat{x}_c, \hat{y}_c)$ is the only local minimum of $f(x,y)$ in G_n^*, we conclude that $(\hat{x}_c, \hat{y}_c)$ is the only local minimum of $f(x,y)$ for $(x,y) \in Int(D)$.

Second, we will show that $(\hat{x}_c, \hat{y}_c)$ is the only global minimum of $f(x,y)$ for $(x,y) \in Int(D)$. Before doing the proof, we need the following theorems.

Theorem 15.41 in Faires [25]: If R is a bounded region of the plane and $f : R \rightarrow E_1$ and f has a global minimum at (x_0, y_0) in R, then either (x_0, y_0) is a critical point of f or (x_0, y_0) is on the boundary of R.

Theorem 7.8 in Curtis [20]: (*extreme value theorem*) Let $(a_1, a_2, \ldots, a_n)$ be a vector of $n-$tuple of real numbers. The set of all such vectors will be written as $V_n(R)$. Let S be a nonempty bounded closed set in $V_n(R)$. If f is a continuous real-valued function defined on S, then there exists a point $X_0 \in S$ such that

$$f(X_0) \geq f(X) \ \forall \ X \in S.$$

Similarly there exists a point $X_1 \in S$ such that

$$f(X_1) \leq f(X) \ \forall \ X \in S.$$

We can combine theorem 15.41 in Faires and theorem 7.8 in Curtis to form the following theorem.

Theorem 1 If T is a compact subset of the plane and $f : T \rightarrow E_1$ and f is a continuous function on T, then there exists a global minimum, say (x_0, y_0), in T such that either (x_0, y_0) is a critical point of f or (x_0, y_0) is on the boundary of T.

Proof B:

1. Given that G_n is the largest closed circumscribed square region centered at $O(0,0)$ such that

$$f(x,y) \leq f(0,0), \quad \text{and}$$
$$G_n \subset Int(D),$$

and $\overline{G}_n$ is the complement of G_n, we obtain

$$f(0,0) < f(\overline{G}_n). \tag{5.25}$$

If there is a global minimum, say (x_{n0}, y_{n0}), in G_n, then

$$f(x_{n0}, y_{n0}) \leq f(0,0). \tag{5.26}$$

By (5.25) and (5.26) we find that

$$f(x_{n0}, y_{n0}) < f(\overline{G}_n). \tag{5.27}$$

By (5.27) it is clear that if there is a global minimum of $f(x,y)$, then the global minimum will not be in $\overline{G}_n$ (i.e., the global minimum of $f(x,y)$ will be in G_n).

2. Given that $f(x,y)$ is a continuous function and G_n is a compact subset of the plane, by Theorem 1 we know that there exists a global minimum of $f(x,y)$ and the global minimum occurs in G_n. The global minimum is either a critical point of $f(x,y)$ or is on the boundary of G_n.

3. Let $Bdry(G_n)$ be the boundary of G_n. We can show that given $n \geq 4$ (see Appendix S)

$$f(Bdry(G_n)) > f(0,0).$$

We know that $(\hat{x}_c, \hat{y}_c)$ is the only global minimum of $f(x, y)$ in G_n^*, and

$$G_n^* \subset G_n, \tag{5.28}$$

therefore, the global minimum cannot occur on the boundary of G_n. Thus the global minimum of $f(x, y)$ occurs only at the critical points in the interior of the G_n (i.e., $Int(G_n)$).

4. Given that $f(x, y)$ is differentiable in $Int(G_n)$, no point outside G_n^* satisfies the FONCs as we have shown. We know that the global minimum occurs only at the critical point of $f(x, y)$ in G_n^* which satisfies the FONCs. Since $(\hat{x}_c, \hat{y}_c)$ is the only global minimum of $f(x, y)$ in G_n^*, thus we conclude that $(\hat{x}_c, \hat{y}_c)$ is the only global minimum of $f(x, y)$ for $(x, y) \in Int(D)$.

This concludes proof of the second step.

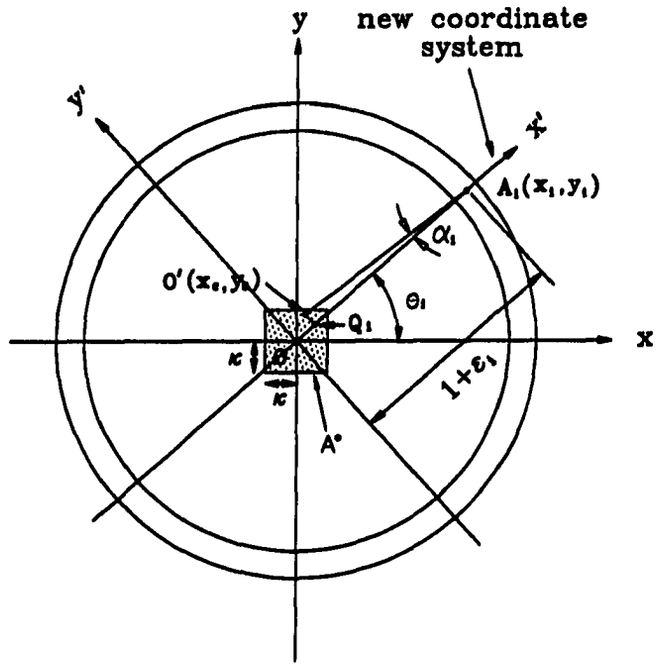

Figure 5.1: An approximation of $\overline{O'A_i}$ by $\overline{Q_iA_i}$.

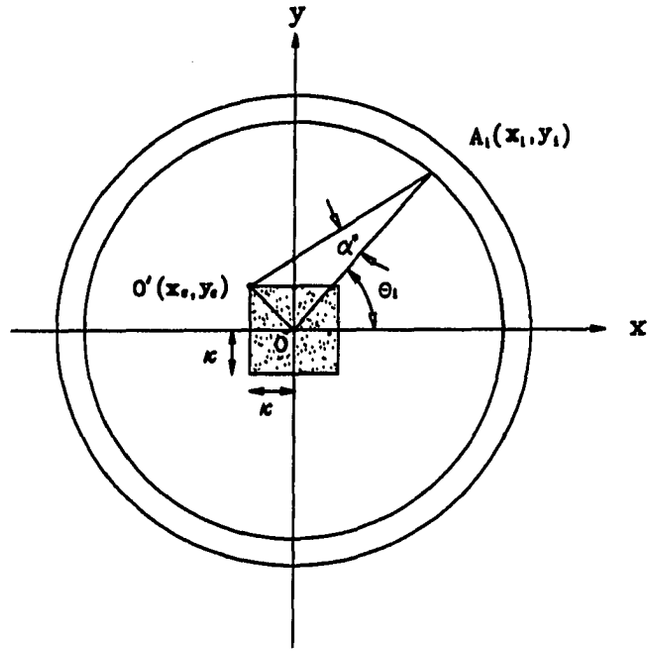

Figure 5.2: The arrangement of $E(\kappa)^*$.

CHAPTER 6. RESTRICTIONS OF THE CRITERIA

Our criteria cover up to 200 data points with n of a multiple of 4. We can show that $s_n > \sqrt{n-1}\kappa$ (see Appendix T). So when $n > 200$ with n of a multiple of 4 (i.e., $n = 204, 208, 212, \ldots, etc.$) and $\kappa = 0.05$, we obtain that

$$\begin{aligned} s_n &> \sqrt{204-1}\kappa \\ &= 0.71239, \end{aligned}$$

which is greater than $\frac{\sqrt{2}}{2} = 0.70711$. As a result, G_n will not be completely in the $Int(D)$ as shown in Figure 6.1. As a result, the function $g_n(x, y, \epsilon_1, \epsilon_2, \ldots, \epsilon_n) = \sum_{i=1}^{n} \sqrt{(x-x_i)^2 + (y-y_i)^2}$ (see Appendix A) is no longer twice differentiable in G_n and therefore we can no longer guarantee that $g_n(x, y, \epsilon_1, \epsilon_2, \ldots, \epsilon_n)$ is strictly convex in G_n. Due derivation of G_n^* becomes invalid for this case. Thus, when $n > 200$ and n is a multiple of 4, it remains to be seen that our criteria can still provide a unique circle for a set of n data points.

The other restriction is that n is a multiple of 4. This restriction is due to the fact that we want to simplify the iterative algorithm to search for the x_n^* of G_n^*. When $n > 4$ and n is not a multiple of 4, it remains to be seen that G_n can be contracted to be within A^*, which in turn, leads to the result of a unique circle.

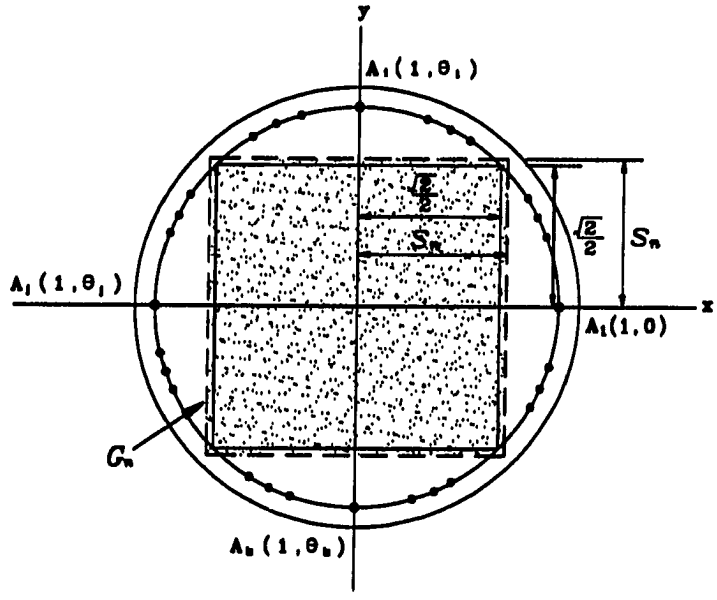

Figure 6.1: The G_n When $n > 200$ and n is a Multiple of 4.

CHAPTER 7. APPLICATION

This methodology is applied to a worn-out bushing to measure its departure from circularity, which indicates the deformation of the bushing. The bushing (which was worn out by the accelerated life testing, i.e., vibrating test) is a prototype of the bushing used in the spring trip standard of John Deere & Company. The spring trip standard is sketched in Figure 7.1. The spring trip standard is mounted on a field cultivator to till the land. When the tip of the spring trip standard dig into the ground, it exerts pressure on the bushing (which connecting standard and bracket) resulting worn out on the bushing. The vibration, which was exerted on the bushing in the vibrating test, was to simulate the effect of the pressure on the bushing of the spring trip standard under plowing. The vibrating test was done at the test laboratory in the John Deere & Company in Ankeny, Iowa. The purpose of study of the bushing is to investigate the relationship between the functionality and the design specification of the bushing.

The worn-out bushing is measured by a Brown & Sharpe CMM [33] [34] in Carver Laboratory of Black Engineering in the Iowa State University. The bushing was mounted on the smaller hole of an aluminum block by a bolt. Then the aluminum block was mounted on the measurement table of CMM by the clamping wedge, bolt and nut. The set up of the measurement is shown in Figure 7.2. The

design specification of the bushing and aluminum block are shown in Figures 7.3 and 7.4. The size of probe of CMM, which we used to take measurement, is of 5.9 mm in diameter.

Using CMM we take the measurement on the outer surface of the worn-out bushing to measure its departure from circularity. Four data points on the outer surface of the worn-out bushing had been preselected to determine the center of the bushing with respect to its outer surface. Then we choose that center as the origin of our new coordinate system. The z coordinate was set zero at the top surface of the aluminum block (see Figure 7.2). Afterwards, We took three levels of measurements and in each level we took 40 equally spacing angle-wise data points with respect to the origin of our new coordinate system. The data is shown in Appendix U. For each level, we project the data points into x, y plane, resulting Figures 7.5, 7.6 and 7.7.

We first want to know that whether this three sets of data (a set in a level) satisfy our criteria of having a unique global minimum of $f(x, y)$. We calculate the distances from $(0, 0)$ to the data points to find out its minimum, say d_{min}, and maximum, say d_{max}. Next, we calculated the converted ratio $\hat{\kappa}$ as follows

$$\hat{\kappa} = \frac{d_{max} - d_{min}}{d_{min}}. \tag{7.1}$$

If $\hat{\kappa} \leq 0.05$, then the data sets satisfy our criteria. The results of d_{min}, d_{max}, and $\hat{\kappa}$ are summarized in Table 7.1 as follows.

All the $\hat{\kappa}$ in each level is less than 0.05. Thus the data points satisfy our criteria. Since we have shown that when the data points satisfy the criteria, there exists only one both local minimum and global minimum point of $f(x, y)$ in $Int(D)$. Thus we can use common optimization software to search for the local minimum of $f(x, y)$. When we find the local minimum, we find its global minimum as well. An optimization

Table 7.1: The Results of d_{min}, d_{max}, and $\hat{\kappa}$.

level	d_{min}	d_{max}	$\hat{\kappa}$
1	.3614130393	.3701276792	.02411268812
2	.3653746431	.3668119394	.00393376039
3	.3631390782	.3721407966	.02478862491

software, MATLAB [10], was used to find the local minima of $f(x, y)$ for the three sets of data points. The results are shown in Table 7.2 as follows.

Table 7.2: The Results of Local Minima of $f(x, y)$ in Each Level.

level	local minimum
1	(-0.000456330499, -0.000719643735)
2	(0.000312615154, 0.000158162625)
3	(0.000231168531, 0.000187560897)

After that, for each level, we calculate the distances from the local minimum (which is also the global minimum) to the data points to find out its minimum, say d'_{min}, and maximum, say d'_{max}. Using the difference between the d'_{min} and the d'_{max}, we obtain a measure of departure from circularity. Let

$$d_{cir} = d'_{max} - d'_{min}. \tag{7.2}$$

The results of d'_{min}, d'_{max} and d_{cir} for each level are shown in Table 7.3 as follows.

Table 7.3: The Results of d'_{min}, d'_{max} and d_{cir}.

level	d'_{min}	d'_{max}	d_{cir}
1	.3618565821	.3704519174	.0085953353
2	.3654141128	.3665951940	.0011810812
3	.3634365693	.3718703352	.0084337659

The results of d_{cir} match our observation on the worn-out bushing, i.e., two ends

of the bushing was worn-out more severely than the middle part of the bushing. This concludes the illustration of our methodology to the worn-out bushing.

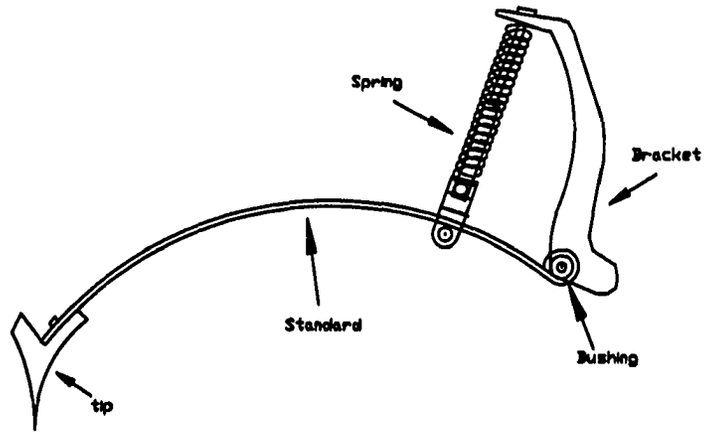

Figure 7.1: The Spring Trip Standard.

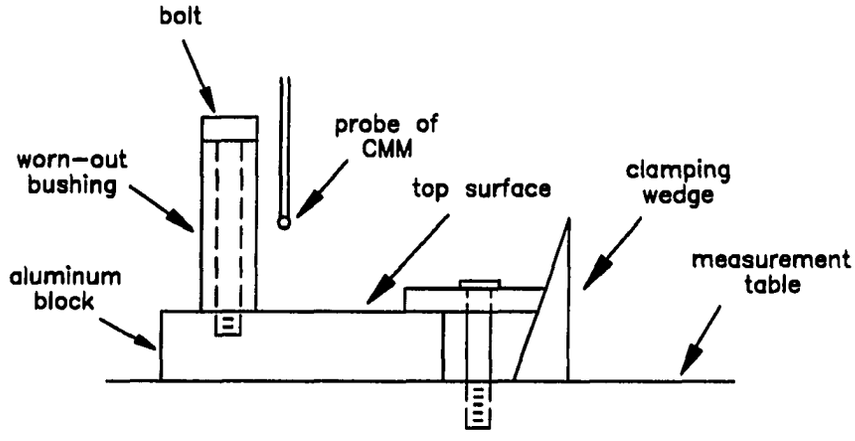

Figure 7.2: The Set Up of the Measurement.

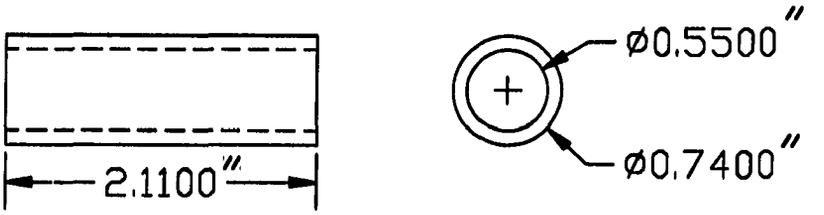

Figure 7.3: The Bushing.

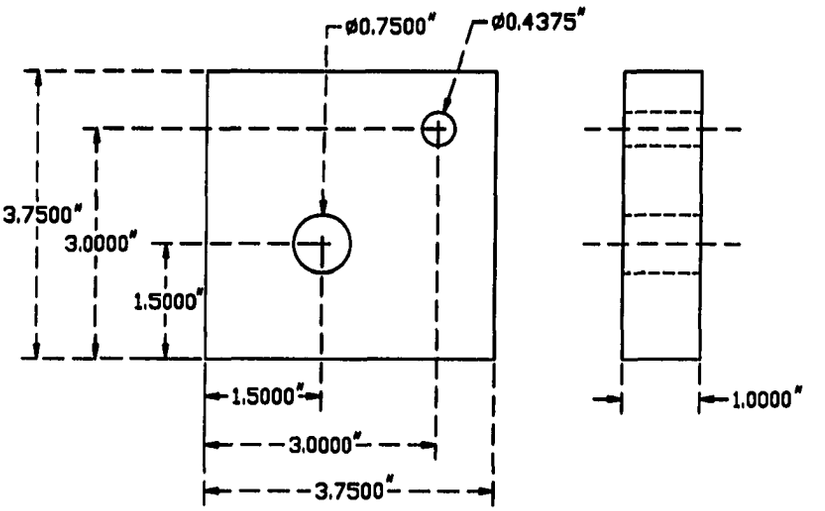

Figure 7.4: The Aluminum Block.

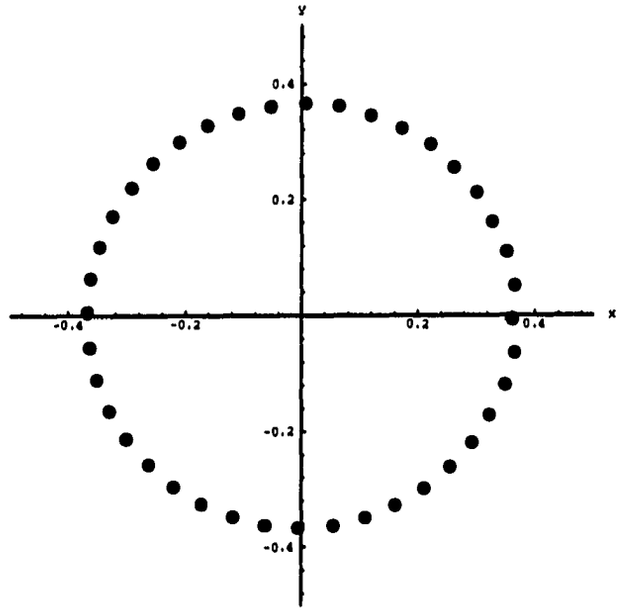

Figure 7.5: The Projection of Data Points in Level 1.

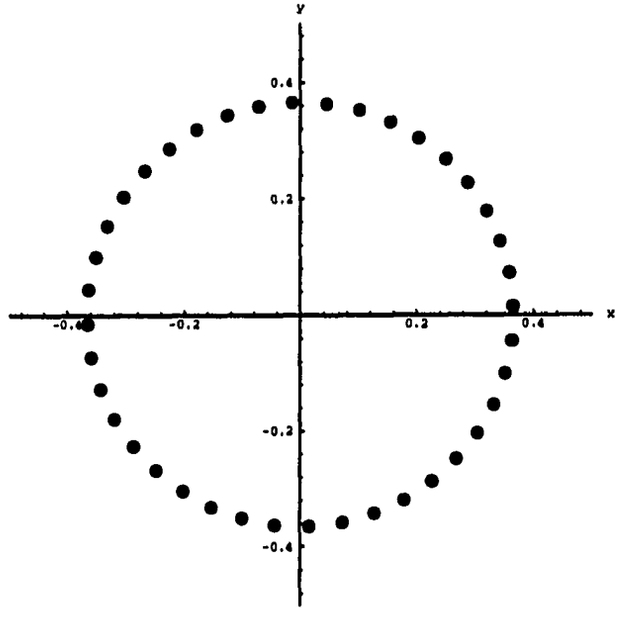

Figure 7.6: The Representation of Data Points in Level 2.

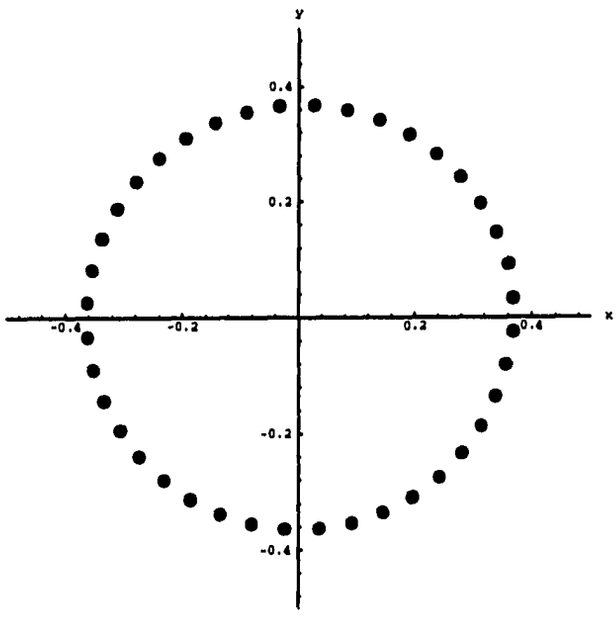

Figure 7.7: The Picture of Data Points in Level 3.

CHAPTER 8. CONCLUSION

In search of a least squares center, we have shown that for $4 \leq n \leq 200$ and n is a multiple of 4, there exists a unique circle which best fits the data points when the data points are scattered around an annulus with equal spacing angle-wise and randomly located radius-wise. The annulus is constructed in such a way that the radius of the inner circle is 1 and the width of annulus, κ, is no greater than 0.05. The inner radius can be regarded as the radius of the hole when the hole is at its MMC. Let us consider three points that make our criterion realistic and practical.

1. By evaluating the diameter before circularity, we can assume that the hole has satisfied the specification of the size tolerance when evaluating the circularity.

2. The ISO standard [17] suggests that κ is almost always less than or equal to 0.05 times the radius at MMC for any design specification.

3. Based on the capabilities of CMMs, the equal spacing angle-wise data points can easily be obtained from the surface of a hole.

Therefore, when evaluating the circularity of cylindrical parts, an annulus larger than κ would indicate that the least squares method is no longer valid. Thus this method provides assurance for engineers in obtaining a unique circle (i.e., a unique center) when they use the ISO least squares method to fit a set of discrete data points as

well as a warning when the criterion is not satisfied. In most cases less than 200 data points are sampled to evaluate the circularity, thus our criterion is very useful in practice.

BIBLIOGRAPHY

[1] *Dimensioning and Tolerancing, ANSI Y14.5M - 1982.* The American Society of Mechanical Engineers, New York, 1982.

[2] *ISO 1101 - 1983. Technical drawings - Geometrical tolerancing - Tolerancing of form, orientation, location and run-out - Generalities, definitions, symbols, indications on drawings.* International Organization for Standardization, Genève, Switzerland.

[3] *ISO 5460 - 1985. Technical Drawings - Geometrical tolerancing - Tolerancing of form, orientation, location and run-out -Verification principles and methods - Guidelines.* International Organization for Standardization, Genève, Switzerland.

[4] *Measurement of Out-Of-Roundness, ANSI B89.3.1 - 1972.* The American Society of Mechanical Engineers, New York, 1972.

[5] A. Thom and A.S. Thom, *A Megalithic Lunar Observatory in Orkney: The Ring of Brogar and its Cairns,* Journal for the History of Astronomy, Volume 4, pp. 111-123, June 1973, Science History Publication Ltd., Cambridge, England.

[6] I. Kasa, *A Circle Fitting Procedure and Its Error Analysis,* IEEE Transactions on Instrumentation and Measurement, pp.8-14, March 1976.

[7] Philip Cox, *Fitting a Circle by Least Squares,* Laboratory Practice, pp. 368-369, May 1962.

[8] John Jackman, Jyh-jeng Deng, Hae-il Ahn, Way Kuo, and Stephen Vardeman, *A Compliance Measure for the Alignment of Cylindrical Part,* to appear in Journal of IIE Transactions.

[9] G. Caskey, Y. Hari, R. Hocken, R. Machireddy, J. Raja, R. Wilson, G. Zhang, K. Chen, and J. Yang *Sampling Techniques for Coordinate Measuring Machines,* Proceedings of the 1992 NSF Design and Manufacturing Systems Conference, pp.983-988.

[10] *MATLAB for Unix Computers, User's Guide* The Math Works, Inc., South Natick, MA, 1990.

[11] Mokhtar S. Bazaraa, and C. M. Shetty, *Nonlinear Programming: Theory and Algorithms,* John Wiley & Sons, Inc., New York, 1979.

[12] Bert Mendelson, *Introduction to Topology,* 3rd ed., Dover Publications, Inc., New York, 1990.

[13] Mark Berman and David Culpin *The Statistical Behavior of Some Least Squares Estimators of the Center and Radius of a Circle,* Journal of the Royal Statistical Society, Series B (methodological), Volume 48, No.2, pp. 183-196, London, England, 1986.

[14] Yu. A. Shreider *What is Distance?,* Translated and Adapted from the Russian by Leslie Cohn and Harvey Edelberg, The University of Chicago Press, Chicago, IL, 1974.

[15] A.H. Money, J.F. Afflect-Graves, M.L. Hart and G.D.I. Barr *The linear regression model: L_p norm estimation and the choice of p,* Communications in Statistics: Simulation and Computation, 11(1), pp. 89-109, 1982.

[16] Lee J. Bain, and Max Engelhardt, *Introduction to Probability and Mathematical Statistics,* Prindle, Weber & Schmidt Publishers, Duxbury Press, Boston, MA, 1987.

[17] *ISO 286-1 - 1988. ISO system of limits and fits - Part 1: Bases of tolerances, deviations and fits.* . International Organization for Standardization, Genève, Switzerland.

[18] David G. Luenberger, *Linear and Nonlinear Programming,* Addison-Wesley Publishing Company, Reading, MA, 2nd ed., 1989.

[19] S. R. Searle, *Linear Model,* John Wiley & Sons, Inc., New York, 1971.

[20] Philip C. Curtis, Jr., *Multivariate Calculus with linear Algebra* John Wiley and Sons, Inc., New York, 1972.

[21] Tom M. Apostol, *Mathematical Analysis,* 2nd ed., Addison-Wesley Publishing Company, Reading, MA, 1974.

[22] Claude J.P. Belisle, H. Edwin Romeijn, and Robert L. Smith, *Hide-and-Seek: A Simulated Annealing Algorithm Global Optimization,* Technical Report No. 90-25, The University of Michigan, Ann Arbor, MI, Sept. 1990.

[23] H. Edwin Romeijn and Robert L. Smith, *Software of Hide-and-Seek: A simulated annealing algorithm for global optimization,* Department of Industrial and Operations Engineering, The University of Michigan, Ann Arbor, MI, April 30, 1990.

[24] Bruce W. Char, Keith O. Geddes, Gaston H. Gonnet, Michael B. Monagan, Stephen M. Watt *Maple: First Leaves, A Tutorial Introduction to Maple* Version 3, Watcom Publications, Waterloo, Ontario Canada, 1990.

[25] J. Douglas Faires and Barbara Trader Faires *Calculus and Analytic Geometry* Prindle, Weber & Schmidt Publishers, Boston, MA, 1983.

[26] Michael Mortenson, *Geometric Modeling,* John Wiley & Sons, Inc., New York, 1985.

[27] Raymond H. Myers and Janet S. Milton, *A first course in the theory of linear statistical models,* PWS-KENT Publishing Company, Boston, MA, 1991.

[28] Leslie Hogben, *Elementary Linear Algebra,* West Publishing Company, St. Paul, MN, 1987.

[29] Shayle R. Searle, *Matrix Algebra Useful for Statistics,* John Wiley & Sons Inc., New York, 1982.

[30] Edward T. Walsh, *A first course in geometry,* Rinehart Press, Corte Madera, CA, 1974.

[31] Louis L. Wilson, and Bill D. New, *Trigonometry,* John Wiley & Sons, Inc., New York, 1972.

[32] Stephen Wolfram, *Mathematica: A system for Doing Mathematics by Computer,* Addision-Wesley Publishing Company, Inc., Redwood City, CA, 1991.

[33] *User's Manual: Xcel Series Machines* , Headquarters: Validator Systems, Brown & Sharpe Mfg. Co., Precision Park, North Kingstown, RI, 1990.

[34] *Software Manual: AVAIL* , Headquarters: Validator Systems, Brown & Sharpe Mfg. Co., Precision Park, North Kingstown, RI, 1990.

[35] John D. Depree, and Charles W. Swartz, *Introduction to Real Analysis,* John Wiley & Sons, Inc., New York, 1988.

[36] Edward C. Wallace, and Stephen F. West, *Roads to Geometry,* Prentice-Hall, Inc., Englewood Cliffs, New Jersey, 1992.

APPENDIX A. $\sum_{i=1}^{n} \delta_i > 0$ IF $(x_c, y_c) \neq (0,0)$

We define a new function $g_n(x, y, \epsilon_1, \epsilon_2, \ldots, \epsilon_n)$ as follows:

$$g_n(x, y, \epsilon_1, \epsilon_2, \ldots, \epsilon_n) = \sum_{i=1}^{n} \sqrt{(x - x_i)^2 + (y - y_i)^2}. \tag{A.1}$$

By (A.1) we know that $g_n(x, y, \epsilon_1, \epsilon_2, \ldots, \epsilon_n)$ is the sum of distances from point (x, y) to point (x_i, y_i) $\forall$ i. We can show that

$$\begin{aligned} \sum_{i=1}^{n} \delta_i &= \sum_{i=1}^{n}(1 + \epsilon_i + \delta_i) - \sum_{i=1}^{n}(1 + \epsilon_i) \\ &= \sum_{i=1}^{n} \overline{O'A_i} - \sum_{i=1}^{n}(1 + \epsilon_i) \qquad (\because \ \overline{O'A_i} = 1 + \epsilon_i + \delta_i) \\ &= g_n(x_c, y_c, \epsilon_1, \epsilon_2, \ldots, \epsilon_n) - g_n(0, 0, \epsilon_1, \epsilon_2, \ldots, \epsilon_n). \end{aligned} \tag{A.2}$$

$(\because \ \sum_{i=1}^{n} \overline{O'A_i} = g_n(x_c, y_c, \epsilon_1, \epsilon_2, \ldots, \epsilon_n)$ and $\sum_{i=1}^{n}(1 + \epsilon_i) = g_n(0, 0, \epsilon_1, \epsilon_2, \ldots, \epsilon_n))$

By (A.2), it is clear that $\sum_{i=1}^{n} \delta_i > 0$ if and only if $g_n(x_c, y_c, \epsilon_1, \epsilon_2, \ldots, \epsilon_n) > g_n(0, 0, \epsilon_1, \epsilon_2, \ldots, \epsilon_n)$. Thus we can show that

If $(x_c, y_c) \neq (0,0)$, then $\sum_{i=1}^{n} \delta_i > 0$.

$\Longleftrightarrow$ If $(x_c, y_c) \neq (0,0)$, then $g_n(x_c, y_c, \epsilon_1, \epsilon_2, \ldots, \epsilon_n) > g_n(0, 0, \epsilon_1, \epsilon_2, \ldots, \epsilon_n)$.

$\Longleftrightarrow$ (0,0) is the only global minimum of $g_n(x, y, \epsilon_1, \epsilon_2, \ldots, \epsilon_n)$ $\forall$ (x, y).

Thus the problem (i.e., if $(x_c, y_c) \neq (0,0)$, then $\sum_{i=1}^{n} \delta_i > 0$) can be rephrased as that $(0,0)$ is the unique global minimum of $g_n(x, y, \epsilon_1, \epsilon_2, \ldots, \epsilon_n)$. We can show that $(0,0)$

is the unique global minimum of $g_n(x, y, \epsilon_1, \epsilon_2, \ldots, \epsilon_n)$ by showing two propositions as follows:

Proposition 3: Function $g_n(x, y, \epsilon_1, \epsilon_2, \ldots, \epsilon_n)$ is strictly convex.

Proposition 4: Function $g_n(x, y, \epsilon_1, \epsilon_2, \ldots, \epsilon_n)$ has the unique global minimum at $(0, 0)$.

The proofs of the two propositions are as follows.

Proposition 3 Function $g_n(x, y, \epsilon_1, \epsilon_2, \ldots, \epsilon_n)$ is strictly convex.

Proof:

1. Taking the first partial derivatives of $g_n(x, y, \epsilon_1, \epsilon_2, \ldots, \epsilon_n)$ with respect to x and y, we obtain

$$\frac{\partial g_n(x, y, \epsilon_1, \epsilon_2, \ldots, \epsilon_n)}{\partial x} = \sum_{i=1}^{n} \frac{x - x_i}{\sqrt{(x - x_i)^2 + (y - y_i)^2}}, \tag{A.3}$$

and

$$\frac{\partial g_n(x, y, \epsilon_1, \epsilon_2, \ldots, \epsilon_n)}{\partial y} = \sum_{i=1}^{n} \frac{y - y_i}{\sqrt{(x - x_i)^2 + (y - y_i)^2}}. \tag{A.4}$$

For the second partial derivatives of $g_n(x, y, \epsilon_1, \epsilon_2, \ldots, \epsilon_n)$, we obtain

$$\frac{\partial^2 g_n(x, y, \epsilon_1, \epsilon_2, \ldots, \epsilon_n)}{\partial x^2} = \sum_{i=1}^{n} \frac{(y - y_i)^2}{((x - x_i)^2 + (y - y_i)^2)^{1.5}}, \tag{A.5}$$

$$\frac{\partial^2 g_n(x, y, \epsilon_1, \epsilon_2, \ldots, \epsilon_n)}{\partial y^2} = \sum_{i=1}^{n} \frac{(x - x_i)^2}{((x - x_i)^2 + (y - y_i)^2)^{1.5}}, \text{ and} \tag{A.6}$$

$$\frac{\partial^2 g_n(x, y, \epsilon_1, \epsilon_2, \ldots, \epsilon_n)}{\partial x \partial y} = -\sum_{i=1}^{n} \frac{(x - x_i)(y - y_i)}{((x - x_i)^2 + (y - y_i)^2)^{1.5}}. \tag{A.7}$$

We then construct a Hessian matrix of $g_n(x, y, \epsilon_1, \epsilon_2, \ldots, \epsilon_n)$ as follows:

$$\mathbf{H} = \begin{bmatrix} \frac{\partial^2 g_n(x,y,\epsilon_1,\epsilon_2,\ldots,\epsilon_n)}{\partial x^2} & \frac{\partial^2 g_n(x,y,\epsilon_1,\epsilon_2,\ldots,\epsilon_n)}{\partial x \partial y} \\ \frac{\partial^2 g_n(x,y,\epsilon_1,\epsilon_2,\ldots,\epsilon_n)}{\partial x \partial y} & \frac{\partial^2 g_n(x,y,\epsilon_1,\epsilon_2,\ldots,\epsilon_n)}{\partial y^2} \end{bmatrix}.$$

The determinants of the principal leading minors of $\mathbf{H}$ are $\det(\mathbf{H}[1,1])$ and $\det(\mathbf{H})$. It is clear that $\det(\mathbf{H}[1,1]) > 0$. By Cauchy's inequality, it is also clear that

$$\begin{aligned} \det(\mathbf{H}) &= \left(\sum_{i=1}^{n} \frac{(y-y_i)^2}{((x-x_i)^2+(y-y_i)^2)^{1.5}}\right)\left(\sum_{i=1}^{n} \frac{(x-x_i)^2}{((x-x_i)^2+(y-y_i)^2)^{1.5}}\right) \\ &\quad - \left(\sum_{i=1}^{n} \frac{(x-x_i)(y-y_i)}{((x-x_i)^2+(y-y_i)^2)^{1.5}}\right)^2 \\ &\geq 0. \end{aligned} \tag{A.8}$$

We can show that when $n \geq 4$, $\det(\mathbf{H}) \neq 0$ (see Lemma 2 in Appendix A.1), thus by (A.8) we obtain that $\det(\mathbf{H}) > 0$. Thus by lemma 1 of chapter 2 in Searle [19] (see section 5.2), we know that Hessian matrix $\mathbf{H}$ is positive definite.

2. Taking the third partial derivatives of $g_n(x, y, \epsilon_1, \epsilon_2, \ldots, \epsilon_n)$, we obtain

$$\frac{\partial^3 g_n(x,y,\epsilon_1,\epsilon_2,\ldots,\epsilon_n)}{\partial x^3} = \sum_{i=1}^{n} \frac{-3(y-y_i)^2(x-x_i)}{((x-x_i)^2+(y-y_i)^2)^{2.5}}, \tag{A.9}$$

$$\frac{\partial^3 g_n(x,y,\epsilon_1,\epsilon_2,\ldots,\epsilon_n)}{\partial x^2 \partial y} = \sum_{i=1}^{n} \frac{2(y-y_i)((x-x_i)^2-2(y-y_i)^2)}{((x-x_i)^2+(y-y_i)^2)^{2.5}}, \tag{A.10}$$

$$\frac{\partial^3 g_n(x,y,\epsilon_1,\epsilon_2,\ldots,\epsilon_n)}{\partial x \partial y^2} = \sum_{i=1}^{n} \frac{2(x-x_i)((y-y_i)^2-2(x-x_i)^2)}{((x-x_i)^2+(y-y_i)^2)^{2.5}}, \tag{A.11}$$

and

$$\frac{\partial^3 g_n(x,y,\epsilon_1,\epsilon_2,\ldots,\epsilon_n)}{\partial y^3} = \sum_{i=1}^{n} \frac{-3(x-x_i)^2(y-y_i)}{((x-x_i)^2+(y-y_i)^2)^{2.5}}. \tag{A.12}$$

By (A.9), (A.10), (A.11) and (A.12) we know that the third partial derivatives of $g_n(x, y, \epsilon_1, \epsilon_2, \ldots, \epsilon_n)$ exist and are continuous, thus by definition 3.3.5 in

Bazaraa [11], theorem 14 of chapter 10 in DePree [35] (see section 5.2) and definition 15 of chapter 10 in DePree [35], we obtain that $g_n(x, y, \epsilon_1, \epsilon_2, \ldots, \epsilon_n)$ is twice differentiable. It is clear that $Int(D)$ is a nonempty open convex set.

3. By proof statements 1 and 2 and theorem 3.3.8 in Bazaraa [11], we conclude that $g_n(x, y, \epsilon_1, \epsilon_2, \ldots, \epsilon_n)$ is strictly convex.

This concludes the proof of Proposition 3.

Proposition 4 Function $g_n(x, y, \epsilon_1, \epsilon_2, \ldots, \epsilon_n)$ has the unique global minimum at $(0, 0)$.

Proof:

1. We can show that if $n \geq 2$, then $\sum_{i=1}^{n} \cos((i-1)\frac{2\pi}{n}) = 0$, and $\sum_{i=1}^{n} \sin((i-1)\frac{2\pi}{n}) = 0$ (see Lemma 3 in Appendix A.1).

2. When $(x, y) = (0, 0)$, by (A.3) we obtain that

$$\begin{aligned}
\frac{\partial g_n(x, y, \epsilon_1, \epsilon_2, \ldots, \epsilon_n)}{\partial x} &= \sum_{i=1}^{n} \frac{x - x_i}{\sqrt{(x - x_i)^2 + (y - y_i)^2}} \\
&= \sum_{i=1}^{n} \frac{-x_i}{\sqrt{x_i^2 + y_i^2}} \qquad (\because \ (x, y) = (0, 0)) \\
&= \sum_{i=1}^{n} -\cos((i-1)\frac{2\pi}{n}) \\
&\qquad (\because \ \frac{x_i}{\sqrt{x_i^2 + y_i^2}} = \cos((i-1)\frac{2\pi}{n})) \\
&= 0. \qquad (\because \text{ proof statement 1})
\end{aligned}$$

Similarly, using (A.4) we obtain that when $(x, y) = (0, 0)$, $\frac{\partial g_n(x, y, \epsilon_1, \epsilon_2, \ldots, \epsilon_n)}{\partial y} = 0$. Therefore, we know that the first partial derivatives of $g_n(x, y, \epsilon_1, \epsilon_2, \ldots, \epsilon_n)$ are zero at $(0, 0)$.

3. Given that $g_n(x, y, \epsilon_1, \epsilon_2, \ldots, \epsilon_n)$ is twice differentiable at $(0,0)$, and the value of Hessian matrix $\mathbf{H}$ at $(0,0)$ is positive definite as we have shown, by theorem 4.1.4 in Bazaraa [11] (see section 5.3.1) we conclude that $(0,0)$ is a local minimum of $g_n(x, y, \epsilon_1, \epsilon_2, \ldots, \epsilon_n)$.

4. Given that $Int(D)$ is a nonempty convex set in E_2, and $g_n(x, y, \epsilon_1, \epsilon_2, \ldots, \epsilon_n)$ is strictly convex, by theorem 3.4.2 in Bazaraa [11] (see section 5.3.1) we conclude that $(0,0)$ is the unique global minimum of $g_n(x, y, \epsilon_1, \epsilon_2, \ldots, \epsilon_n)$.

This concludes the proof of Proposition 4.

A.1

Lemma 2 When $n \geq 4$, $\det(\mathbf{H}) \neq 0$

This proof is shown by contradiction. We first assume that $\det(\mathbf{H}) = 0$, then we show that there is a contradiction in the assumption of $\det(\mathbf{H}) = 0$. Thus we obtain that $\det(\mathbf{H}) \neq 0$. The details are as follows.

Proof:

1. Assuming that $\det(\mathbf{H}) = 0$ (see (A.8)), then by the proof of lemma 8.1 of chapter 2 in Mendelson [12] (see Appendix A.1.1), there exists a $\lambda \in R$, such that

$$\sum_{i=1}^{n} \left[\frac{y - y_i}{((x - x_i)^2 + (y - y_i)^2)^{0.75}} + \lambda \frac{x - x_i}{((x - x_i)^2 + (y - y_i)^2)^{0.75}} \right]^2 = 0.$$

$$\Leftrightarrow \sum_{i=1}^{n} [y - y_i + \lambda(x - x_i)]^2 = 0.$$

$$\Leftrightarrow y - y_i + \lambda(x - x_i) = 0 \quad \forall \quad i. \quad \text{(A.13)}$$

2. When n is a positive even number, say n = 2m, substituting $i = 1, 2$ into (A.13), we obtain

$$y - y_1 + \lambda(x - x_1) = 0, \text{ and} \tag{A.14}$$

$$y - y_2 + \lambda(x - x_2) = 0. \tag{A.15}$$

Where

$$x_1 = 1 + \epsilon_1, \tag{A.16}$$

$$y_1 = 0, \tag{A.17}$$

$$x_2 = (1 + \epsilon_2)\cos(\frac{2\pi}{n}), \text{ and} \tag{A.18}$$

$$y_2 = (1 + \epsilon_2)\sin(\frac{2\pi}{n}). \tag{A.19}$$

Solving λ by (A.14) and (A.15), we have

$$\lambda = -\frac{y_1 - y_2}{x_1 - x_2}$$
$$\neq 0. \quad (\because \; y_1 = 0 \quad \text{and} \quad y_2 \neq 0) \tag{A.20}$$

Similarly, substituting $i = 1, m + 1$ into (A.13) and solving λ, we get

$$\lambda = -\frac{y_1 - y_{m+1}}{x_1 - x_{m+1}}. \tag{A.21}$$

Where

$$y_{m+1} = (1 + \epsilon_{m+1})\sin[(m + 1 - 1)\frac{2\pi}{2m}]$$
$$= (1 + \epsilon_{m+1})\sin\pi$$
$$= 0. \tag{A.22}$$

Substituting (A.22) and (A.17) into (A.21), we obtain $\lambda = 0$, which contradicts (A.20) (where we show $\lambda \neq 0$). Thus when n is a positive even number, there is no $\lambda \in R$ satisfies (A.13).

3. When n is a positive odd number, say n = 2m+1, using the analogy in proof statement 2, we can easily show that substituting $i = 1, m+1$ into (A.13) and solving λ, we obtain

$$\begin{aligned} \lambda &= -\frac{y_1 - y_{m+1}}{x_1 - x_{m+1}} \\ &> 0, \end{aligned} \tag{A.23}$$

and substituting $i = 1, m+2$ into (A.13) and solving λ, we obtain

$$\begin{aligned} \lambda &= -\frac{y_1 - y_{m+2}}{x_1 - x_{m+2}} \\ &< 0. \end{aligned} \tag{A.24}$$

It is clear that the λ in (A.23) contradicts the λ in (A.24). Thus when n is a positive odd number, there is no $\lambda \in R$ satisfies (A.13).

4. Given that when n is a positive integer number, there is no $\lambda \in R$ satisfies (A.13) as we have shown, we know that the assumption of $\det(\mathbf{H}) = 0$ is not true. Thus, we conclude that $\det(\mathbf{H}) \neq 0$.

This concludes the proof of Lemma 2.

Lemma 3 If $n \geq 2$, and n is a positive integer, then $\sum_{i=1}^{n} \cos\left((i-1)\frac{2\pi}{n}\right) = 0$, and $\sum_{i=1}^{n} \sin\left((i-1)\frac{2\pi}{n}\right) = 0$.

The proof of this lemma is provided by Dr. R. H. Sprague.

Proof:

1. Let S be a summation of complex numbers such that

$$S = \sum_{j=1}^{n}[\cos((j-1)\frac{2\pi}{n}) + i\sin((j-1)\frac{2\pi}{n})], \tag{A.25}$$

where $i = \sqrt{-1}$. By DeMoivre's theorem [21], we know that

$$(\cos\theta + i\sin\theta)^a = \cos(a\theta) + i\sin(a\theta) \tag{A.26}$$
$$\forall \quad a \in R, \quad \& -\pi < \theta \leq \pi.$$

Substituting (A.26) into (A.25) with $a = j-1$ and $\theta = \frac{2\pi}{n}$, we obtain

$$S = \sum_{j=1}^{n}[\cos\frac{2\pi}{n} + i\sin\frac{2\pi}{n}]^{j-1}. \tag{A.27}$$

2. By definition [21], we know

$$\cos\alpha + i\sin\alpha = e^{i\alpha}. \tag{A.28}$$

So, substituting (A.28) into (A.27) with $\alpha = \frac{2\pi}{n}$, we obtain

$$\begin{aligned} S &= \sum_{j=1}^{n}(e^{\frac{2\pi i}{n}})^{j-1} \\ &= \frac{1-e^{2\pi i}}{1-e^{\frac{2\pi i}{n}}} \\ &= \frac{1-\cos 2\pi - i\sin 2\pi}{1-\cos\frac{2\pi}{n} - i\sin\frac{2\pi}{n}} \qquad (\because \text{(A.28)}) \\ &= 0. \end{aligned} \tag{A.29}$$

3. Thus, by (A.29) we know that both the real and imaginary units of S are 0. So, by (A.25) we find that

$$\sum_{j=1}^{n}\cos((j-1)\frac{2\pi}{n}) = 0, \tag{A.30}$$

and

$$\sum_{j=1}^{n} \sin((j-1)\frac{2\pi}{n}) \;=\; 0. \qquad \text{(A.31)}$$

4. Since the j in (A.30) and (A.31) is a dummy variable, we can rewrite (A.30) and (A.31) as

$$\sum_{i=1}^{n} \cos((i-1)\frac{2\pi}{n}) \;=\; 0,$$

and

$$\sum_{i=1}^{n} \sin((i-1)\frac{2\pi}{n}) \;=\; 0.$$

This concludes the proof of Lemma 3.

A.1.1

Lemma 8.1 of chapter 2 in Mendelson [12]: Let $(u_1, u_2, \ldots, u_n)$, $(v_1, v_2, \ldots, v_n)$ be n-tuples of real numbers, then

$$\sum_{i=1}^{n} u_i v_i \leq \left[\sum_{i=1}^{n} u_i^2\right]^{\frac{1}{2}} \left[\sum_{i=1}^{n} v_i^2\right]^{\frac{1}{2}}.$$

APPENDIX B. IF $(x_c, y_c) \neq (0,0)$, THEN AT LEAST ONE OF $\delta_i's < 0$

Proof:

1. Suppose $(x_c, y_c) \neq (0,0)$, $\delta_i \geq 0 \; \forall \; i$. By definition we obtain

$$\overline{O'A_i} \;=\; 1 + \epsilon_i + \delta_i, \tag{B.1}$$

and

$$\overline{OA_i} \;=\; 1 + \epsilon_i, \tag{B.2}$$

$\forall \; i$. Thus by (B.1) and (B.2) and our assumption, we have

$$\begin{aligned} \delta_i \;&\geq\; 0 \quad \forall \; i \\ \Longleftrightarrow 1 + \epsilon_i + \delta_i \;&\geq\; 1 + \epsilon_i \quad \forall \; i \\ \Longleftrightarrow \overline{O'A_i} \;&\geq\; \overline{OA_i} \quad \forall \; i. \end{aligned} \tag{B.3}$$

(B.3) states that $\overline{O'A_i}$ is no less than $\overline{OA_i} \; \forall \; i$.

2. Let the inner circle of the annulus be divided into n equal sectors as shown in Figure B.1. Let's suppose that the $O'(x_c, y_c)$ falls arbitrarily into the ith sector of the inner circle as shown in the shaded area of Figure B.1. The ith sector is formed by two radii, say $\overline{OA_i'}$ and $\overline{OA_{i+1}'}$, and their intercepted arc. When

$O'(x_c, y_c)$ is in the ith sector and $O'(x_c, y_c) \neq O(0,0)$, we can show that (see Appendix B.1)

$$\overline{OA_i} + \overline{OA_{i+1}} \;>\; \overline{O'A_i} + \overline{O'A_{i+1}}. \tag{B.4}$$

However by (B.3) we know that

$$\overline{O'A_i} + \overline{O'A_{i+1}} \;\geq\; \overline{OA_i} + \overline{OA_{i+1}}. \tag{B.5}$$

(B.4) and (B.5) contradict to each other. So we know that our assumption is not true. i.e., if $(x_c, y_c) \neq (0,0)$, then there exists at least one of $\delta_i's < 0$.

This concludes the proof.

B.1

The ith sector is composed of three parts such as two edges $\overline{OA_i'}$ and $\overline{OA_{i+1}'}$, the central triangle $\Delta OA_i'A_{i+1}'$ not including the two edges, and the segment not including the chord $\overline{A_i'A_{i+1}'}$ (see Figure B.2). We will show that if $O'(x_c, y_c)$ is in either one of the three parts of the ith sector, then

$$\overline{OA_i} + \overline{OA_{i+1}} \;>\; \overline{O'A_i} + \overline{O'A_{i+1}}. \tag{B.6}$$

The details are as follows.

Before doing the proof, we need the following theorems.

Theorem 34 in Walsh [30]: *The Triangle Inequality:* The sum of the lengths of two sides of a triangle is greater than the length of the third side.

Theorem 7.5 in Wilson [31]: *Law of Sines:* In any triangle **ABC** ,

$$\frac{\sin A}{a} = \frac{\sin B}{b} = \frac{\sin C}{c}.$$

That is, the ratio of any side of a triangle to the sine of the angle opposite the side is constant in any triangle.

Theorem 3.3.6 in Wallace [36]: If two angles of a triangle are not congruent, then the sides opposite them are not congruent and the larger side is opposite the larger angle. i.e., given a triangle **ABC**, if $\angle A > \angle B$, then $\overline{BC} > \overline{AC}$.

Proof:

1. Suppose that O' is in the edge $\overline{OA_i'}$ and $O' \neq O$ as shown in Figure B.3. Knowing that $\theta = \frac{2\pi}{n}$ and $n \geq 4$, we obtain

$$\theta \leq \frac{\pi}{2}. \tag{B.7}$$

Since $\theta \leq \frac{\pi}{2}$, O' is in the edge $\overline{OA_i'}$, and $O' \neq O$, we can always form a triangle $\Delta OO'A_{i+1}$. Applying theorem 34 in Walsh [30] to $\Delta OO'A_{i+1}$, we get

$$\begin{aligned} & \overline{O'A_{i+1}} < \overline{OO'} + \overline{OA_{i+1}} \\ \Longleftrightarrow\ & \overline{O'A_i} + \overline{O'A_{i+1}} < \overline{O'A_i} + \overline{OO'} + \overline{OA_{i+1}} \\ \Longleftrightarrow\ & \overline{O'A_i} + \overline{O'A_{i+1}} < \overline{OA_i} + \overline{OA_{i+1}}. \quad (\because\ \overline{OA_i} = \overline{O'A_i} + \overline{OO'}) \end{aligned}$$

Similarly, we can show that if O' is in the edge $\overline{OA_{i+1}'}$ and $O' \neq O$, then

$$\overline{O'A_i} + \overline{O'A_{i+1}} < \overline{OA_i} + \overline{OA_{i+1}}.$$

2. Suppose that O' is in the central triangle $\Delta OA_i'A_{i+1}'$ not including the two edges, $\overline{OA_i'}$ and $\overline{OA_{i+1}'}$, as shown in Figure B.4. Knowing $\theta \leq \frac{\pi}{2}$, we can always draw a line $\overleftrightarrow{O'A_{i+1}}$ which intersects the edge $\overline{OA_i'}$ at a point Q. Therefore

we can always form two triangles such as $\Delta O'QA_i$ and ΔOQA_{i+1}. Applying theorem 34 in Walsh [30] to $\Delta O'QA_i$, we acquire

$$\overline{O'A_i} < \overline{QA_i} + \overline{O'Q}. \tag{B.8}$$

Applying the same theorem to ΔOQA_{i+1}, we procure

$$\begin{aligned} \overline{QA_{i+1}} &< \overline{OA_{i+1}} + \overline{OQ} \\ \Longleftrightarrow \overline{O'Q} + \overline{O'A_{i+1}} &< \overline{OA_{i+1}} + \overline{OQ}. \\ (\because \overline{QA_{i+1}} &= \overline{O'Q} + \overline{O'A_{i+1}}) \end{aligned} \tag{B.9}$$

Combining (B.8) and (B.9), we obtain

$$\begin{aligned} \overline{O'A_i} + \overline{O'Q} + \overline{O'A_{i+1}} &< \overline{QA_i} + \overline{O'Q} + \overline{OA_{i+1}} + \overline{OQ} \\ \Longleftrightarrow \overline{O'A_i} + \overline{O'A_{i+1}} &< \overline{QA_i} + \overline{OA_{i+1}} + \overline{OQ} \\ \Longleftrightarrow \overline{O'A_i} + \overline{O'A_{i+1}} &< \overline{OA_i} + \overline{OA_{i+1}}. \\ (\because \overline{OA_i} &= \overline{QA_i} + \overline{OQ}) \end{aligned} \tag{B.10}$$

3. Suppose that O' is in the segment not including the chord $\overline{A_i'A_{i+1}'}$ as shown in Figure B.5. Knowing $\theta \leq \frac{\pi}{2}$, we can show that every point in the segment can be reflected by the chord $\overline{A_i'A_{i+1}'}$ onto $\Delta OA_i'A_{i+1}'$ (see Lemma 4). Let point S be the reflection of the point $O'(x_c, y_c)$ (see Figure B.5). Drawing a line from point S to point A_i, we can always intersect the chord $\overline{A_i'A_{i+1}'}$ at a point P_1. Considering $\Delta O'P_1S$, we have

$$\overline{P_1S} = \overline{P_1O'}. \tag{B.11}$$

Applying theorem 34 in Walsh [30] to $\Delta O'P_1A_i$, we get

$$\overline{O'A_i} \leq \overline{A_iP_1} + \overline{P_1O'}$$

$$\Longleftrightarrow \overline{O'A_i} \leq \overline{A_iP_1} + \overline{P_1S} \quad (\because \text{(B.11)})$$

$$\Longleftrightarrow \overline{O'A_i} \leq \overline{A_iS}. \tag{B.12}$$

Equal sign in (B.12) occurs when $\Delta O'P_1A_i$ degenerates into a line. Applying the same procedure to $\Delta O'A_{i+1}S$, we obtain

$$\overline{O'A_{i+1}} \leq \overline{A_{i+1}S}. \tag{B.13}$$

Equal sign in (B.13) occurs when $\Delta O'P_2A_{i+1}$ degenerates into a line. Combining (B.12) and (B.13), we acquire

$$\overline{O'A_i} + \overline{O'A_{i+1}} \leq \overline{A_iS} + \overline{A_{i+1}S}. \tag{B.14}$$

Given that

$$\overline{A_iS} + \overline{A_{i+1}S} < \overline{OA_i} + \overline{OA_{i+1}}, \tag{B.15}$$

as we have shown, by (B.14) we get

$$\overline{O'A_i} + \overline{O'A_{i+1}} < \overline{OA_i} + \overline{OA_{i+1}}. \tag{B.16}$$

This concludes the proof.

Lemma 4 If $\theta \leq \frac{\pi}{2}$, then all the points in the segment of the ith sector can be reflected by the chord $\overline{A_i'A_{i+1}'}$ onto $\Delta OA_i'A_{i+1}'$.

Proof:

1. Let O'' be the reflection of O, and the arc $\overset{\frown}{A_i'R_2A_{i+1}'}$ be the reflection of arc $\overset{\frown}{A_i'R_1A_{i+1}'}$ by the chord $\overline{A_i'A_{i+1}'}$ (see Figure B.6). If arc $\overset{\frown}{A_i'R_2A_{i+1}'}$ is in $\Delta OA_i'A_{i+1}'$, then all the points in the segment of the ith sector can be reflected by the chord $\overline{A_i'A_{i+1}'}$ onto $\Delta OA_i'A_{i+1}'$.

2. Let α be the angle of $\angle OA_i'O''$. Considering $\Delta OA_i'A_{i+1}'$, we have

$$\begin{aligned} \angle OA_i'A_{i+1}' &= \frac{\alpha}{2} \\ &= \frac{1}{2}(\pi - \theta) \\ \Longrightarrow \alpha &= \pi - \theta. \end{aligned} \tag{B.17}$$

Knowing $\theta \leq \frac{\pi}{2}$, by (B.17) we obtain

$$\alpha \geq \frac{\pi}{2}. \tag{B.18}$$

3. Let S_1' be an arbitrary point in arc $\overset{\frown}{A_i'R_2}$ such that $S_1' \neq A_i'$, then we can draw a line $\overleftrightarrow{O''S_1'}$ which will always intersect the edge $\overline{OA_i'}$ at a point S_1. Applying theorem 7.5 in Wilson [31] to $\Delta O''A_i'S_1$, we get

$$\begin{aligned} &\frac{\overline{O''S_1}}{\sin\alpha} = \frac{\overline{O''A_i'}}{\sin\angle A_i'S_1O''} \\ \Longleftrightarrow\ &\overline{O''S_1} = \frac{\sin\alpha}{\sin\angle A_i'S_1O''}\overline{O''A_i'} \\ \Longrightarrow\ &\overline{O''S_1} > \overline{O''A_i'} \quad (\because \quad \alpha > \angle A_i'S_1O'' \text{ and theorem 3.3.6 in Wallace[36]}) \\ \Longrightarrow\ &\overline{O''S_1} > \overline{O''S_1'}. \quad (\because \quad \overline{O''A_1'} = \overline{O''S_1'}) \end{aligned} \tag{B.19}$$

By (B.19) we conclude that the point S_1' is in $\Delta OA_i'Z$. Since S_1' is an arbitrary point in arc $\overset{\frown}{A_i'R_2}$, thus we conclude that arc $\overset{\frown}{A_i'R_2}$ is completely in $\Delta OA_i'Z$. Similarly we can show that the arc $\overset{\frown}{A_{i+1}'R_2}$ is completely in $\Delta OA_{i+1}'Z$. Therefore we conclude that the arc $\overset{\frown}{A_i'R_2A_{i+1}'}$ is in $\Delta OA_i'A_{i+1}'$.

This concludes the proof.

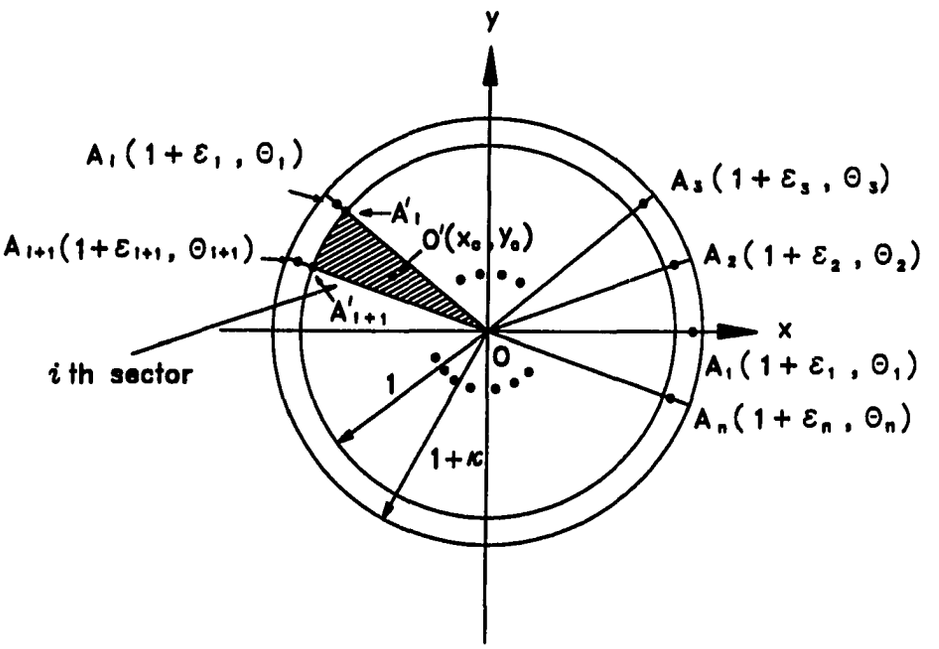

Figure B.1: A Division of n Equal Sectors in the Inner Circle of the Annulus.

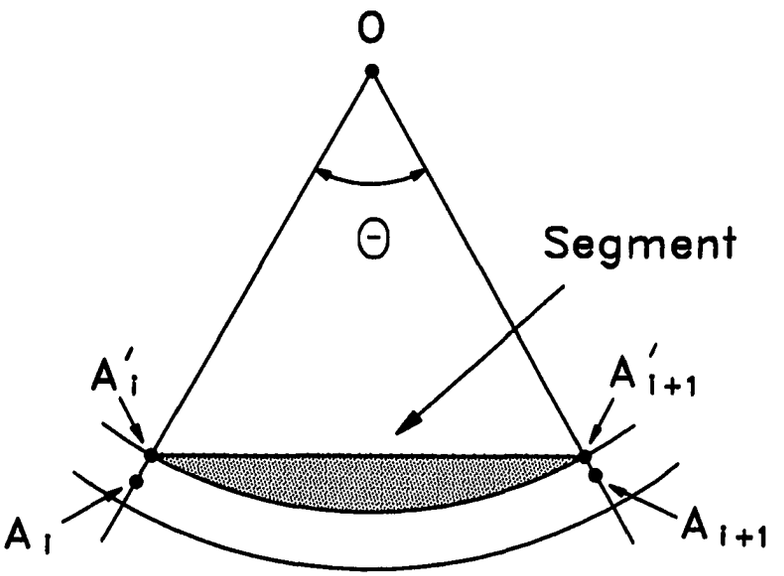

Figure B.2: The Components of the ith Sector.

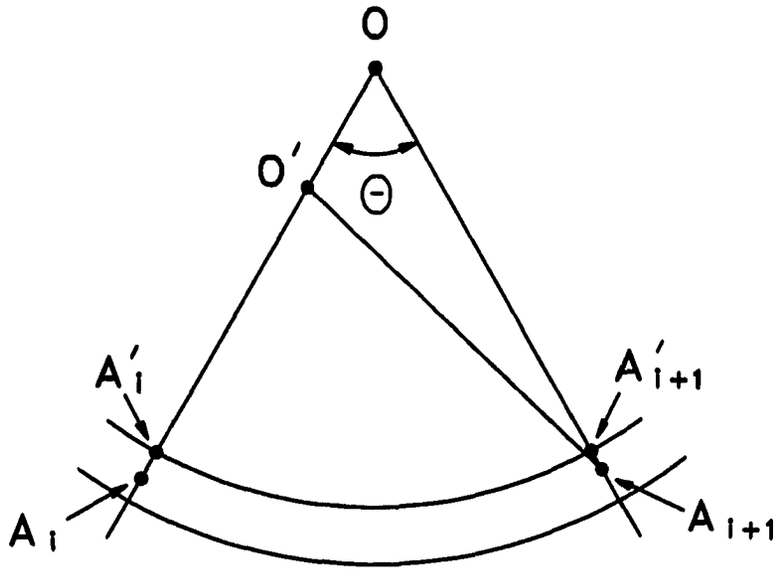

Figure B.3: The O' in the Edge $\overline{OA'_i}$.

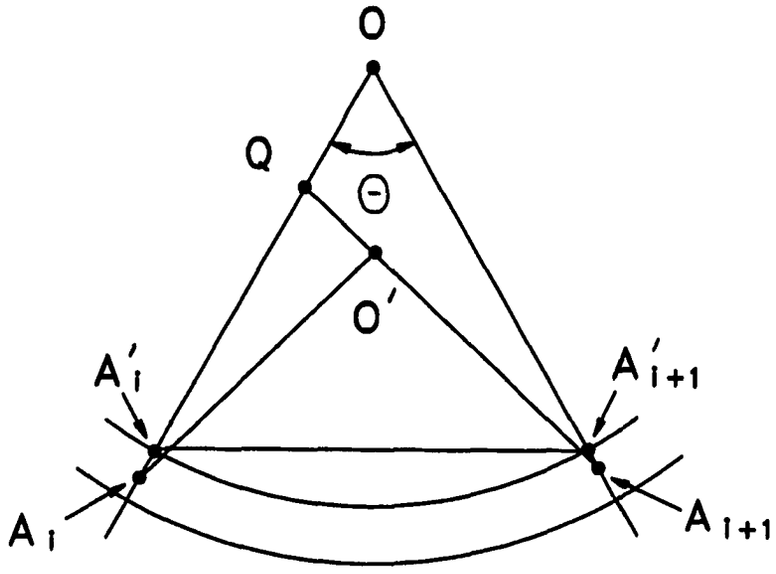

Figure B.4: The O' in the Triangle $\Delta OA'_iA'_{i+1}$.

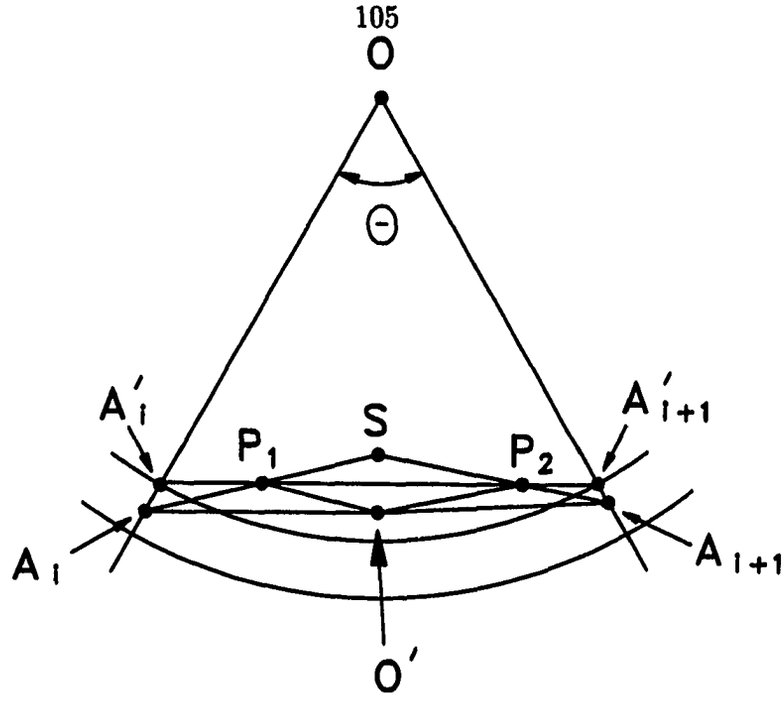

Figure B.5: The O' in the Segment of the ith Sector.

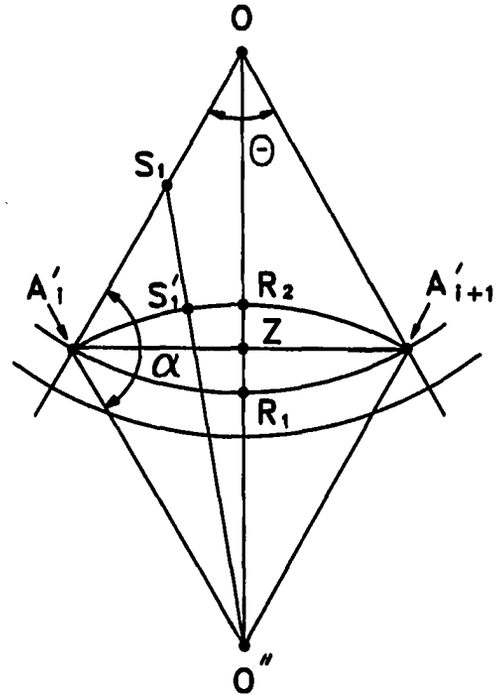

Figure B.6: The Reflection of the Segment of the ith Sector by the Chord $\overline{A'_iA'_{i+1}}$.

APPENDIX C. THE GLOBAL MINIMUM CONDITIONS OF Δ_n

We reformulate the constrained minimization problem in section 4.1.1.2 as follows.

$$\text{Minimize} \qquad \Delta_n$$

$$\begin{aligned} \text{subject to} \quad & 1. \quad \textstyle\sum_{i=1}^{n}(\Delta_i - \overline{\Delta})^2 \leq c, \\ & 2. \quad \textstyle\sum_{i=1}^{n}\Delta_i \geq 0, \\ & 3. \quad \text{at least one of } \Delta_i's \leq 0. \end{aligned}$$

Here $c = 4\sum_{i=1}^{n}(\epsilon_i - \overline{\epsilon})^2$, $\overline{\Delta} = \frac{1}{n}\sum_{i=1}^{n}\Delta_i$, and Δ_n is the minimum of $\Delta_i \ \forall\ i$.

Proof:

1. Because of both Δ_n is the minimum of $\Delta_i \ \forall\ i$ and the constraint 3, we obtain that if Δ_n reaches its global minimum, say Δ_{n*}, then

$$\Delta_{n*} \ \leq \ 0. \tag{C.1}$$

2. We can show that if Δ_n reaches its global minimum, Δ_{n*}, and the corresponding values of other Δ_i are $\Delta_{i*} \ \forall\ i = 1, 2, \ldots, n-1$, then (see Appendix C.1)

$$\sum_{i=1}^{n}\Delta_{i*} \ = \ 0. \tag{C.2}$$

3. Given $\sum_{i=1}^{n-1} \Delta_{i*} = k_1 \geq 0$, we can show that if $\sum_{i=1}^{n-1} \Delta_{i*}^2$ reaches its global minimum, then (see Appendix C.2)

$$\Delta_{1*} = \Delta_{2*} = \ldots = \Delta_{(n-1)*} = \frac{k_1}{n-1}. \tag{C.3}$$

4. Given condition 1 and (C.2), we know that when Δ_n reaches its global minimum,

$$\begin{aligned} \sum_{i=1}^{n} (\Delta_i - \overline{\Delta})^2 &= \sum_{i=1}^{n} \Delta_i^2 \\ &\leq c. \end{aligned}$$

Since c is a constant, thus $\sum_{i=1}^{n-1} \Delta_i^2$ must be minimum. By (C.3) we know that $\sum_{i=1}^{n-1} \Delta_i^2$ reaches its minimum when

$$\Delta_1 = \Delta_2 = \ldots = \Delta_{n-1} = -\frac{1}{n-1}\Delta_n.$$

This concludes the proof.

C.1

We can show (C.2) by contradiction. We first assume that when Δ_n reaches its global minimum, Δ_{n*}, $\sum_{i=1}^{n} \Delta_{i*} \neq 0$. Then we can find a new arrangement of Δ_i, say Δ'_{i*}, $\forall\ i$ such that $\sum_{i=1}^{n} \Delta'_{i*} = 0$ and the new value of Δ_n, i.e., Δ'_{n*}, is smaller than Δ_{n*}. This then contradicts the assumption that Δ_{n*} is the global minimum of Δ_n. The details are as follows.

1. Suppose that when Δ_n reaches its global minimum, say Δ_{n*}, $\sum_{i=1}^{n} \Delta_{i*} \neq 0$. For the sake of argument, let's assume that the arrangement of Δ_{i*} $\forall\ i$ is as shown

in Figure C.1. In this arrangement we know that by the constraints 2 and 1, we obtain

$$\sum_{i=1}^{n} \Delta_{i*} > 0, \tag{C.4}$$

and

$$\sum_{i=1}^{n} (\Delta_{i*} - \overline{\Delta}_*)^2 \leq c. \tag{C.5}$$

Where

$$\overline{\Delta}_* = \frac{1}{n} \sum_{i=1}^{n} \Delta_{i*}. \tag{C.6}$$

2. By (C.4) and (C.6) we know that $\overline{\Delta}_* > 0$. We can find a new arrangement of Δ_i, say Δ'_{i*}, (see Figure C.2) such that

$$\Delta'_{i*} = \Delta_{i*} - \overline{\Delta}_*, \ \forall \ i. \tag{C.7}$$

In this new arrangement, it is easy to show that the constraint 1 is satisfied as follows:

$$\begin{aligned} \sum_{i=1}^{n} (\Delta'_{i*} - \overline{\Delta}'_*)^2 &= \sum_{i=1}^{n} (\Delta_{i*} - \overline{\Delta}_*)^2 \\ &\leq c. \quad (\because \ (C.5)) \end{aligned} \tag{C.8}$$

We can show that this new arrangement satisfies the constraint 2 as follows:

$$\begin{aligned} \sum_{i=1}^{n} \Delta'_{i*} &= \sum_{i=1}^{n} (\Delta_{i*} - \overline{\Delta}_*) \\ &= \sum_{i=1}^{n} \Delta_{i*} - n\overline{\Delta}_* \\ &= 0. \quad (\because \ \overline{\Delta}_* = \frac{1}{n} \sum_{i=1}^{n} \Delta_{i*}) \end{aligned}$$

It is clear that the new arrangement satisfies the constraint 3. Thus we conclude that the new arrangement, $\Delta'_{i*}\ \forall\ i$, is a valid solution to the constrained minimization problem.

3. It is clear that

$$\begin{aligned} \Delta'_{n*} &= \Delta_{n*} - \overline{\Delta}_{*} \\ &< \Delta_{n*}. \end{aligned} \tag{C.9}$$

By (C.9) we know that it contradicts the assumption that Δ_{n*} is the global minimum of Δ_n.

This concludes the proof.

C.2

We show (C.3) as follows. Let

$$\overline{\mathbf{x}} = \left[\begin{array}{cccc} \frac{k_1}{n-1} & \frac{k_1}{n-1} & \cdots & \frac{k_1}{n-1} \end{array} \right]_{1\mathbf{x}(n-2).} \tag{C.10}$$

Furthermore, let

$$\begin{aligned} g &= \sum_{i=1}^{n-1} \Delta_{i*}^2 \\ &= \sum_{i=1}^{n-2} \Delta_{i*}^2 + (k_1 - \sum_{i=1}^{n-2} \Delta_{i*})^2. \qquad (\because\ \Delta_{(n-1)*} = k_1 - \sum_{i=1}^{n-2} \Delta_{i*}) \end{aligned} \tag{C.11}$$

By (C.11) we know that $g : E_{n-2} \longrightarrow E_1$. We will show that g is strictly convex on E_{n-2} and $\overline{\mathbf{x}}$ is the global minimum of g on E_{n-2}. Then using the constraint of $\sum_{i=1}^{n-1} \Delta_{i*} = k_1$, we obtain that if $\sum_{i=1}^{n-1} \Delta_{i*}^2$ reaches its global minimum, then

$$\Delta_{1*} = \Delta_{2*} = \ldots = \Delta_{(n-1)*} = \frac{k_1}{n-1}.$$

Before doing the proof, we need the following definition and theorems.

Theorem 2.1.1 in Myers & Milton [27]: A symmetric matrix **A** is positive definite if and only if all its eigenvalues are positive.

Definition 1 in section 1 of chapter 2 in Hogben [28]: Let **A** be a nxn matrix. The i,j-minor of **A** is the $(n-1)$x$(n-1)$ matrix obtained from **A** by deleting row i and column j. The i,j-minor is denoted $\mathbf{M}_{ij}$.

Theorem 5 in section 3 of chapter 2 in Hogben [28]: The determinant of a nxn matrix **A** may be computed by expanding by cofactors on any row or column. That is,

$$\begin{aligned}&\det(\mathbf{A})\\ &= a_{i1}(-1)^{i+1}\det(\mathbf{M}_{i1}) + a_{i2}(-1)^{i+2}\det(\mathbf{M}_{i2}) + \ldots + a_{in}(-1)^{i+n}\det(\mathbf{M}_{in})\\ &= a_{1j}(-1)^{1+j}\det(\mathbf{M}_{1j}) + a_{2j}(-1)^{2+j}\det(\mathbf{M}_{2j}) + \ldots + a_{nj}(-1)^{n+j}\det(\mathbf{M}_{nj}),\end{aligned}$$

for any $i,j = 1,\ldots,n$. Here a_{ij} is the entry in row i and column j of the matrix **A**. The quantity $(-1)^{i+j}\det(\mathbf{M}_{ij})$ is called the i,j-cofactor of **A** and is denoted $\mathbf{A}_{ij}$.

Theorem 2 in section 1 of chapter 7 in Hogben [28]: Let **A** be a nxn matrix. The real number λ is an eigenvalue of **A** if and only if $\det(\mathbf{A} - \lambda\mathbf{I}) = 0$. Here **I** is a nxn identity matrix.

Theorem d in section 3 of chapter 4 in Searle [29]: Adding to one row (column) of a determinant any multiple of another row (column) does not affect the value of the determinant.

Proof:

1. We show that all the first partial derivatives of g are zero at $\overline{\mathbf{x}}$ as follows. Taking the first partial derivatives of g with respect to $\Delta_{i*}\ \forall\ i$, we obtain

$$\frac{\partial g}{\partial \Delta_{i*}} = 2\Delta_{i*} + 2(k_1 - \sum_{i=1}^{n-2}\Delta_{i*})(-1) \quad \forall\ i. \tag{C.12}$$

Making (C.12) equal to zero, we obtain

$$\Delta_{1*} - (k_1 - \sum_{i=1}^{n-2} \Delta_{i*}) = 0, \tag{C.13}$$

$$\Delta_{2*} - (k_1 - \sum_{i=1}^{n-2} \Delta_{i*}) = 0, \tag{C.14}$$

$$\vdots$$

$$\Delta_{(n-2)*} - (k_1 - \sum_{i=1}^{n-2} \Delta_{i*}) = 0. \tag{C.15}$$

Summing up (C.13) through (C.15), we obtain

$$\begin{aligned} \sum_{i=1}^{n-2} \Delta_{i*} - (n-2)(k_1 - \sum_{i=1}^{n-2} \Delta_{i*}) &= 0 \\ \Longleftrightarrow (n-1) \sum_{i=1}^{n-2} \Delta_{i*} &= (n-2)k_1 \\ \Longleftrightarrow \sum_{i=1}^{n-2} \Delta_{i*} &= \frac{(n-2)k_1}{n-1} . \end{aligned} \tag{C.16}$$

Substituting (C.16) into (C.13) through (C.15), we obtain

$$\Delta_{i*} = \frac{k_1}{n-1} \ \forall \ i.$$

Thus we know that all the first partial derivatives of g are zero at $\bar{\mathbf{x}}$.

2. We show that the Hessian matrix of g is positive definite on E_{n-2} as follows. Using (C.12), we take the second partial derivatives of g with respect to Δ_{i*} and Δ_{j*}, obtaining

$$\frac{\partial^2 g}{\partial \Delta_{i*}^2} = 4, \ \forall \ i, \tag{C.17}$$

and

$$\frac{\partial^2 g}{\partial \Delta_{i*} \partial \Delta_{j*}} = 2, \ \forall \ i \neq j. \tag{C.18}$$

So we obtain the Hessian matrix of g, $\mathbf{H}$, as follows:

$$\mathbf{H} = \begin{bmatrix} \frac{\partial^2 g}{\partial \Delta_{1*}^2} & \frac{\partial^2 g}{\partial \Delta_{1*}\Delta_{2*}} & \frac{\partial^2 g}{\partial \Delta_{1*}\Delta_{3*}} & \cdot\ \cdot & \frac{\partial^2 g}{\partial \Delta_{1*}\Delta_{(n-2)*}} \\ \frac{\partial^2 g}{\partial \Delta_{2*}\Delta_{1*}} & \frac{\partial^2 g}{\partial \Delta_{2*}^2} & \frac{\partial^2 g}{\partial \Delta_{2*}\Delta_{3*}} & \cdot\ \cdot & \frac{\partial^2 g}{\partial \Delta_{2*}\Delta_{(n-2)*}} \\ \frac{\partial^2 g}{\partial \Delta_{3*}\Delta_{1*}} & \frac{\partial^2 g}{\partial \Delta_{3*}\Delta_{2*}} & \frac{\partial^2 g}{\partial \Delta_{3*}^2} & \cdot\ \cdot & \frac{\partial^2 g}{\partial \Delta_{3*}\Delta_{(n-2)*}} \\ \cdot & \cdot & \cdot & \cdot\ \cdot & \cdot \\ \cdot & \cdot & \cdot & \cdot\ \cdot & \cdot \\ \frac{\partial^2 g}{\partial \Delta_{(n-2)*}\Delta_{1*}} & \frac{\partial^2 g}{\partial \Delta_{(n-2)*}\Delta_{2*}} & \frac{\partial^2 g}{\partial \Delta_{(n-2)*}\Delta_{3*}} & \cdot\ \cdot & \frac{\partial^2 g}{\partial \Delta_{(n-2)*}^2} \end{bmatrix}_{(n-2)\mathbf{x}(n-2).}$$

$$= \begin{bmatrix} 4 & 2 & 2 & . & . & 2 \\ 2 & 4 & 2 & . & . & 2 \\ 2 & 2 & 4 & . & . & 2 \\ . & . & . & . & . & . \\ . & . & . & . & . & . \\ 2 & 2 & 2 & . & . & 4 \end{bmatrix}_{(n-2)\mathbf{x}(n-2).}$$

3. Let $\mathbf{I}$ be a $(n-2)\mathbf{x}(n-2)$ identity matrix. Thus we obtain $\mathbf{H} - \lambda\mathbf{I}$, $\mathbf{H_1}$, as follows:

$$\mathbf{H_1} = \begin{bmatrix} 4-\lambda & 2 & 2 & . & . & 2 \\ 2 & 4-\lambda & 2 & . & . & 2 \\ 2 & 2 & 4-\lambda & . & . & 2 \\ . & . & . & . & . & . \\ . & . & . & . & . & . \\ 2 & 2 & 2 & . & . & 4-\lambda \end{bmatrix}_{(n-2)\mathbf{x}(n-2).}$$

4. Let the manipulation of rows (columns) of a matrix $\mathbf{A}$,

$$\text{row (column) } i \text{ - } k \text{ [row (column) } j\text{]} \longrightarrow \text{row (column) } i$$

stand for subtracting a multiple of k of row (column) j from row (column) i and putting the result into row (column) i in the matrix **A**. We then do the manipulation of rows of $\mathbf{H_1}$ as follows:

$$\begin{gathered}
\text{row 3 - row 2} \longrightarrow \text{row 3,} \\
\text{row 4 - row 2} \longrightarrow \text{row 4,} \\
\text{row 5 - row 2} \longrightarrow \text{row 5,} \\
\vdots \\
\text{row } (n-2) \text{ - row 2} \longrightarrow \text{row } (n-2), \\
\text{row 2 - row 1} \longrightarrow \text{row 2,}
\end{gathered}$$

resulting a new matrix $\mathbf{H_2}$ as follows:

$$\mathbf{H_2} = \begin{bmatrix}
4-\lambda & 2 & 2 & . & . & 2 \\
-2+\lambda & 2-\lambda & 0 & . & . & 0 \\
0 & -2+\lambda & 2-\lambda & . & . & 0 \\
. & . & . & . & . & . \\
. & . & . & . & . & . \\
0 & -2+\lambda & 0 & . & . & 2-\lambda
\end{bmatrix}_{(n-2)\mathrm{x}(n-2).}$$

We transform $\mathbf{H_2}$ as follows:

$$\begin{gathered}
\text{column 1 + column 2} \longrightarrow \text{column 2,} \\
\text{column 3 + column 2} \longrightarrow \text{column 2,} \\
\text{column 4 + column 2} \longrightarrow \text{column 2,}
\end{gathered}$$

$$\text{column } 5 + \text{column } 2 \longrightarrow \text{column } 2,$$

$$\vdots$$

$$\text{column } (n-2) + \text{column } 2 \longrightarrow \text{column } 2,$$

and obtain

$$\mathbf{H_3} = \begin{bmatrix} 4-\lambda & 2(n-1)-\lambda & 2 & . & . & 2 \\ -2+\lambda & 0 & 0 & . & . & 0 \\ 0 & 0 & 2-\lambda & . & . & 0 \\ . & . & . & . & . & . \\ . & . & . & . & . & . \\ 0 & 0 & 0 & . & . & 2-\lambda \end{bmatrix}_{(n-2)\mathbf{x}(n-2).}$$

By theorem d in section 3 of chapter 4 in Searle [29], we obtain

$$\begin{aligned} \det(\mathbf{H}-\lambda\mathbf{I}) &= \det(\mathbf{H_1}) \\ &= \det(\mathbf{H_2}) \\ &= \det(\mathbf{H_3}) \\ &= \begin{vmatrix} 4-\lambda & 2(n-1)-\lambda & 2 & . & . & 2 \\ -2+\lambda & 0 & 0 & . & . & 0 \\ 0 & 0 & 2-\lambda & . & . & 0 \\ . & . & . & . & . & . \\ . & . & . & . & . & . \\ 0 & 0 & 0 & . & . & 2-\lambda \end{vmatrix}_{(n-2)\mathbf{x}(n-2).} \end{aligned} \tag{C.19}$$

By theorem 5 in section 3 of chapter 2 in Hogben [28], we can find the determinant of $\mathbf{H_3}$ by expanding by cofactors on column 2 of $\mathbf{H_3}$, resulting in

$$\det(\mathbf{H_3}) = (2(n-1)-\lambda)(-1)^{1+2}\det(\mathbf{M}_{1,2}) + 0 * \det(\mathbf{M}_{2,2}) +$$

$$0 * \det(\mathbf{M}_{3,2}) + \ldots + 0 * \det(\mathbf{M}_{(n-2),2})$$

$$= -(2(n-1) - \lambda)\det(\mathbf{M}_{1,2}). \qquad \text{(C.20)}$$

By definition 1 in section 1 of chapter 2 in Hogben [28], we obtain $\det(\mathbf{M}_{1,2})$ as follows:

$$\det(\mathbf{M}_{1,2}) = \begin{vmatrix} -2+\lambda & 0 & 0 & . & . & 0 \\ 0 & 2-\lambda & 0 & . & . & 0 \\ 0 & 0 & 2-\lambda & . & . & 0 \\ . & . & . & . & . & . \\ . & . & . & . & . & . \\ 0 & 0 & 0 & . & . & 2-\lambda \end{vmatrix}_{(n-3)\mathbf{x}(n-3)}$$

$$= (-2+\lambda)(2-\lambda)^{n-4}. \qquad \text{(C.21)}$$

Substituting (C.20) and (C.21) into (C.19), we obtain

$$\det(\mathbf{H} - \lambda\mathbf{I}) = -(2(n-1) - \lambda)(-2+\lambda)(2-\lambda)^{n-4}$$

$$= (2(n-1) - \lambda)(2-\lambda)^{n-3}. \qquad \text{(C.22)}$$

According to theorem 2 in section 1 of chapter 7 in Hogben [28], we make (C.22) equal to zero to find the eigenvalues, λ, of $\mathbf{H}$, resulting,

$$\lambda = 2, \text{ or } 2(n-1). \qquad \text{(C.23)}$$

By (C.23) it is clear that all the eigenvalues of $\mathbf{H}$ are greater than zero. Therefore by theorem 2.1.1 in Myers & Milton [27], we know that $\mathbf{H}$ is positive definite on E_{n-2}.

5. We show that g is strictly convex on E_{n-2} as follows. Taking the third partial derivatives of g, we obtain

$$\frac{\partial^3 g}{\partial \Delta_{i*}^3} = 0, \quad \forall\, i, \tag{C.24}$$

$$\frac{\partial^3 g}{\partial \Delta_{i*}^2 \partial \Delta_{j*}} = 0, \quad \forall\, i \neq j, \tag{C.25}$$

$$\frac{\partial^3 g}{\partial \Delta_{i*} \partial \Delta_{j*} \partial \Delta_{k*}} = 0, \quad \forall\, i \neq j \neq k. \tag{C.26}$$

By (C.24), (C.25) and (C.26) we know that the third partial derivatives of g exist and are continuous on E_{n-2}. Thus by definition 3.3.5 in Bazaraa [11], theorem 14 of chapter 10 in DePree [35] and definition 15 of chapter 10 in DePree [35] (see section 5.2), we obtain that g is twice differentiable on E_{n-2}. It is clear that E_{n-2} is a nonempty open convex set. Given that $\mathbf{H}$ is positive definite on E_{n-2} as we have shown, by theorem 3.3.8 in Bazaraa [11] (see section 5.2) we conclude that g is strictly convex.

6. We show that $\overline{\mathbf{x}}$ is a local minimum of g as follows. Given that all the first partial derivatives of g are zero at $\overline{\mathbf{x}}$, $\mathbf{H}$ is positive definite at $\overline{\mathbf{x}}$ and g is twice differentiable at $\overline{\mathbf{x}}$ as we have shown, by theorem 4.1.4 in Bazaraa [11] (see section 5.3.1) we conclude that $\overline{\mathbf{x}}$ is a local minimum of g.

7. Given $\overline{\mathbf{x}}$ is a local minimum of g, g is strictly convex, and E_{n-2} is a nonempty convex set as we have shown, by theorem 3.4.2 in Bazaraa [11] (see section 5.3.1) we conclude that $\overline{\mathbf{x}}$ is the unique global minimum.

This concludes the proof.

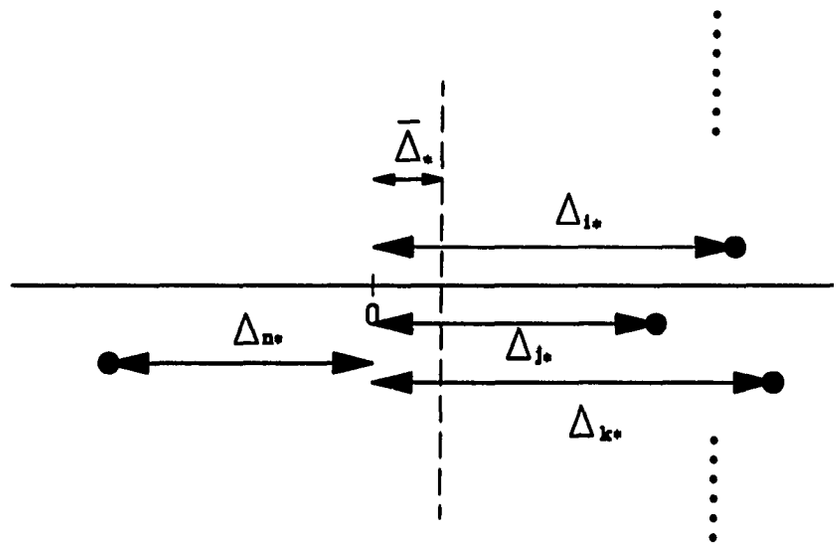

Figure C.1: A Possible Arrangement of Δ_i, Δ_{i*}.

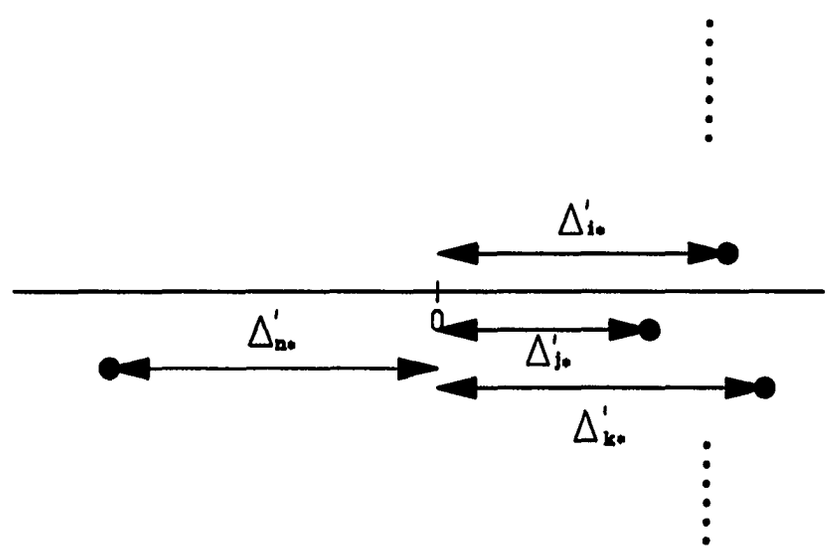

Figure C.2: A New Arrangement of Δ_i, Δ'_{i*}.

APPENDIX D. $\sum_{i=1}^{n}(\epsilon_i - \bar{\epsilon})^2 \leq \frac{n}{4}\kappa^2$

Before doing the proof, we need the following definitions and theorems.

Theorem 4.5 in section 4 of chapter 5 in Mendelson [12]: A subset A of R^n is compact if and only if A is closed and bounded.

Definition 2.5.1 in Bazaraa [11]: A nonempty set S in E_n is called a polyhedral set if it is the intersection of a finite number of closed half spaces; that is, $S = \{\mathbf{x} : \mathbf{p}_i^t\mathbf{x} \leq \alpha_i \ \forall\ i = 1, 2, \ldots, m\}$, where $\mathbf{p}_i$ is a nonzero vector and α_i is a scalar $\forall\ i$.

Definition 2.5.2 in Bazaraa [11]: Let S be a nonempty convex set in E_n. A vector $\mathbf{x} \in S$ is called an extreme point of S if $\mathbf{x} = \lambda\mathbf{x}_1 + (1-\lambda)\mathbf{x}_2$ with $\mathbf{x}_1, \mathbf{x}_2 \in S$, and $\lambda \in (0,1)$ implies that $\mathbf{x} = \mathbf{x}_1 = \mathbf{x}_2$.

Theorem 3.4.6 in Bazaraa [11]: Let $f : E_n \rightarrow E_1$ be a convex function, and let S be a nonempty compact polyhedral set in E_n. Consider the problem to maximize $f(\mathbf{x})$ subject to $\mathbf{x} \in S$. There then exists an optimal solution $\bar{\mathbf{x}}$ to the problem, where $\bar{\mathbf{x}}$ is an extreme point of S.

Proof:

1. Let

$$S = \{(\epsilon_1, \epsilon_2, \ldots, \epsilon_n) \mid 0 \leq \epsilon_i \leq \kappa, \ \forall\ i\}, \tag{D.1}$$

and

$$f = \sum_{i=1}^{n}(\epsilon_i - \bar{\epsilon})^2. \tag{D.2}$$

By (D.1) and (D.2) we know that $f : S \longrightarrow E_1$. We can show that f is convex on S (see Appendix D.1).

2. It is clear that S is closed and bounded, thus by theorem 4.5 in section 4 of chapter 5 in Mendelson [12], we know that S is compact. Let

$$\mathbf{p}_{i1}^t = [0_1, 0_2, 0_3, \ldots, 0_{i-1}, -1_i, 0_{i+1}, \ldots, 0_n]_{1\mathbf{x}n}$$

be an array with the ith element equal to -1 and all other elements are 0. Let

$$\mathbf{p}_{i2}^t = [0_1, 0_2, 0_3, \ldots, 0_{i-1}, 1_i, 0_{i+1}, \ldots, 0_n]_{1\mathbf{x}n}$$

be an array with the ith element equal to 1 and all other elements are 0. Then we can represent S in a different form as

$$S = \{\mathbf{x} : \mathbf{p}_{i1}^t\mathbf{x} \leq 0, \text{ and } \mathbf{p}_{i2}^t\mathbf{x} \leq \kappa, \forall\, i\}$$

Thus by definition 2.5.1 in Bazaraa [11], we know that S is a polyhedral set in E_n. By definition 2.5.2 in Bazaraa [11] we obtain a set of extreme points in S, say SE, as

$$SE = \{(\epsilon_1, \epsilon_2, \ldots, \epsilon_n) \mid \epsilon_i = 0 \text{ or } \kappa, \ \forall \text{ i}\}. \tag{D.3}$$

Given that S is both a compact set and a polyhedral set, S is a nonempty set, and f is convex on S as we have shown, by theorem 3.4.6 in Bazaraa [11] we know that there exists a global maximum, say $\overline{\mathbf{x}}$, of f $\forall$ $(\epsilon_1, \epsilon_2, \ldots, \epsilon_n) \in S$ where $\overline{\mathbf{x}} \in SE$.

3. Let $SE_1 = (\epsilon_{1*}, \epsilon_{2*}, \ldots, \epsilon_{n*})$ be an arbitrary element in SE such that m of ϵ_{i*} in SE_1 are zero, and the other in SE_1 are κ. Thus we obtain the value of f at

SE_1 as

$$\begin{aligned} f(SE_1) &= \sum_{i=1}^{n}(\epsilon_{i*} - \bar{\epsilon}_*)^2 \quad (\text{Here } \bar{\epsilon}_* = \frac{1}{n}\sum_{i=1}^{n}\epsilon_{i*}) \\ &= \sum_{i=1}^{n}\epsilon_{i*}^2 - n\bar{\epsilon}_*{}^2 \\ &= (n-m)\kappa^2 - n(\frac{(n-m)\kappa}{n})^2 \end{aligned}$$

$$(\because \quad \textstyle\sum_{i=1}^{n}\epsilon_{i*}^2 = (n-m)\kappa^2, \quad \text{and} \quad \bar{\epsilon}_* = \frac{(n-m)\kappa}{n})$$

$$= (n-m)\kappa^2 - \frac{(n-m)^2}{n}\kappa^2. \tag{D.4}$$

By (D.4) it is clear that $f(SE_1)$ is a function of m where m is a nonnegative integer such that $0 \leq m \leq n$. We can show that an upper bound of $f(SE_1)$ is given by (see Appendix D.2)

$$f(SE_1) \leq \frac{n}{4}\kappa^2. \tag{D.5}$$

Since SE_1 is an arbitrary element in SE, thus we know that

$$f(\epsilon_1, \epsilon_2, \ldots, \epsilon_n) \leq \frac{n}{4}\kappa^2 \quad \forall\ (\epsilon_1, \epsilon_2, \ldots, \epsilon_n) \in SE, \tag{D.6}$$

which in turn, gives

$$f(\epsilon_1, \epsilon_2, \ldots, \epsilon_n) \leq \frac{n}{4}\kappa^2 \quad \forall\ (\epsilon_1, \epsilon_2, \ldots, \epsilon_n) \in S.$$

This concludes the proof.

D.1

It suffices to show that f is convex on E_n. We show that f is convex by showing that the Hessian matrix of f is positive semidefinite on E_n. The details are as follows. Before doing the proof, we need the following theorems.

Theorem 2.1.2 in Myers & Milton [27]: A symmetric matrix **A** is positive semidefinite if and only if its eigenvalues are all nonnegative and at least one eigenvalue is zero.

Theorem 3.3.6 in Bazaraa [11]: Let S be a nonempty open convex set in E_n, and let $f : S \longrightarrow E_1$ be twice differentiable on S. Then f is convex if and only if the Hessian matrix is positive semidefinite at each point in S.

Proof:

1. We show that the Hessian matrix of f is positive semidefinite as follows. Taking the first partial derivatives of f with respect to $\epsilon_i \ \forall \ i$, we obtain

$$\begin{aligned}
\frac{\partial f}{\partial \epsilon_i} &= 2(\epsilon_1 - \bar{\epsilon})(-\frac{1}{n}) + 2(\epsilon_2 - \bar{\epsilon})(-\frac{1}{n}) + \ldots + 2(\epsilon_{i-1} - \bar{\epsilon})(-\frac{1}{n}) \\
&\quad +2(\epsilon_i - \bar{\epsilon})(1 - \frac{1}{n}) + 2(\epsilon_{i+1} - \bar{\epsilon})(-\frac{1}{n}) + \ldots + 2(\epsilon_n - \bar{\epsilon})(-\frac{1}{n}) \\
&= 2(\epsilon_i - \bar{\epsilon})(1 - \frac{1}{n}) + \sum_{1 \le j \ne i \le n} 2(\epsilon_j - \bar{\epsilon})(-\frac{1}{n}) \\
&= 2(\epsilon_i - \bar{\epsilon})(1 - \frac{1}{n}) - \frac{2}{n} \sum_{1 \le j \ne i \le n} (\epsilon_j - \bar{\epsilon}) \\
&= 2(\epsilon_i - \bar{\epsilon})(1 - \frac{1}{n}) - \frac{2}{n}(-(\epsilon_i - \bar{\epsilon})) \quad \left(\because \ \sum_{i=1}^{n} (\epsilon_i - \bar{\epsilon}) = 0 \right) \\
&= 2(\epsilon_i - \bar{\epsilon})(1 - \frac{1}{n}) + \frac{2}{n}(\epsilon_i - \bar{\epsilon}) \\
&= 2(\epsilon_i - \bar{\epsilon}). \qquad \text{(D.7)}
\end{aligned}$$

2. Using (D.7), we take the second partial derivatives of f with respect to ϵ_i and ϵ_j, obtaining

$$\frac{\partial^2 f}{\partial \epsilon_i^2} = 2(1 - \frac{1}{n}) \quad \forall \ i, \qquad \text{(D.8)}$$

and

$$\frac{\partial^2 f}{\partial \epsilon_i \partial \epsilon_j} = -\frac{2}{n} \quad \forall \ i \ne j. \qquad \text{(D.9)}$$

The Hessian matrix of f, $\mathbf{F}$, is given by

$$\mathbf{F} = \begin{bmatrix} \frac{\partial^2 f}{\partial \epsilon_1^2} & \frac{\partial^2 f}{\partial \epsilon_1 \partial \epsilon_2} & \frac{\partial^2 f}{\partial \epsilon_1 \partial \epsilon_3} & . & . & \frac{\partial^2 f}{\partial \epsilon_1 \partial \epsilon_n} \\ \frac{\partial^2 f}{\partial \epsilon_2 \partial \epsilon_1} & \frac{\partial^2 f}{\partial \epsilon_2^2} & \frac{\partial^2 f}{\partial \epsilon_2 \partial \epsilon_3} & . & . & \frac{\partial^2 f}{\partial \epsilon_2 \partial \epsilon_n} \\ \frac{\partial^2 f}{\partial \epsilon_3 \partial \epsilon_1} & \frac{\partial^2 f}{\partial \epsilon_3 \partial \epsilon_2} & \frac{\partial^2 f}{\partial \epsilon_3^2} & . & . & \frac{\partial^2 f}{\partial \epsilon_3 \partial \epsilon_n} \\ . & . & . & . & . & . \\ . & . & . & . & . & . \\ \frac{\partial^2 f}{\partial \epsilon_n \partial \epsilon_1} & \frac{\partial^2 f}{\partial \epsilon_n \partial \epsilon_2} & \frac{\partial^2 f}{\partial \epsilon_n \partial \epsilon_3} & . & . & \frac{\partial^2 f}{\partial \epsilon_n^2} \end{bmatrix}_{n \mathbf{X} n.}$$

$$= \begin{bmatrix} 2(1-\frac{1}{n}) & -\frac{2}{n} & -\frac{2}{n} & . & . & -\frac{2}{n} \\ -\frac{2}{n} & 2(1-\frac{1}{n}) & -\frac{2}{n} & . & . & -\frac{2}{n} \\ -\frac{2}{n} & -\frac{2}{n} & 2(1-\frac{1}{n}) & . & . & -\frac{2}{n} \\ . & . & . & . & . & . \\ . & . & . & . & . & . \\ -\frac{2}{n} & -\frac{2}{n} & -\frac{2}{n} & . & . & 2(1-\frac{1}{n}) \end{bmatrix}_{n \mathbf{X} n.}$$

3. Let $\mathbf{I}$ be a $n\mathbf{x}n$ identity matrix. Thus we obtain $\mathbf{F} - \lambda\mathbf{I}$, $\mathbf{F_1}$, as

$$\mathbf{F_1} = \begin{bmatrix} 2(1-\frac{1}{n})-\lambda & -\frac{2}{n} & -\frac{2}{n} & . & . & -\frac{2}{n} \\ -\frac{2}{n} & 2(1-\frac{1}{n})-\lambda & -\frac{2}{n} & . & . & -\frac{2}{n} \\ -\frac{2}{n} & -\frac{2}{n} & 2(1-\frac{1}{n})-\lambda & . & . & -\frac{2}{n} \\ . & . & . & . & . & . \\ . & . & . & . & . & . \\ -\frac{2}{n} & -\frac{2}{n} & -\frac{2}{n} & . & . & 2(1-\frac{1}{n})-\lambda \end{bmatrix}_{n \mathbf{X} n.}$$

4. We transform $\mathbf{F_1}$

$$\text{row } 1 + \text{row } 2 \longrightarrow \text{row } 1,$$

$$\text{row } 1 + \text{row } 3 \longrightarrow \text{row } 1,$$

$$\text{row } 1 + \text{row } 4 \longrightarrow \text{row } 1,$$

$$\vdots$$

$$\text{row } 1 + \text{row } n \longrightarrow \text{row } 1,$$

giving a new matrix $\mathbf{F_2}$ as follows:

$$\mathbf{F_2} = \begin{bmatrix} -\lambda & -\lambda & -\lambda & . \; . & -\lambda \\ -\frac{2}{n} & 2(1-\frac{1}{n})-\lambda & -\frac{2}{n} & . \; . & -\frac{2}{n} \\ -\frac{2}{n} & -\frac{2}{n} & 2(1-\frac{1}{n})-\lambda & . \; . & -\frac{2}{n} \\ . & . & . & . \; . & . \\ . & . & . & . \; . & . \\ -\frac{2}{n} & -\frac{2}{n} & -\frac{2}{n} & . \; . & 2(1-\frac{1}{n})-\lambda \end{bmatrix}_{n\mathbf{X}n.}$$

We transform $\mathbf{F_2}$

$$\text{column } 2 \text{ - column } 1 \longrightarrow \text{column } 2,$$

$$\text{column } 3 \text{ - column } 1 \longrightarrow \text{column } 3,$$

$$\text{column } 4 \text{ - column } 1 \longrightarrow \text{column } 4,$$

$$\vdots$$

$$\text{column } n \text{ - column } 1 \longrightarrow \text{column } n,$$

obtaining a new matrix $\mathbf{F_3}$ as follows:

$$\mathbf{F_3} = \begin{bmatrix} -\lambda & 0 & 0 & . & . & 0 \\ -\frac{2}{n} & 2-\lambda & 0 & . & . & 0 \\ -\frac{2}{n} & 0 & 2-\lambda & . & . & 0 \\ . & . & . & . & . & . \\ . & . & . & . & . & . \\ -\frac{2}{n} & 0 & 0 & . & . & 2-\lambda \end{bmatrix}_{n\mathbf{x}n.}$$

By theorem d in section 3 of chapter 4 in Searle [29], we obtain

$$\begin{aligned} & \det(\mathbf{F}-\lambda\mathbf{I}) \\ = \ & \det(\mathbf{F_1}) \\ = \ & \det(\mathbf{F_2}) \\ = \ & \det(\mathbf{F_3}) \\ = \ & \begin{vmatrix} -\lambda & 0 & 0 & . & . & 0 \\ -\frac{2}{n} & 2-\lambda & 0 & . & . & 0 \\ -\frac{2}{n} & 0 & 2-\lambda & . & . & 0 \\ . & . & . & . & . & . \\ . & . & . & . & . & . \\ -\frac{2}{n} & 0 & 0 & . & . & 2-\lambda \end{vmatrix}_{n\mathbf{x}n.} \end{aligned} \tag{D.10}$$

By theorem 5 in section 3 of chapter 2 in Hogben [28], we can find the determinant of $\mathbf{F_3}$ by expanding by cofactors on row 1 of $\mathbf{F_3}$, resulting

$$\begin{aligned} \det(\mathbf{F_3}) &= -\lambda(-1)^{1+1}\det(\mathbf{M}_{1,1}) + 0 * \det(\mathbf{M}_{1,2}) + \\ &\quad 0 * \det(\mathbf{M}_{1,3}) + \ldots + 0 * \det(\mathbf{M}_{1,n}) \\ &= -\lambda\det(\mathbf{M}_{1,1}). \end{aligned} \tag{D.11}$$

By definition 1 in section 1 of chapter 2 in Hogben [28], we obtain $\det(\mathbf{M}_{1,1})$ as follows:

$$\begin{aligned}\det(\mathbf{M}_{1,1}) &= \begin{vmatrix} 2-\lambda & 0 & 0 & . & . & 0 \\ 0 & 2-\lambda & 0 & . & . & 0 \\ 0 & 0 & 2-\lambda & . & . & 0 \\ . & . & . & . & . & . \\ . & . & . & . & . & . \\ 0 & 0 & 0 & . & . & 2-\lambda \end{vmatrix}_{(n-1)\mathbf{x}(n-1)} \\ &= (2-\lambda)^{n-1}. \end{aligned} \tag{D.12}$$

Substituting (D.11) and (D.12) into (D.10), we obtain

$$\det(\mathbf{F}-\lambda\mathbf{I}) = -\lambda(2-\lambda)^{n-1}. \tag{D.13}$$

According to theorem 2 in section 1 of chapter 7 in Hogben [28], we make (D.13) equal to zero to find the eigenvalues, λ, of $\mathbf{F}$, resulting,

$$\lambda = 0, \text{ or } 2. \tag{D.14}$$

By (D.14) it is clear that all the eigenvalues of $\mathbf{F}$ are nonnegative and one of them is zero. Therefore by theorem 2.1.2 in Myers & Milton [27], we know that $\mathbf{F}$ is positive semidefinite.

5. We show that f is convex as follows. Taking the third partial derivatives of f, we obtain

$$\frac{\partial^3 f}{\partial \epsilon_i^3} = 0, \quad \forall\, i, \tag{D.15}$$

$$\frac{\partial^3 f}{\partial \epsilon_i^2 \partial \epsilon_j} = 0, \quad \forall\, i \neq j, \tag{D.16}$$

$$\frac{\partial^3 f}{\partial \epsilon_i \partial \epsilon_j \partial \epsilon_k} = 0, \quad \forall\, i \neq j \neq k. \tag{D.17}$$

By (D.15), (D.16) and (D.17) we know that the third partial derivatives of f exist and are continuous. Thus by definition 3.3.5 in Bazaraa [11], theorem 14 of chapter 10 in DePree [35] and definition 15 of chapter 10 in DePree [35] (see section 5.2), we obtain that f is twice differentiable. Given that f is twice differentiable, E_n is a nonempty open convex set, and $\mathbf{F}$ is positive semidefinite on E_n as we have shown, by theorem 3.3.6 in Bazaraa [11] we conclude that f is convex.

This concludes the proof.

D.2

We first show that if n is a positive real number and m is a nonnegative real number such that $0 \leq m \leq n$, then $f(SE_1)$ has a global maximum at $m = \frac{n}{2}$ with the corresponding global maximum value as $\frac{n}{4}\kappa^2$. Since in our original problem $(m,n) \in (I^+ \cup \{0\}, I^+) \subset (R^+ \cup \{0\}, R^+)$, thus we know that if m is a nonnegative integer and n is a positive integer such that $0 \leq m \leq n$, then $f(SE_1) \leq \frac{n}{4}\kappa^2$. The details are as follows.

Proof:

1. Let's assume that m is a nonnegative real number and n is a positive real number such that $0 \leq m \leq n$. Taking the first partial derivatives of $f(SE_1)$ with respect to m, we obtain

$$\frac{\partial f(SE_1)}{\partial m} = \left(-1 - \frac{2(n-m)}{n}(-1)\right)\kappa^2. \tag{D.18}$$

Making (D.18) equal to zero, we obtain

$$\begin{aligned}\left(-1-\frac{2(n-m)}{n}(-1)\right) &= 0\\ \Longleftrightarrow -n+2(n-m) &= 0\\ \Longleftrightarrow n &= 2m\\ \Longleftrightarrow m &= \frac{n}{2}.\end{aligned} \tag{D.19}$$

2. Taking the second partial derivative of $f(SE_1)$ with respect to m, we obtain

$$\begin{aligned}\frac{\partial^2 f(SE_1)}{\partial m^2} &= -\frac{2}{n}\kappa^2\\ &< 0.\end{aligned} \tag{D.20}$$

By (D.20) we know that $f(SE_1)$ is a strictly concave function of m. Thus it is clear that $f(SE_1)$ has a global maximum at $m = \frac{n}{2}$. i.e.,

$$\begin{aligned}f(SE_1) &= (n-m-\frac{(n-m)^2}{n})\kappa^2\\ &\leq f(\frac{n}{2})\\ &= \frac{n}{4}\kappa^2.\end{aligned}$$

This concludes the proof.

APPENDIX E. THE CONDITIONS OF THE LARGEST G_n'

Proof:

1. Let IND be the intersection of the complements of $Int(D_i)\ \forall\ i$. i.e.,

$$\text{IND} \ = \ \cap_{i=1}^{n} C(Int(D_i)).$$

Given that

$$\delta_* \ \geq \ -\sqrt{n-1}\kappa, \tag{E.1}$$

as we have shown, we can show that the largest value of IND occurs when $\delta_* = -\sqrt{n-1}\kappa$. The argument is as follows.

If we choose a value of δ_*, say δ_*', such that $\delta_*' > -\sqrt{n-1}\kappa$, then we obtain

$$1 + \epsilon_i + \delta_*' \ > \ 1 + \epsilon_i - \sqrt{n-1}\kappa$$

$\forall\ i$. Let D_i' and D_i'' be two concentric discs with a common center of polar coordinate of $(1+\epsilon_i, \theta_i)$ and with the radii of $1 + \epsilon_i + \delta_*'$ and $1 + \epsilon_i - \sqrt{n-1}\kappa$ respectively. It is clear that

$$D_i'' \ \subset \ D_i',\ \forall\ i.$$

Thus we obtain

$$\begin{aligned} C(Int(D_i'')) \ &\supset \ C(Int(D_i'))\ \forall\ i. \\ \Rightarrow \cap_{i=1}^{n} C(Int(D_i'')) \ &\supseteq \ \cap_{i=1}^{n} C(Int(D_i')). \end{aligned} \tag{E.2}$$

We observe from (E.2) that the intersection of the complements of $Int(D_i'')\ \forall\ i$ contains the intersection of the complements of $Int(D_i')\ \forall\ i$. Thus we conclude that the largest value of IND occurs when $\delta_* = -\sqrt{n-1}\kappa$.

2. Now, we want to show that the largest value of IND occurs when $\epsilon_i = 0\ \forall\ i$. Let $\delta_* = -\sqrt{n-1}\kappa$. We obtain

$$1 + \epsilon_i + \delta_* \ \geq\ 1 + \delta_*\ \forall\ i.$$

Let D_i^0 be a disc with center of polar coordinate of $(1, \theta_i)$ and radius of $1 + \delta_*$. Then it is clear that (see Figure E.1)

$$D_i^0 \ \subseteq\ D_i\ \forall\ i.$$

Thus we obtain

$$\begin{aligned} C(Int(D_i^0)) \ &\supseteq\ C(Int(D_i))\ \forall\ i. \\ \Rightarrow \cap_{i=1}^n C(Int(D_i^0)) \ &\supseteq\ \cap_{i=1}^n C(Int(D_i)). \end{aligned} \tag{E.3}$$

We observe from (E.3) that the intersection of the complements of $Int(D_i^0)\ \forall\ i$ contains the intersection of the complements of $Int(D_i)\ \forall\ i$. Thus we conclude that the largest value of IND occurs when $\epsilon_i = 0\ \forall\ i$.

This concludes the proof.

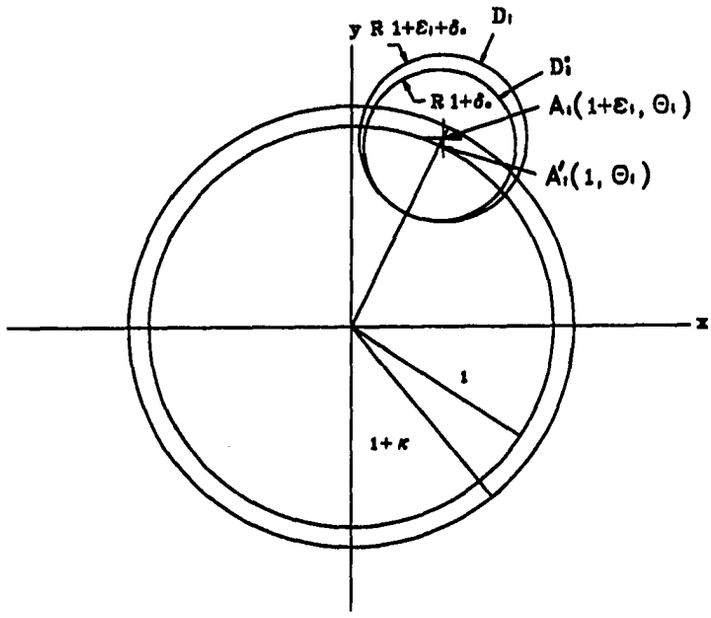

Figure E.1: Illustration of $D_i^0 \subseteq D_i$.

APPENDIX F. $L_{nc\theta'} = -U_{nc\theta'}$

Let

$$h_n(x, y, \epsilon_1, \epsilon_2, \ldots, \epsilon_n) = \sum_{i=1}^{n} \frac{x_i - x}{\sqrt{(x_i - x)^2 + (y_i - y)^2}}.$$

Before doing the proof, we need the following theorem and corollary.

Theorem 3.5 of chapter 5 in Mendelson [12]: A subset A of the real line is compact if and only if A is closed and bounded.

Corollary 4.3 of chapter 5 in Mendelson [12]: Let $X_1, X_2, \ldots, X_n$ be compact topological spaces. Then $\prod_{i=1}^{n} X_i$ is also compact.

Proof:

1. Given $(x_i, y_i) = (x_{i1}, y_{i1})\ \forall\ i$ and its corresponding value of $(\epsilon_1, \epsilon_2, \ldots, \epsilon_n)$, say $(\epsilon_{11}, \epsilon_{21}, \ldots, \epsilon_{n1})$, we take the first partial derivatives of $h_n(x, y, \epsilon_{11}, \epsilon_{21}, \ldots, \epsilon_{n1})$ with respect to x and y and obtain

$$\frac{\partial h_n(x, y, \epsilon_{11}, \epsilon_{21}, \ldots, \epsilon_{n1})}{\partial x} = \sum_{i=1}^{n} \frac{-(y_{i1} - y)^2}{((x_{i1} - x)^2 + (y_{i1} - y)^2)^{1.5}} \qquad \text{(F.1)}$$

$$< 0, \quad \text{and}$$

$$\frac{\partial h_n(x, y, \epsilon_{11}, \epsilon_{21}, \ldots, \epsilon_{n1})}{\partial y} = \sum_{i=1}^{n} \frac{(x_{i1} - x)(y_{i1} - y)}{((x_{i1} - x)^2 + (y_{i1} - y)^2)^{1.5}}. \qquad \text{(F.2)}$$

Given that $h_n(x, y, \epsilon_{11}, \epsilon_{21}, \ldots, \epsilon_{n1})$ is continuous and G_n is compact, by theorem 7.8 in Curtis [20] (see section 5.3.2) we know that there exists a global

maximum, say $U_1(x_1, y_1)$ in G_n. By (F.1) we know that $h_n(x, y, \epsilon_{11}, \epsilon_{21}, \ldots, \epsilon_{n1})$ is a decreasing function of x given y. Thus we know that the global maximum of $h_n(x, y, \epsilon_{11}, \epsilon_{21}, \ldots, \epsilon_{n1})$ occurs at the left boundary of G_n. Figure F.1 is shown to illustrate a possible location of $U_1(x_1, y_1)$ in G_n.

2. Given n is even, $(x, y) = (x_1, y_1)$ and $(x_i, y_i) = (x_{i1}, y_{i1})$ $\forall$ i, we can construct a new layout of (x, y), say $U_2(x_2, y_2)$, and (x_i, y_i), say (x_{i2}, y_{i2}), $\forall$ i such that

$$(x_2, y_2) = (-x_1, -y_1), \tag{F.3}$$

$$(x_{i2}, y_{i2}) = (-x_{i1}, -y_{i1}) \ \forall \ i. \tag{F.4}$$

As an illustration, Figure F.2 is shown as a symmetrical counterpart of Figure F.1 which satisfies (F.3) and (F.4). From (F.3) and (F.4), we obtain

$$\frac{x_{i1} - x_1}{\sqrt{(x_{i1} - x_1)^2 + (y_{i1} - y_1)^2}} = -\frac{x_{i2} - x_2}{\sqrt{(x_{i2} - x_2)^2 + (y_{i2} - y_2)^2}} \ \forall \ i,$$

$$\Rightarrow \sum_{i=1}^{n} \frac{x_{i1} - x_1}{\sqrt{(x_{i1} - x_1)^2 + (y_{i1} - y_1)^2}} = -\sum_{i=1}^{n} \frac{x_{i2} - x_2}{\sqrt{(x_{i2} - x_2)^2 + (y_{i2} - y_2)^2}}. \tag{F.5}$$

We observe from (F.5) that we can construct two layouts of (x, y) and (x_i, y_i) $\forall$ i such that the value of $h_n(x, y, \epsilon_1, \epsilon_2, \ldots, \epsilon_n)$ of one layout is the negative value of its counterpart of the other layout.

3. Since $(x, y) \in G_n$ and $0 \leq \epsilon_i \leq \kappa$ $\forall$ i, thus we know that $x, y, \epsilon_1, \epsilon_2, \ldots, \epsilon_n$ are closed and bounded. Therefore, by theorem 3.5 of chapter 5 in Mendelson [12], we know that $\{(x, y) : (x, y) \in G_n\}$, $\{\epsilon_i : 0 \leq \epsilon_i \leq \kappa\}$ $\forall$ i, are compact. As a result, by corollary 4.3 of chapter 5 in Mendelson [12], we know that the set $\{(x, y, \epsilon_1, \epsilon_2, \ldots, \epsilon_n) : (x, y) \in G_n$ and $0 \leq \epsilon_i \leq \kappa, \forall\ i\}$ is compact. Consequently, by theorem 4.5 of chapter 5 in Mendelson [12] (see Appendix D),

we know that the set $\{(x, y, \epsilon_1, \epsilon_2, \ldots, \epsilon_n) : (x, y) \in G_n$ and $0 \leq \epsilon_i \leq \kappa$, $\forall\ i\}$ is closed and bounded. It is clear that $h_n(x, y, \epsilon_1, \epsilon_2, \ldots, \epsilon_n)$ is continuous, therefore, by theorem 7.8 in Curtis [20] there exists a global maximum of $h_n(x, y, \epsilon_1, \epsilon_2, \ldots, \epsilon_n)$.

4. Let's say that the global maximum of $h_n(x, y, \epsilon_1, \epsilon_2, \ldots, \epsilon_n)$ occurs when

$$\begin{aligned} (x, y) &= (x_u^*, y_u^*), \text{ and} \\ (x_i, y_i) &= (x_i^*, y_i^*)\ \forall\ i. \end{aligned}$$

In addition, let's say the global maximum value is $U_{nc\theta'}$. i.e.,

$$h_n(x_u^*, y_u^*, \epsilon_1^*, \epsilon_2^*, \ldots, \epsilon_n^*) = U_{nc\theta'}. \tag{F.6}$$

Furthermore, there exists another set of (x, y), say (x_{u*}, y_{u*}), and (x_i, y_i), say (x_{i*}, y_{i*}), $\forall\ i$ such that

$$\begin{aligned} (x_{u*}, y_{u*}) &= (-x_u^*, -y_u^*), \\ (x_{i*}, y_{i*}) &= (-x_i^*, -y_i^*)\ \forall\ i, \text{ and} \\ h_n(x_{u*}, y_{u*}, \epsilon_{1*}, \epsilon_{2*}, \ldots, \epsilon_{n*}) &= -h_n(x_u^*, y_u^*, \epsilon_1^*, \epsilon_2^*, \ldots, \epsilon_n^*). \end{aligned} \tag{F.7}$$

Let

$$h_n(x_{u*}, y_{u*}, \epsilon_{1*}, \epsilon_{2*}, \ldots, \epsilon_{n*}) = L_{nc\theta'}. \tag{F.8}$$

By (F.6), (F.7), and (F.8), we obtain

$$L_{nc\theta'} = -U_{nc\theta'}. \tag{F.9}$$

5. We claim that $L_{nc\theta'}$ is a global minimum value of $h_n(x, y, \epsilon_1, \epsilon_2, \ldots, \epsilon_n)$. The argument is as follows. Suppose that $L_{nc\theta'}$ is not a global minimum value of $h_n(x, y, \epsilon_1, \epsilon_2, \ldots, \epsilon_n)$, then there exists a global minimum such that $(x, y) = (x_{s*}, y_{s*})$, and $(x_i, y_i) = (x_{si}, y_{si})\ \forall\ i$, resulting

$$h_n(x_{s*}, y_{s*}, \epsilon_{s1}, \epsilon_{s2}, \ldots, \epsilon_{sn}) \ < \ L_{nc\theta'}. \tag{F.10}$$

Furthermore, there exists a set of (x, y), say (x_s^*, y_s^*), and (x_i, y_i), say (x_{ti}, y_{ti}), $\forall\ i$ such that

$$\begin{aligned} (x_s^*, y_s^*) &= (-x_{s*}, -y_{s*}) \\ (x_{ti}, y_{ti}) &= (-x_{si}, -y_{si})\ \forall\ i, \text{ and} \\ h_n(x_s^*, y_s^*, \epsilon_{t1}, \epsilon_{t2}, \ldots, \epsilon_{tn}) &= -h_n(x_{s*}, y_{s*}, \epsilon_{s1}, \epsilon_{s2}, \ldots, \epsilon_{sn}). \end{aligned} \tag{F.11}$$

By (F.10), (F.9) and (F.11) we obtain

$$\begin{aligned} -h_n(x_{s*}, y_{s*}, \epsilon_{s1}, \epsilon_{s2}, \ldots, \epsilon_{sn}) &> -L_{nc\theta'}. \\ \Longleftrightarrow h_n(x_s^*, y_s^*, \epsilon_{t1}, \epsilon_{t2}, \ldots, \epsilon_{tn}) &> U_{nc\theta'}. \end{aligned} \tag{F.12}$$

We observe from (F.12) that $U_{nc\theta'}$ is not a global maximum of $h_n(x, y, \epsilon_1, \epsilon_2, \ldots, \epsilon_n)$. This contradicts the fact that $U_{nc\theta'}$ is a global maximum of $h_n(x, y, \epsilon_1, \epsilon_2, \ldots, \epsilon_n)$. Thus we know that our assumption is not true. i.e., $L_{nc\theta'}$ is a global minimum of $h_n(x, y, \epsilon_1, \epsilon_2, \ldots, \epsilon_n)$.

This concludes the proof.

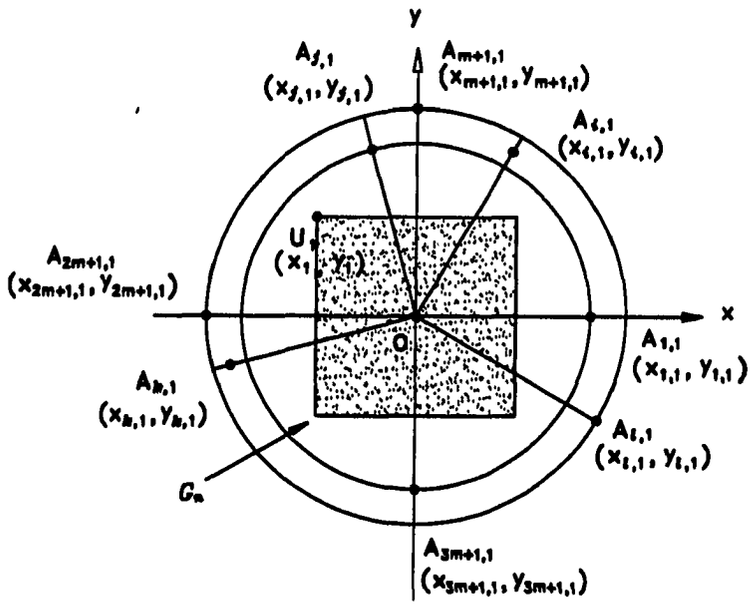

Figure F.1: A Possible Location of Global Maximum Point $U_1(x_1, y_1)$ of $h_n(x, y, \epsilon_{11}, \epsilon_{21}, \ldots, \epsilon_{n1})$.

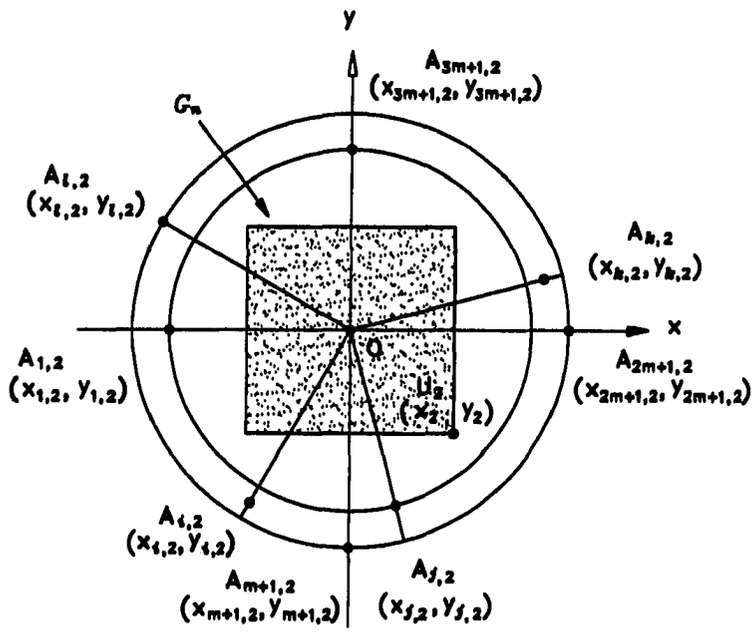

Figure F.2: A Symmetrical Counterpart of Figure F.1 Reflected by $O(0, 0)$.

APPENDIX G. $L_{n\kappa c} = -U_{n\kappa c}$

We will do the proof in two parts. First, we will show that when n is a multiple of 4, then $L_{n\kappa c} = -U_{n\kappa c}$. Next, we will show that when n is even but not a multiple of 4, then $L_{n\kappa c} = -U_{n\kappa c}$ also. The detail is as follows.

Proof:

1. Since n is even, let $n = 2m$. Recall that

$$L_{n\kappa c} = \sum_{i=t_1+2}^{n-t_1} \kappa \cos\left((i-1)\frac{2\pi}{n}\right), \text{ and} \tag{G.1}$$

$$U_{n\kappa c} = \kappa + 2\kappa \sum_{i=2}^{t_1+1} \cos\left((i-1)\frac{2\pi}{n}\right). \tag{G.2}$$

2. Case 1: If m is even, then let $m = 2l$. So we obtain $n = 4l$, resulting in

$$t_1 = \lfloor \frac{n}{4} \rfloor = l. \tag{G.3}$$

Substituting t_1 in (G.3) into (G.2) and (G.1), we obtain

$$U_{n\kappa c} = \kappa + 2\kappa \sum_{i=2}^{l+1} \cos\left((i-1)\frac{2\pi}{4l}\right), \text{ and} \tag{G.4}$$

$$\begin{aligned} L_{n\kappa c} &= \sum_{i=l+2}^{3l} \kappa \cos\left((i-1)\frac{2\pi}{4l}\right) \\ &= \sum_{i=l+2}^{2l} \kappa \cos\left((i-1)\frac{2\pi}{4l}\right) - \kappa + \sum_{i=2l+2}^{3l} \kappa \cos\left((i-1)\frac{2\pi}{4l}\right) \end{aligned}$$

$$
\begin{aligned}
&= -\kappa + 2\kappa \sum_{i=l+2}^{2l} \cos\left((i-1)\frac{2\pi}{4l}\right) \\
&= -\kappa - 2\kappa \sum_{i=l+2}^{2l} \cos\left(\pi - (i-1)\frac{2\pi}{4l}\right) \\
&= -\kappa - 2\kappa \sum_{i=1}^{l-1} \cos\left(i\frac{2\pi}{4l}\right) \\
&= -\kappa - 2\kappa \sum_{i=2}^{l+1} \cos\left((i-1)\frac{2\pi}{4l}\right) \qquad (\because \cos(l\frac{2\pi}{4l}) = 0) \\
&= -U_{n\kappa c} \qquad \text{(G.5)}
\end{aligned}
$$

3. Case 2: If m is not even, then let $m = 2l+1$. So we obtain $n = 4l+2$, resulting in

$$t_1 = \lfloor \frac{n}{4} \rfloor = l. \qquad \text{(G.6)}$$

Substituting t_1 in (G.6) into (G.2) and (G.1), we obtain

$$
\begin{aligned}
U_{n\kappa c} &= \kappa + 2\kappa \sum_{i=2}^{l+1} \cos\left((i-1)\frac{2\pi}{4l+2}\right), \text{ and} \qquad \text{(G.7)} \\
L_{n\kappa c} &= \sum_{i=l+2}^{3l+2} \kappa \cos\left((i-1)\frac{2\pi}{4l+2}\right) \\
&= \sum_{i=l+2}^{2l+1} \kappa \cos\left((i-1)\frac{2\pi}{4l+2}\right) - \kappa + \sum_{i=2l+3}^{3l+2} \kappa \cos\left((i-1)\frac{2\pi}{4l+2}\right) \\
&= -\kappa + 2\kappa \sum_{i=l+2}^{2l+1} \cos\left((i-1)\frac{2\pi}{4l+2}\right) \\
&= -\kappa - 2\kappa \sum_{i=l+2}^{2l+1} \cos\left(\pi - (i-1)\frac{2\pi}{4l+2}\right) \\
&= -\kappa - 2\kappa \sum_{i=2}^{l+1} \cos\left((i-1)\frac{2\pi}{4l+2}\right) \\
&= -U_{n\kappa c} \qquad \text{(G.8)}
\end{aligned}
$$

This concludes the proof.

APPENDIX H. $U_{nc\theta'} = U_{ns\theta'}$

Let

$$h_n(x, y, \epsilon_1, \epsilon_2, \ldots, \epsilon_n) = \sum_{i=1}^{n} \frac{x_i - x}{\sqrt{(x_i - x)^2 + (y_i - y)^2}}, \text{ and}$$

$$t_n(x, y, \epsilon_1, \epsilon_2, \ldots, \epsilon_n) = \sum_{i=1}^{n} \frac{y_i - y}{\sqrt{(x_i - x)^2 + (y_i - y)^2}}.$$

We show that

$$U_{ns\theta'} = U_{nc\theta'},$$

where $U_{nc\theta'}$ is a global maximum value of $h_n(x, y, \epsilon_1, \epsilon_2, \ldots, \epsilon_n)$ and $U_{ns\theta'}$ is a global maximum value of $t_n(x, y, \epsilon_1, \epsilon_2, \ldots, \epsilon_n)$.

Proof:

1. Let's say a global maximum of $h_n(x, y, \epsilon_1, \epsilon_2, \ldots, \epsilon_n)$ occurs when

$$(x, y) = (x_u, y_u),$$

$$(x_i, y_i) = (x_{iu}, y_{iu}) \ \forall \ i. \tag{H.1}$$

Figure H.1 shows a possible location of the global maximum point $U(x_u, y_u)$ and $A_{iu}(x_{iu}, y_{iu}) \ \forall \ i$ with the corresponding value of $(\epsilon_1, \epsilon_2, \ldots, \epsilon_n)$, say $(\epsilon_{1u}, \epsilon_{2u}, \ldots, \epsilon_{nu})$, in the annulus. Thus we obtain that

$$h_n(x_u, y_u, \epsilon_{1u}, \epsilon_{2u}, \ldots, \epsilon_{nu}) = U_{nc\theta'}. \tag{H.2}$$

2. Given $n = 4m$ and the layout of (x, y) and (x_i, y_i) $\forall$ i in Figure H.1, we can construct a new layout of (x, y), say $V(x_v, y_v)$, and (x_i, y_i), say (x_{iv}, y_{iv}), $\forall$ i such that

$$(x_v, y_v) = (y_u, x_u), \tag{H.3}$$

$$(x_{iv}, y_{iv}) = (y_{iu}, x_{iu}) \ \forall \ i. \tag{H.4}$$

We observe from (H.3) and (H.4) that (x_v, y_v) and (x_{iv}, y_{iv}) $\forall$ i are the reflection of (x_u, y_u) and (x_{iu}, y_{iu}) $\forall$ i by line $x = y$. Figure H.2 shows a reflection of Figure H.1 by line $x = y$. From (H.3) and (H.4) we obtain

$$\frac{x_{iu} - x_u}{\sqrt{(x_{iu} - x_u)^2 + (y_{iu} - y_u)^2}} = \frac{y_{iv} - y_v}{\sqrt{(y_{iv} - y_v)^2 + (x_{iv} - x_v)^2}} \ \forall \ i,$$

$$\Rightarrow \sum_{i=1}^{n} \frac{x_{iu} - x_u}{\sqrt{(x_{iu} - x_u)^2 + (y_{iu} - y_u)^2}} = \sum_{i=1}^{n} \frac{y_{iv} - y_v}{\sqrt{(y_{iv} - y_v)^2 + (x_{iv} - x_v)^2}}. \tag{H.5}$$

We observe from (H.5) that we can construct two layouts of (x, y) and (x_i, y_i) $\forall$ i such that the value of $h_n(x, y, \epsilon_1, \epsilon_2, \ldots, \epsilon_n)$ of one layout is equal to its counterpart of the other layout.

3. We claim that $U_{ns\theta'} = U_{nc\theta'}$. The argument is as follows. Suppose that $U_{ns\theta'} \neq U_{nc\theta'}$, then $U_{ns\theta'} > U_{nc\theta'}$ or $U_{ns\theta'} < U_{nc\theta'}$. Let's say $U_{ns\theta'} > U_{nc\theta'}$, then there exists a global maximum point, say $(x, y) = (x_{s*}, y_{s*})$ and $(x_i, y_i) = (x_{is}, y_{is})$ $\forall$ i, of $t_n(x, y, \epsilon_1, \epsilon_2, \ldots, \epsilon_n)$, with corresponding value of $(\epsilon_1, \epsilon_2, \ldots, \epsilon_n)$, say $(\epsilon_{1s}, \epsilon_{2s}, \ldots, \epsilon_{ns})$. Thus we obtain

$$t_n(x_{s*}, y_{s*}, \epsilon_{1s}, \epsilon_{2s}, \ldots, \epsilon_{ns}) > U_{nc\theta'}. \tag{H.6}$$

Furthermore, there exists a set of (x, y), say (x_{w*}, y_{w*}), and (x_i, y_i), say (x_{iw}, y_{iw}), $\forall$ i with the corresponding value of $(\epsilon_1, \epsilon_2, \ldots, \epsilon_n)$, say $(\epsilon_{1w}, \epsilon_{2w}, \ldots, \epsilon_{nw})$, such

that

$$\begin{aligned}(x_{w*}, y_{w*}) &= (y_{s*}, x_{s*}) \\ (x_{iw}, y_{iw}) &= (y_{is}, x_{is}) \ \forall \ i, \text{ and} \\ h_n(x_{w*}, y_{w*}, \epsilon_{1w}, \epsilon_{2w}, \ldots, \epsilon_{nw}) &= t_n(x_{s*}, y_{s*}, \epsilon_{1s}, \epsilon_{2s}, \ldots, \epsilon_{ns}). \qquad \text{(H.7)}\end{aligned}$$

Substituting (H.7) into (H.6), we obtain

$$h_n(x_{w*}, y_{w*}, \epsilon_{1w}, \epsilon_{2w}, \ldots, \epsilon_{nw}) > U_{nc\theta'}. \qquad \text{(H.8)}$$

We observe from (H.8) that $U_{nc\theta'}$ is not a global maximum value of $h_n(x, y, \epsilon_1, \epsilon_2, \ldots, \epsilon_n)$. This contradicts the fact that $U_{nc\theta'}$ is a global maximum value of $h_n(x, y, \epsilon_1, \epsilon_2, \ldots, \epsilon_n)$. Thus we know that our assumption is not true. i.e., $U_{ns\theta'} \not> U_{nc\theta'}$.

4. Applying the same procedure to the case of $U_{ns\theta'} < U_{nc\theta'}$, we can show that $U_{ns\theta'} \not< U_{nc\theta'}$.

This concludes the proof.

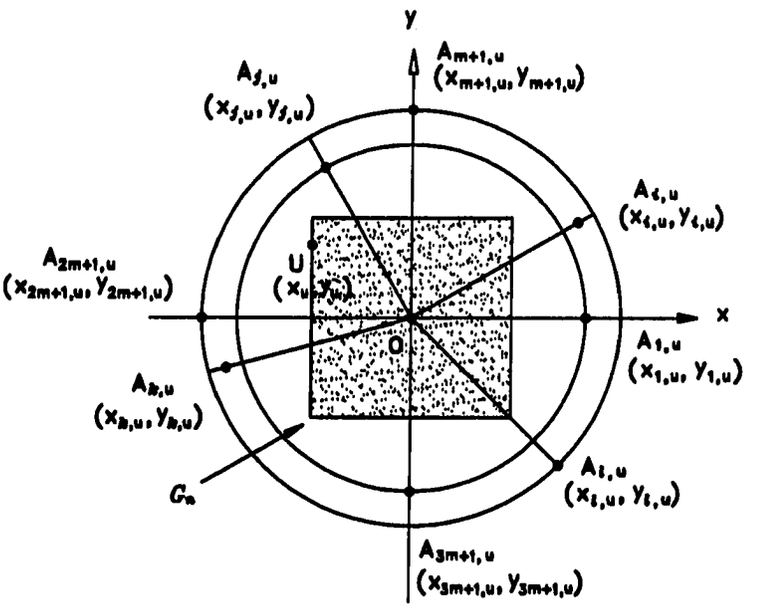

Figure H.1: A Possible Location of Global Maximum Point $U(x_u, y_u)$ and $A_{iu}(x_{iu}, y_{iu})\ \forall\ i$ in the Annulus.

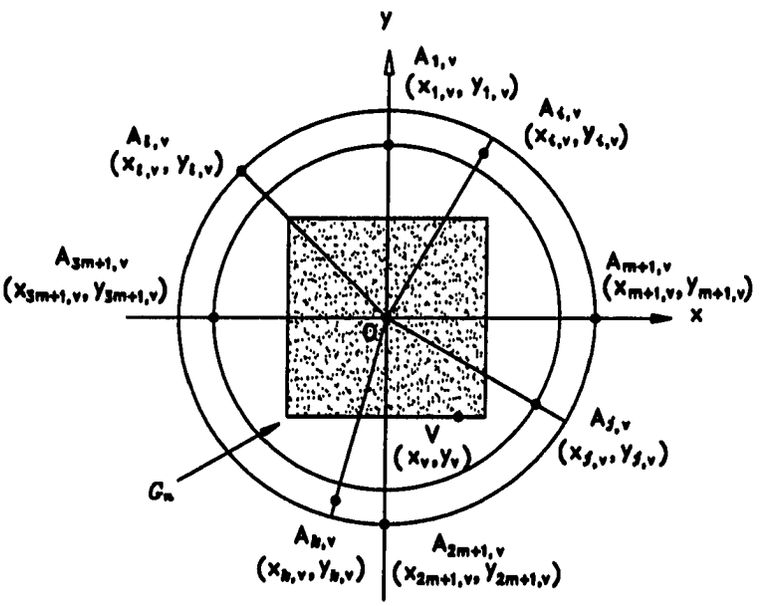

Figure H.2: A Counterpart of Figure H.1 Reflected by Line $x = y$.

APPENDIX I. $U_{n\kappa c} = U_{n\kappa s}$

Recall that

$$U_{n\kappa c} = \kappa + 2\kappa \sum_{i=2}^{t_1+1} \cos\left((i-1)\frac{2\pi}{n}\right), \text{ and} \tag{I.1}$$

$$U_{n\kappa s} = \kappa \sum_{i=1}^{t_2+1} \sin\left((i-1)\frac{2\pi}{n}\right). \tag{I.2}$$

Proof:

1. Given that $n = 4m$, we obtain $t_1 = m$ and $t_2 = 2m$. Substituting t_1 into (I.1), we obtain

$$\begin{aligned} U_{n\kappa c} &= \kappa + 2\kappa \sum_{i=2}^{m+1} \cos\left((i-1)\frac{2\pi}{4m}\right) \\ &= \kappa + 2\kappa \sum_{i=2}^{m} \cos\left((i-1)\frac{\pi}{2m}\right). \end{aligned} \tag{I.3}$$

Substituting t_2 into (I.2), we obtain

$$\begin{aligned} U_{n\kappa s} &= \kappa \sum_{i=1}^{2m+1} \sin\left((i-1)\frac{\pi}{2m}\right) \\ &= \kappa \sum_{i=1}^{m} \sin\left((i-1)\frac{\pi}{2m}\right) + \kappa \sin\left((m+1-1)\frac{\pi}{2m}\right) \\ &\quad + \kappa \sum_{i=m+2}^{2m+1} \sin\left((i-1)\frac{\pi}{2m}\right) \\ &= \kappa + 2\kappa \sum_{i=1}^{m} \sin\left((i-1)\frac{\pi}{2m}\right) \end{aligned}$$

$$
\begin{aligned}
&= \kappa + 2\kappa \sum_{i=2}^{m} \sin\left((i-1)\frac{\pi}{2m}\right) \\
&= \kappa + 2\kappa \sum_{i=2}^{m} \cos\left(\frac{\pi}{2} - (i-1)\frac{\pi}{2m}\right) \\
&= \kappa + 2\kappa \sum_{i=2}^{m} \cos\left((m-i+1)\frac{\pi}{2m}\right) \\
&= \kappa + 2\kappa \sum_{i=2}^{m} \cos\left((i-1)\frac{\pi}{2m}\right) \\
&= U_{n\kappa c}. \qquad \text{(I.4)}
\end{aligned}
$$

This concludes the proof.

APPENDIX J. THEOREM 2

Theorem 2 Let S be a nonempty compact polyhedral set in E_n, and let $f : E_n \rightarrow E_1$ be a strictly convex function and continuous on S. Consider the problem to maximize $f(\mathbf{x})$ subject to $\mathbf{x} \in$ S. There then exists an optimal solution $\overline{\mathbf{x}}$ to the problem, where $\overline{\mathbf{x}}$ only occurs at an extreme point of S.

Before doing the proof we need the following definitions and theorem.

Definition 2.5.3 in Bazaraa [11]: Let S be a closed convex set in E_n. A nonzero vector $\mathbf{d}$ in E_n is called a *direction* of S if for each $\mathbf{x} \in S$, $\mathbf{x} + \lambda\mathbf{d} \in S$ $\forall$ $\lambda \geq 0$. Two directions $\mathbf{d_1}$ and $\mathbf{d_2}$ of S are called *distinct* if $\mathbf{d_1} \neq \alpha\mathbf{d_2}$ $\forall$ $\alpha > 0$. A direction $\mathbf{d}$ of S is called an *extreme direction* if it cannot be written as a positive linear combination of two distinct directions, i.e., if $\mathbf{d} = \lambda_1\mathbf{d_1} + \lambda_2\mathbf{d_2}$ $\forall$ $\lambda_1, \lambda_2 > 0$ then $\mathbf{d_1} = \alpha\mathbf{d_2}$ for some $\alpha > 0$.

Theorem 2.5.7 in Bazaraa [11]: (*Representation Theorem*) Let S be a nonempty polyhedral set in E_n of the form $\{\mathbf{x} : \mathbf{Ax} \leq \mathbf{b} \text{ and } \mathbf{x} \geq \mathbf{0}\}$, where $\mathbf{A}$ is an mxn matrix with rank m and $\mathbf{b}$ is an m vector. Let $\mathbf{x_1}, \ldots, \mathbf{x_k}$ be the extreme points of S and $\mathbf{d_1}, \ldots, \mathbf{d_l}$ be the extreme directions of S. Then $\mathbf{x} \in S$ if and only if $\mathbf{x}$ can be written as

$$\mathbf{x} = \sum_{i=1}^{k} \lambda_i \mathbf{x_i} + \sum_{i=1}^{l} \mu_i \mathbf{d_i},$$

$$\sum_{i=1}^{k} \lambda_i = 1,$$

$$\lambda_i \geq 0 \ \forall \ i = 1, 2, \ldots, k,$$

$$\mu_i \geq 0 \ \forall \ i = 1, 2, \ldots, l.$$

Proof:

This proof is modified from the proof of theorem 3.4.6 in Bazaraa [11].

1. Since S is compact and f is continuous on S, f assumes a maximum at $\mathbf{x}' \in S$. If $\mathbf{x}'$ is an extreme point of S, then we are done. Otherwise, by thereon 2.5.7 in Bazaraa [11], $\mathbf{x}' = \sum_{i=1}^{k} \lambda_i \mathbf{x}_i$, where $\sum_{i=1}^{k} \lambda_i = 1$, $\lambda_i > 0 \ \forall \ i$, and $\mathbf{x}_i$ is an extreme point of $S \ \forall \ i$. By strictly convexity of f, we have

$$f(\mathbf{x}') = f\left(\sum_{i=1}^{k} \lambda_i \mathbf{x}_i\right) < \sum_{i=1}^{k} \lambda_i f(\mathbf{x}_i). \tag{J.1}$$

But since $f(\mathbf{x}') \geq f(\mathbf{x}_i) \ \forall \ i$, we obtain

$$\begin{aligned} & f(\mathbf{x}') \geq f(\mathbf{x}_i) \ \forall \ i \\ \Longrightarrow \ & \lambda_i f(\mathbf{x}') \geq \lambda_i f(\mathbf{x}_i) \ \forall \ i \quad (\because \ \lambda_i > 0) \\ \Longrightarrow \ & \sum_{i=1}^{k} \lambda_i f(\mathbf{x}') \geq \sum_{i=1}^{k} \lambda_i f(\mathbf{x}_i) \\ \Longrightarrow \ & f(\mathbf{x}') \geq \sum_{i=1}^{k} \lambda_i f(\mathbf{x}_i). \quad (\because \ \sum_{i=1}^{k} \lambda_i = 1) \end{aligned} \tag{J.2}$$

(J.2) contradicts (J.1). Thus we know that $\mathbf{x}'$ cannot be a non-extreme point.

This concludes the proof.

APPENDIX K. THE GLOBAL MAXIMUM OF $g_n(x, y, \epsilon_1, \epsilon_2, \ldots, \epsilon_n)$ IS INVARIANT WHEN (x, y) IS AT ANY OF THE VERTICES OF G_n

We show that there exists a global maximum of $g_n(x, y, \epsilon_1, \epsilon_2, \ldots, \epsilon_n)$. Furthermore, given that s_n is one half the length of a side of G_n, P_1, P_2, P_3, P_4 are the four vertices of G_n such that P_1 has Cartesian coordinate of (s_n, s_n), and P_2 has Cartesian coordinate of $(-s_n, s_n)$, and P_3 has Cartesian coordinate of $(-s_n, -s_n)$, and P_4 has Cartesian coordinate of $(s_n, -s_n)$, then the global maximum of $g_n(x, y, \epsilon_1, \epsilon_2, \ldots, \epsilon_n)$ occurs only when (x, y) is at one of the vertices of G_n, moreover, the global maximum value of $g_n(x, y, \epsilon_1, \epsilon_2, \ldots, \epsilon_n)$ is invariant when (x, y) is at any of the vertices of G_n.

Proof:

1. Given that $g_n(x, y, \epsilon_1, \epsilon_2, \ldots, \epsilon_n)$ is continuous, and the set $\{(x, y, \epsilon_1, \epsilon_2, \ldots, \epsilon_n) : (x, y) \in G_n \text{ and } 0 \leq \epsilon_i \leq \kappa \ \forall \ i\}$ is closed and bounded, by theorem 7.8 in Curtis [20] (see section 5.3.2) we obtain that there exists a global maximum of $g_n(x, y, \epsilon_1, \epsilon_2, \ldots, \epsilon_n)$. Let's say the global maximum of $g_n(x, y, \epsilon_1, \epsilon_2, \ldots, \epsilon_n)$ occurs when

$$\begin{aligned} (x, y) &= (x_b, y_b) \\ (x_i, y_i) &= (x_{bi}, y_{bi}) \ \forall \ i, \end{aligned} \tag{K.1}$$

with the corresponding value of $(\epsilon_1, \epsilon_2, \ldots, \epsilon_n)$, say $(\epsilon_{b1}, \epsilon_{b2}, \ldots, \epsilon_{bn})$. Given ϵ_{bi} $\forall \ i$, by Proposition 3 in Appendix A we obtain that $g_n(x, y, \epsilon_{b1}, \epsilon_{b2}, \ldots, \epsilon_{bn})$

is strictly convex for (x, y). As a result, by Theorem 2 in Appendix J, the maximum of $g_n(x, y, \epsilon_{b1}, \epsilon_{b2}, \ldots, \epsilon_{bn})$ occurs only when (x, y) is at an extreme point. Thus we claim that (x_b, y_b) must be at one of the vertices of G_n.

2. Now we want to show that the global maximum value of $g_n(x, y, \epsilon_1, \epsilon_2, \ldots, \epsilon_n)$ with (x, y) of $P_1(s_n, s_n)$ is equal to the global maximum value of $g_n(x, y, \epsilon_1, \epsilon_2, \ldots, \epsilon_n)$ with (x, y) of $P_3(-s_n, -s_n)$. The argument is as follows. Let's say a global maximum of $g_n(x, y, \epsilon_1, \epsilon_2, \ldots, \epsilon_n)$ with (x, y) of $P_1(s_n, s_n)$ occurs when

$$(x_i, y_i) \;=\; (x_{is}, y_{is}) \;\forall\; i,$$

and with the corresponding global maximum value, say U_{r1}. i.e.,

$$U_{r1} \;=\; \sum_{i=1}^{n} \sqrt{(x_{is} - s_n)^2 + (y_{is} - s_n)^2}.$$

Furthermore, let's say the global maximum of $g_n(x, y, \epsilon_1, \epsilon_2, \ldots, \epsilon_n)$ with (x, y) of $P_3(-s_n, -s_n)$ occurs when

$$(x_i, y_i) \;=\; (x_{ip}, y_{ip}) \;\forall\; i,$$

and with the corresponding global maximum value, say U_{r3}. i.e.,

$$U_{r3} \;=\; \sum_{i=1}^{n} \sqrt{(x_{ip} - (-s_n))^2 + (y_{ip} - (-s_n))^2}.$$

Suppose that $U_{r1} \neq U_{r3}$ and $U_{r1} > U_{r3}$. Given $n = 4m$, we construct a new layout of (x_i, y_i), say (x_{iq}, y_{iq}) $\forall\, i$ such that

$$(x_{iq}, y_{iq}) \;=\; (-x_{is}, -y_{is}) \;\forall\; i. \qquad \text{(K.2)}$$

Thus by (K.2), we obtain

$$\sqrt{(x_{is} - s_n)^2 + (y_{is} - s_n)^2} = \sqrt{(-x_{is} - (-s_n))^2 + (-y_{is} - (-s_n))^2} \;\forall\; i,$$

$$\Rightarrow \sum_{i=1}^{n} \sqrt{(x_{is} - s_n)^2 + (y_{is} - s_n)^2} = \sum_{i=1}^{n} \sqrt{(-x_{is} - (-s_n))^2 + (-y_{is} - (-s_n))^2},$$

$$\Rightarrow U_{r1} = \sum_{i=1}^{n} \sqrt{(-x_{is} - (-s_n))^2 + (-y_{is} - (-s_n))^2}. \qquad \text{(K.3)}$$

Observing from (K.3) that when $(x, y) = (-s_n, -s_n)$, we obtain a value of U_{r1} for $g_n(x, y, \epsilon_1, \epsilon_2, \ldots, \epsilon_n)$ which, by our assumption is greater than U_{r3}. This contradicts the fact that U_{r3} is the global maximum value of $g_n(x, y, \epsilon_1, \epsilon_2, \ldots, \epsilon_n)$ when $(x, y) = (-s_n, -s_n)$. Thus our assumption of $U_{r1} > U_{r3}$ is not true. i.e., $U_{r1} \not> U_{r3}$. Applying the same procedure to the assumption of $U_{r1} < U_{r3}$, we can show easily that this assumption is not true either. Therefore, we conclude that $U_{r1} = U_{r3}$.

3. Next, we want to show that the global maximum value of $g_n(x, y, \epsilon_1, \epsilon_2, \ldots, \epsilon_n)$ with (x, y) of $P_1(s_n, s_n)$ is equal to the global maximum value of $g_n(x, y, \epsilon_1, \epsilon_2, \ldots, \epsilon_n)$ with (x, y) of $P_2(-s_n, s_n)$. The argument is as follows. Let's say the global maximum of $g_n(x, y, \epsilon_1, \epsilon_2, \ldots, \epsilon_n)$ with (x, y) of $P_2(-s_n, s_n)$ occurs when

$$(x_i, y_i) \;=\; (x_{io}, y_{io}) \;\; \forall \;\; i,$$

and with the corresponding global maximum value, say U_{r2}. i.e.,

$$U_{r2} \;=\; \sum_{i=1}^{n} \sqrt{(x_{io} - (-s_n))^2 + (y_{io} - s_n)^2}.$$

Suppose that $U_{r1} \neq U_{r2}$ and $U_{r1} > U_{r2}$. Given $n = 4m$, we construct a new layout of (x_i, y_i), say (x_{iz}, y_{iz}) $\forall$ i such that

$$(x_{iz}, y_{iz}) \;=\; (-x_{is}, y_{is}) \;\; \forall \;\; i. \qquad \text{(K.4)}$$

Thus by (K.4), we obtain

$$\sqrt{(x_{is} - s_n)^2 + (y_{is} - s_n)^2} = \sqrt{(-x_{is} - (-s_n))^2 + (y_{is} - s_n)^2} \;\; \forall \;\; i,$$

$$\Rightarrow \sum_{i=1}^{n} \sqrt{(x_{is} - s_n)^2 + (y_{is} - s_n)^2} = \sum_{i=1}^{n} \sqrt{(-x_{is} - (-s_n))^2 + (y_{is} - s_n)^2},$$

$$\Rightarrow U_{r1} = \sum_{i=1}^{n} \sqrt{(-x_{is} - (-s_n))^2 + (y_{is} - s_n)^2}. \qquad \text{(K.5)}$$

Following the argument in proof statement 2, we conclude that $U_{r1} = U_{r2}$.

4. Let's say the global maximum of $g_n(x, y, \epsilon_1, \epsilon_2, \ldots, \epsilon_n)$ with (x, y) of $P_4(s_n, -s_n)$ occurs when

$$(x_i, y_i) \;=\; (x_{ic}, y_{ic}) \;\; \forall \;\; i,$$

and with the corresponding global maximum value, say U_{r4}. i.e.,

$$U_{r4} \;=\; \sum_{i=1}^{n} \sqrt{(x_{ic} - s_n)^2 + (y_{ic} - (-s_n))^2}.$$

Following the procedure in proof statement 3, we can show that $U_{r1} = U_{r4}$.

5. Given that $U_{r1} = U_{r3}$, $U_{r1} = U_{r2}$, and $U_{r1} = U_{r4}$ as we have shown, we obtain

$$U_{r1} = U_{r2} = U_{r3} = U_{r4}.$$

This concludes the proof.

APPENDIX L. THE GLOBAL MAXIMUM OF $g_n(s_n, s_n, \epsilon_1, \epsilon_2, \ldots, \epsilon_n)$ OCCURS WHEN $\epsilon_i = \kappa, \forall\ i$

Recall that $g_n(x, y, \epsilon_1, \epsilon_2, \ldots, \epsilon_n) = \sum_{i=1}^{n} \sqrt{(x_i - x)^2 + (y_i - y)^2}$. We show that for any element in $g_n(s_n, s_n, \epsilon_1, \epsilon_2, \ldots, \epsilon_n)$, say $g_{ni}\ (\epsilon_i) = \sqrt{(x_i - s_n)^2 + (y_i - s_n)^2}$, the global maximum of $g_{ni}(\epsilon_i)$ for $0 \leq \epsilon_i \leq \kappa$ occurs when $\epsilon_i = \kappa$. Then it is clear that the global maximum of $g_n(s_n, s_n, \epsilon_1, \epsilon_2, \ldots, \epsilon_n)$ occurs when $\epsilon_i = \kappa\ \forall\ i$.

Proof:

1. Taking the first partial derivative of $g_{ni}(\epsilon_i)$ with respect to ϵ_i, we obtain

$$\begin{aligned} \frac{\partial g_{ni}(\epsilon_i)}{\partial \epsilon_i} &= \frac{1}{2} \frac{2((1+\epsilon_i)\cos\theta_i - s_n)\cos\theta_i + 2((1+\epsilon_i)\sin\theta_i - s_n)\sin\theta_i}{\sqrt{((1+\epsilon_i)\cos\theta_i - s_n)^2 + ((1+\epsilon_i)\sin\theta_i - s_n)^2}} \\ &= \frac{1}{2} \frac{2(1+\epsilon_i) - 2s_n(\cos\theta_i + \sin\theta_i)}{\sqrt{((1+\epsilon_i)\cos\theta_i - s_n)^2 + ((1+\epsilon_i)\sin\theta_i - s_n)^2}}. \end{aligned} \tag{L.1}$$

Since $(x, y) \in G_n$ where $G_n \subset Int(D)$ and (s_n, s_n) is the upper right vertex of G_n, we obtain

$$s_n < \frac{\sqrt{2}}{2}. \tag{L.2}$$

2. Investigating the numerator of the right hand side of (L.1), we obtain

$$2(1+\epsilon_i) - 2s_n(\cos\theta_i + \sin\theta_i)$$

$$
\begin{aligned}
&\geq 2 - 2s_n(\cos\theta_i + \sin\theta_i) \qquad (\because \epsilon_i \geq 0) \\
&> 2 - 2\frac{\sqrt{2}}{2}(\cos\theta_i + \sin\theta_i) \qquad (\because \text{(L.2)}) \\
&= 2 - \sqrt{2}(\cos\theta_i + \sin\theta_i) \\
&\geq 2 - \sqrt{2}\text{x}\sqrt{2} \qquad (\because \sin\theta_i + \cos\theta_i \leq \sqrt{2}) \\
&= 0. \qquad \text{(L.3)}
\end{aligned}
$$

Substituting (L.3) into (L.1), we obtain

$$\frac{\partial g_{ni}(\epsilon_i)}{\partial \epsilon_i} > 0. \qquad \text{(L.4)}$$

By (L.4) we know that $g_{ni}(\epsilon_i)$ is a strictly increasing function of ϵ_i. Thus we know that the global maximum of $g_{ni}(\epsilon_i)$ occurs when $\epsilon_i = \kappa$.

This concludes the proof.

APPENDIX M. THE GLOBAL MINIMUM VALUES OF $h_n(s_n, s_n, \epsilon_1, \epsilon_2, \ldots, \epsilon_n)\ \forall\ \epsilon_i$ AND $h_n(s_n, -s_n, \epsilon_1, \epsilon_2, \ldots, \epsilon_n)\ \forall\ \epsilon_i$ ARE EQUAL

Proof:

1. Recall that

$$h_n(x, y, \epsilon_1, \epsilon_2, \ldots, \epsilon_n) \;=\; \sum_{i=1}^{n} \frac{x_i - x}{\sqrt{(x_i - x)^2 + (y_i - y)^2}}.$$

Let $L_{nc\theta' p1}$ be a global minimum value of $h_n(s_n, s_n, \epsilon_1, \epsilon_2, \ldots, \epsilon_n)\ \forall\ \epsilon_i$ and $L_{nc\theta' p2}$ be a global minimum value of $h_n(s_n, -s_n, \epsilon_1, \epsilon_2, \ldots, \epsilon_n)\ \forall\ \epsilon_i$. Suppose that $L_{nc\theta' p1} \neq L_{nc\theta' p2}$, and $L_{nc\theta' p1} < L_{nc\theta' p2}$. Let's say $L_{nc\theta' p1}$ occurs when

$$(x_i, y_i) \;=\; (x_{i1}, y_{i1}) \quad \forall\ i. \tag{M.1}$$

Then we construct a new layout of (x_i, y_i), say (x_{i2}, y_{i2}), such that

$$(x_{i2}, y_{i2}) \;=\; (x_{i1}, -y_{i1}) \quad \forall\ i. \tag{M.2}$$

From (M.2) we obtain

$$\frac{x_{i1} - s_n}{\sqrt{(x_{i1} - s_n)^2 + (y_{i1} - s_n)^2}} = \frac{x_{i2} - s_n}{\sqrt{(x_{i2} - s_n)^2 + (y_{i2} - (-s_n))^2}} \quad \forall\ i$$

$$\Rightarrow \sum_{i=1}^{n} \frac{x_{i1} - s_n}{\sqrt{(x_{i1} - s_n)^2 + (y_{i1} - s_n)^2}} = \sum_{i=1}^{n} \frac{x_{i2} - s_n}{\sqrt{(x_{i2} - s_n)^2 + (y_{i2} - (-s_n))^2}}$$

$$\Rightarrow L_{nc\theta' p1} = \sum_{i=1}^{n} \frac{x_{i2} - s_n}{\sqrt{(x_{i2} - s_n)^2 + (y_{i2} - (-s_n))^2}}. \tag{M.3}$$

We observe from (M.3) that when $(x, y) = (s_n, -s_n)$, the layout of $(x_i, y_i) = (x_{i2}, y_{i2})$ $\forall$ i will render a value of $L_{nc\theta' p1}$ for $h_n(x, y, \epsilon_1, \epsilon_2, \ldots, \epsilon_n)$, which by our assumption is less than $L_{nc\theta' p2}$. This contradicts the fact the $L_{nc\theta' p2}$ is a global minimum value of $h_n(s_n, -s_n, \epsilon_1, \epsilon_2, \ldots, \epsilon_n)$ $\forall$ ϵ_i. Thus we know that our assumption of $L_{nc\theta' p1} < L_{nc\theta' p2}$ is not true. Applying the same procedure to the assumption of $L_{nc\theta' p1} > L_{nc\theta' p2}$, we can show easily that this assumption is not true either. Therefore, we obtain

$$L_{nc\theta' p1} = L_{nc\theta' p2}.$$

This concludes the proof.

APPENDIX N. Subroutine of finding $L_{nc\theta'}$

In light of the result of chapter 4.2.3, we can use the following subroutine to find the $L_{nc\theta'}$.

Subroutine LCTHETA $(s_n, n, L_{nc\theta'})$

κ:= 0.05;

test1:= 0;

test2:= 0;

test3:= 0;

test4:= 0;

θ:= $(i-1)\frac{2\pi}{n}$;

*** Divide the annulus into four divisions by finding the four

*** dividing points n1, n2, n3, and n4.

for i from 1 to n do

if (test1 = 0) then

t1:= $\sin\theta$;

if t1 > s_n then

```
                n1:= i;
                test1:= 1;
            endif;
        endif;
        if (test2 = 0) then
            if (test1 = 1) and (θ > π/4) then
                n2:= i;
                test2:= 1;
            endif;
        endif;
        if (test3 = 0) then
            t3:= sin θ;
            if (test2 = 1) and (t3 < s_n) then
                n3:= i;
                test3:= 1;
            endif;
        endif;
        if (test4 = 0) then
            if (test3 = 1) and (θ > 5/4 π) then
                n4:= i;
                test4:= 1;
            endif;
        endif;
enddo;
```

*** Calculate the minimum sum of $\frac{(1+\epsilon_i)\cos\theta - s_n}{\sqrt{((1+\epsilon_i)\cos\theta - s_n)^2 + ((1+\epsilon_i)\sin\theta - s_n)^2}}$

*** when ϵ_i falls in the second part of division IV where $y \geq 0$.

for i from 1 to (n1 - 1) do

x[i]:= $\cos\theta$;

y[i]:= $\sin\theta$;

*** Calculate the minimum sum of $\frac{(1+\epsilon_i)\cos\theta - s_n}{\sqrt{((1+\epsilon_i)\cos\theta - s_n)^2 + ((1+\epsilon_i)\sin\theta - s_n)^2}}$

*** when ϵ_i falls between the boundary of divisions I & IV.

if $((1+\kappa)\sin\theta > s_n)$ then

testa1:= $\frac{\cos\theta - s_n}{\sqrt{(\cos\theta - s_n)^2 + (\sin\theta - s_n)^2}}$;

testa2:= $\frac{(1+\kappa)\cos\theta - s_n}{\sqrt{((1+\kappa)\cos\theta - s_n)^2 + ((1+\kappa)\sin\theta - s_n)^2}}$;

endif;

if (testa1 > testa2) then

x[i]:= $(1+\kappa)\cos\theta$

y[i]:= $(1+\kappa)\sin\theta$

endif;

enddo;

cos1:= $\sum_{i=1}^{n1-1} \frac{x[i] - s_n}{\sqrt{(x[i] - s_n)^2 + (y[i] - s_n)^2}}$;

*** Calculate the minimum sum of $\frac{(1+\epsilon_i)\cos\theta - s_n}{\sqrt{((1+\epsilon_i)\cos\theta - s_n)^2 + ((1+\epsilon_i)\sin\theta - s_n)^2}}$

*** when ϵ_i falls in division I.

for i from n1 to (n2 - 1) do

x[i]:= $(1+\kappa)\cos\theta$;

y[i]:= $(1+\kappa)\sin\theta$;

enddo;

cos2:= $\sum_{i=n1}^{n2-1} \frac{x[i]-s_n}{\sqrt{(x[i]-s_n)^2+(y[i]-s_n)^2}}$;

*** Calculate the minimum sum of $\frac{(1+\epsilon_i)\cos\theta - s_n}{\sqrt{((1+\epsilon_i)\cos\theta - s_n)^2 + ((1+\epsilon_i)\sin\theta - s_n)^2}}$

*** when ϵ_i falls in division II.

for i from n2 to (n3 - 1) do

x[i]:= $\cos\theta$;

y[i]:= $\sin\theta$;

enddo;

cos3:= $\sum_{i=n2}^{n3-1} \frac{x[i]-s_n}{\sqrt{(x[i]-s_n)^2+(y[i]-s_n)^2}}$;

*** Calculate the minimum sum of $\frac{(1+\epsilon_i)\cos\theta - s_n}{\sqrt{((1+\epsilon_i)\cos\theta - s_n)^2 + ((1+\epsilon_i)\sin\theta - s_n)^2}}$

*** when ϵ_i falls in division III.

count3:= 0;

for i from n3 to (n4 - 1) do

*** Calculate the minimum sum of $\frac{(1+\epsilon_i)\cos\theta - s_n}{\sqrt{((1+\epsilon_i)\cos\theta - s_n)^2 + ((1+\epsilon_i)\sin\theta - s_n)^2}}$

*** when ϵ_i falls between the boundary of divisions II & III.

if $((1+\kappa)\sin\theta > s_n)$ then

count3:= count3 + 1;

endif;

x[i]:= $(1+\kappa)\cos\theta$;

y[i]:= $(1+\kappa)\sin\theta$;

enddo;

if (count3 = 0) then

cos4:= $\sum_{i=n3}^{n4-1} \frac{x[i]-s_n}{\sqrt{(x[i]-s_n)^2+(y[i]-s_n)^2}}$;

else

cos4:= -count3 + $\sum_{n3+count3}^{n4-1} \frac{x[i]-s_n}{\sqrt{(x[i]-s_n)^2+(y[i]-s_n)^2}}$;

endif;

*** Calculate the minimum sum of $\frac{(1+\epsilon_i)\cos\theta - s_n}{\sqrt{((1+\epsilon_i)\cos\theta - s_n)^2 + ((1+\epsilon_i)\sin\theta - s_n)^2}}$

*** when ϵ_i falls in the first part of division IV where $y < 0$.

for i from n4 to n do

x[i]:= $\cos\theta$;

y[i]:= $\sin\theta$;

enddo;

cos5:= $\sum_{i=n4}^{n} \frac{x[i]-s_n}{\sqrt{(x[i]-s_n)^2+(y[i]-s_n)^2}}$;

$L_{nc\theta'}$:= cos1 + cos2 + cos3 + cos4 + cos5;

APPENDIX O. VALUES OF s_n AND x_n^*

Recall that $\kappa = 0.05$ and $x_n^* = a(n)\kappa$. The results of x_n^* are obtained in Table O.1 by implementing the iterative algorithm through Maple programming language [24]. It is clear that all the values of $x_n^* < \kappa$, thus we know that $a(n) < 1 \; \forall \; n$.

Table O.1: Values of s_n and x^*.

n	s_n	x^*
4	0.091163	.0263719
8	0.134066	.0250855
12	0.167033	.0328793
16	0.194579	.0292820
20	0.218713	.0333798
24	0.240451	.0307184
28	0.260389	.0335166
32	0.278911	.0314445
36	0.296281	.0335726
40	0.31269	.0318829
44	0.328282	.0336008
48	0.343168	.0321762
52	0.357435	.0336170
56	0.371155	.0323863
60	0.384387	.0336271
64	0.397178	.0325441
68	0.409571	.0336338
72	0.4216	.0326671
76	0.433296	.0336385
80	0.444685	.0327655

Table O.1 (Continued)

n	s_n	x^*
84	0.455789	.0336418
88	0.466629	.0328462
92	0.477224	.0336444
96	0.487588	.0329134
100	0.497737	.0336463
104	0.507684	.0329704
108	0.517439	.0336479
112	0.527014	.0330192
116	0.536418	.0336491
120	0.54566	.0330616
124	0.554749	.0336500
128	0.563691	.0330987
132	0.572493	.0336509
136	0.581163	.0331314
140	0.589705	.0336515
144	0.598125	.0331605
148	0.606428	.0336521
152	0.61462	.0331865
156	0.622703	.0336525
160	0.630684	.0332100
164	0.638564	.0336530
168	0.646349	.0332312
172	0.654041	.0336533
176	0.661644	.0332505
180	0.669161	.0336536
184	0.676594	.0332681
188	0.683946	.0336539
192	0.691221	.0332842
196	0.69842	.0336541
200	0.705545	.0332991

APPENDIX P. GLOBAL MAXIMUM VALUES OF $\frac{\partial^2 h_n(x,y,\epsilon_1,\epsilon_2,\ldots,\epsilon_n)}{\partial y^2} < 0$

Let U_{hn} be the global maximum value of $\frac{\partial^2 h_n(x,y,\epsilon_1,\epsilon_2,\ldots,\epsilon_n)}{\partial y^2}$ for $a(n)\kappa \leq x \leq s_n$, $-x \leq y \leq x$, and $0 \leq \epsilon_i \leq \kappa \; \forall \; i$. Recall that $\kappa = 0.05$ and $x^* = a(n)\kappa$. Let U_{hn}^i be the simulated value of global maximum of $\frac{\partial^2 h_n(x,y,\epsilon_1,\epsilon_2,\ldots,\epsilon_n)}{\partial y^2}$ when the simulated annealing was run for i times of $10,000$ iterations. The simulated results of U_{hn}, say U_{hn}^1 and U_{hn}^2, are obtained in Table P.1 by simulated annealing [22] [23] as follows. The corresponding s_n value is obtained by Maple [24].

Table P.1: Values of s_n, U_{hn}^1, and U_{hn}^2.

n	s_n	U_{hn}^1	U_{hn}^2
4	0.091163	-0.205188	-0.205200
8	0.134066	-0.017482	-0.018358
12	0.167033	-0.039753	-0.038604
16	0.194579	-0.043691	-0.041682
20	0.218713	-0.068897	-0.065078
24	0.240451	-0.073370	-0.076663
28	0.260389	-0.099554	-0.099569
32	0.278911	-0.105222	-0.109910
36	0.296281	-0.127764	-0.126346
40	0.31269	-0.142120	-0.132072
44	0.328282	-0.165959	-0.159925
48	0.343168	-0.169063	-0.156165
52	0.357435	-0.193227	-0.188526
56	0.371155	-0.199142	-0.193109
60	0.384387	-0.235228	-0.226890

Table P.1 (Continued)

n	s_n	U^1_{hn}	U^2_{hn}
64	0.397178	-0.236724	-0.233487
68	0.409571	-0.266254	-0.263201
72	0.4216	-0.275337	-0.262480
76	0.433296	-0.295563	-0.291862
80	0.444685	-0.296339	-0.302680
84	0.455789	-0.327015	-0.332363
88	0.466629	-0.336041	-0.325248
92	0.477224	-0.363474	-0.355351
96	0.487588	-0.371998	-0.370609
100	0.497737	-0.393707	-0.380711
104	0.507684	-0.407889	-0.392792
108	0.517439	-0.430777	-0.430309
112	0.527014	-0.434817	-0.452850
116	0.536418	-0.462311	-0.455117
120	0.54566	-0.491376	-0.473234
124	0.554749	-0.501548	-0.505898
128	0.563691	-0.514511	-0.507112
132	0.572493	-0.534201	-0.525151
136	0.581163	-0.541742	-0.534663
140	0.589705	-0.575636	-0.555629
144	0.598125	-0.578072	-0.579330
148	0.606428	-0.616998	-0.610064
152	0.61462	-0.623307	-0.593199
156	0.622703	-0.644200	-0.636165
160	0.630684	-0.654850	-0.647470
164	0.638564	-0.668033	-0.673575
168	0.646349	-0.690696	-0.664614
172	0.654041	-0.712634	-0.684492
176	0.661644	-0.739486	-0.707006
180	0.669161	-0.741105	-0.741567
184	0.676594	-0.758325	-0.757780
188	0.683946	-0.761139	-0.770920
192	0.691221	-0.767522	-0.753039
196	0.69842	-0.802727	-0.817525
200	0.705545	-0.817639	-0.814140

It is clear that both U_{hn}^1 and $U_{hn}^1 < 0$. The simulated annealing [22] [23] states that when the iterations approach infinity, the corresponding simulated value of $\frac{\partial^2 h_n(x,y,\epsilon_1,\epsilon_2,\ldots,\epsilon_n)}{\partial y^2}$ converges to U_{hn}. Note that for each n, U_{hn}^1 is very close to U_{hn}^2. This indicates that the simulated annealing results of $\frac{\partial^2 h_n(x,y,\epsilon_1,\epsilon_2,\ldots,\epsilon_n)}{\partial y^2}$ start to converge when the iteration is larger than $10,000$ and shows that both U_{hn}^1 and U_{hn}^2 are good approximations of U_{hn}. Thus we conclude that $U_{hn} < 0 \ \forall \ n$.

APPENDIX Q. DERIVATION OF $\hat{f}(x, y)$

If $O'(x_c, y_c) \in A^*$, then we can use Taylor theorem to approximate $\overline{O'A_i}$ by $\overline{Q_iA_i}$. Here $\overline{Q_iA_i}$ is the projection of $\overline{O'A_i}$ over line $\overleftrightarrow{OA_i}$ (see Figure 5.1). Thus we obtain

$$\begin{aligned} \overline{O'A_i} &\approx \overline{Q_iA_i} \\ &= 1 + \epsilon_i - \overline{OQ_i}. \end{aligned} \tag{Q.1}$$

Here $\overline{OQ_i}$ is the x coordinate of point $O'(x_c, y_c)$ with respect to a new coordinate system where its new origin is $O(0, 0)$ and its new x axis, say x', is on line $\overleftrightarrow{OA_i}$ (see Figure 5.1). By the transformation formula (8.8) in Mortenson [26], we can show that

$$\overline{OQ_i} = x_c \cos\theta_i + y_c \sin\theta_i. \tag{Q.2}$$

Substituting (Q.2) into (Q.1), we obtain

$$\overline{Q_iA_i} = 1 + \epsilon_i - x_c \cos\theta_i - y_c \sin\theta_i. \tag{Q.3}$$

Thus we can approximate $f(x_c, y_c)$ by $\hat{f}(x_c, y_c)$ as follows:

$$\begin{aligned} & f(x_c, y_c) \\ &= \sum_{i=1}^{n} \left(\sqrt{(x_i - x_c)^2 + (y_i - y_c)^2} - \frac{1}{n} \sum_{j=1}^{n} \sqrt{(x_j - x_c)^2 + (y_j - y_c)^2} \right)^2 \qquad (\because (3.1)) \end{aligned}$$

$$= \sum_{i=1}^{n}\left(\overline{O'A_i} - \frac{1}{n}\sum_{j=1}^{n}\overline{O'A_j}\right)^2 \qquad \left(\because \ \overline{O'A_i} = \sqrt{(x_i - x_c)^2 + (y_i - y_c)^2}\right)$$

$$\approx \sum_{i=1}^{n}\left(\overline{Q_iA_i} - \frac{1}{n}\sum_{j=1}^{n}\overline{Q_jA_j}\right)^2 \qquad (\because \ \text{(Q.1)})$$

$$= \hat{f}(x_c, y_c) \qquad \text{(by definition)}$$

$$= \sum_{i=1}^{n}\left(1 + \epsilon_i - x_c\cos\theta_i - y_c\sin\theta_i - \frac{1}{n}\sum_{j=1}^{n}(1 + \epsilon_j - x_c\cos\theta_j - y_c\sin\theta_j)\right)^2$$

$$(\because \ \text{(Q.3)})$$

$$= \sum_{i=1}^{n}\left(1 + \epsilon_i - x_c\cos\theta_i - y_c\sin\theta_i - (1 + \frac{1}{n}\sum_{j=1}^{n}\epsilon_j - \frac{x_c}{n}\sum_{j=1}^{n}\cos\theta_j - \frac{y_c}{n}\sum_{j=1}^{n}\sin\theta_j)\right)^2$$

$$= \sum_{i=1}^{n}\left(1 + \epsilon_i - x_c\cos\theta_i - y_c\sin\theta_i - (1 + \frac{1}{n}\sum_{j=1}^{n}\epsilon_j)\right)^2$$

$$(\because \ \theta_i = (i-1)\frac{2\pi}{n} \ \text{and Lemma 3 in Appendix A.1})$$

$$= \sum_{i=1}^{n}\left(\epsilon_i - x_c\cos\theta_i - y_c\sin\theta_i - \frac{1}{n}\sum_{j=1}^{n}\epsilon_j\right)^2. \qquad \text{(Q.4)}$$

Since (x_c, y_c) are dummy variables, thus we can rewrite (Q.4) as follows:

$$\hat{f}(x, y) = \sum_{i=1}^{n}\left(\epsilon_i - x\cos\theta_i - y\sin\theta_i - \frac{1}{n}\sum_{j=1}^{n}\epsilon_j\right)^2.$$

This concludes the derivation of $\hat{f}(x, y)$ for n data points.

APPENDIX R. FINDING THE GLOBAL MINIMUM OF $\cos\alpha_i$

Let $\cos\alpha^*$ be the global minimum value of $\cos\alpha_i$. We develop five steps to determine it.

1. $\cos\alpha^*$ occurs when $\epsilon_i = 0$.
2. $\cos\alpha^*$ occurs when $(x_c, y_c) \in Bdry(A^*)$.
3. $\cos\alpha^*$ occurs when (x_c, y_c) is at a vertex of A^*.
4. The global minimum of $\cos\alpha_i \; \forall \; 0 \leq \theta_i \leq 2\pi$ is invariant when (x_c, y_c) is at any one of the vertices of A^*.
5. Based on steps 3 and 4, we can choose $(x_c, y_c) = (-\kappa, \kappa)$ to find $\cos\alpha^*$ without loss of generality. Given $(x_c, y_c) = (-\kappa, \kappa)$, $\cos\alpha^*$ occurs when $\cos\theta_i = \frac{-2\kappa+\sqrt{2-4\kappa^2}}{2}$ and $\sin\theta_i = \frac{2\kappa+\sqrt{2-4\kappa^2}}{2}$.

The details are as follows.

Proof:

1. Suppose that $\cos\alpha^*$ occurs when $\theta_i = \theta_*$ and $A_i = A_*$ where A_* has a polar coordinate of $(1+\epsilon_*, \theta_*)$ such that $\epsilon_* > 0$ as shown in Figure R.1. Then we obtain

$$\cos\alpha_* = \frac{\overline{Q_*A_*}}{\overline{O'A_*}}.$$

Here by the assumption, we know that $\cos\alpha_* = \cos\alpha^*$. However we can find a point A'_* with a polar coordinate $(1, \theta_*)$ and obtain a new value of $\cos\alpha_i$, say $\cos\alpha'_*$, such that

$$\begin{aligned} \cos\alpha'_* &= \frac{\overline{Q_*A'_*}}{\overline{O'A'_*}} \\ &< \cos\alpha_*. \end{aligned} \tag{R.1}$$

By (R.1) we know that it contradicts the assumption that $\cos\alpha_*$ is the global minimum value of $\cos\alpha_i$. Thus we know that $\cos\alpha^*$ occurs only when $\epsilon_i = 0$. This concludes the proof of step 1.

2. Suppose that $\cos\alpha^*$ occurs when (x_c, y_c) is not on the boundary of A^*, and $(x_i, y_i) = (x_*, y_*)$ as shown in Figure R.2. Then we obtain

$$\cos\alpha_* = \frac{\overline{Q_*A_*}}{\overline{O'A_*}}.$$

Here by our assumption, we know that $\cos\alpha_* = \cos\alpha^*$. We can find a point $O'' \in A^*$ such that O'' is the intersection of half line $\overrightarrow{Q_*O'}$ and the boundary of A^*. Then we obtain a new value of $\cos\alpha_i$, say $\cos\alpha'_*$, such that

$$\begin{aligned} \cos\alpha'_* &= \frac{\overline{Q_*A_*}}{\overline{O''A_*}} \\ &< \cos\alpha_*. \end{aligned} \tag{R.2}$$

Following the argument in proof statement 1, we know that $\cos\alpha^*$ occurs only when $(x_c, y_c) \in Bdry(A^*)$. This concludes the proof of step 2.

3. Since both $\{\theta_i : 0 \leq \theta_i \leq 2\pi\}$ and A^* are symmetrical at $O(0,0)$, we can restrict the possible location of $O'(x_c, y_c)$ to one side of $Bdry(A^*)$, say $y = \kappa$

and $-\kappa \leq x \leq \kappa$. Suppose that $\cos\alpha^*$ occurs when (x_c, y_c) is not at the vertex and $(x_i, y_i) = (x_*, y_*)$ as shown in Figure R.3. Then we obtain

$$\cos\alpha_* = \frac{\overline{Q_*A_*}}{\overline{O'A_*}}.$$

Here by our assumption, we know that $\cos\alpha_* = \cos\alpha^*$. We can reduce (or maintain) the value $\cos\alpha_*$ by moving the point $O'(x_c, y_c)$ along the line $y = \kappa$ towards positive (or negative) x direction. In the case of Figure R.3, we move $O'(x_c, y_c)$ towards positive x direction in order to reduce the $\cos\alpha_*$. Following the argument in proof statement 1, we know that $\cos\alpha^*$ occurs when (x_c, y_c) is at the vertex of A^*. This concludes the proof of step 3.

4. $\{\theta_i : 0 \leq \theta_i \leq 2\pi\}$ is symmetrical to point $O(0,0)$. Therefore, the global minimum value of $\cos\alpha_i \; \forall \; 0 \leq \theta_i \leq 2\pi$ is invariant when (x_c, y_c) is at any one of the vertices of A^*. This concludes the proof of step 4.

5. Let's say $\cos\alpha^*$ occurs when $(x_c, y_c) = (-\kappa, \kappa)$. Then the problem is simplified to find a angle θ_i to minimize the $\cos\alpha_i$ as shown in Figure 5.2. Applying the law of cosine [31] to the triangle shown in Figure 5.2, we obtain

$$\begin{aligned}\cos\alpha_i &= \frac{1 + \overline{O'A_i}^2 - 2\kappa^2}{2\overline{O'A_i}} \\ &= \frac{1 + \kappa\cos\theta_i - \kappa\sin\theta_i}{\sqrt{(\cos\theta_i + \kappa)^2 + (\sin\theta_i - \kappa)^2}}.\end{aligned}$$

Taking the first partial derivative of $\cos\alpha_i$ with respect to θ_i, we obtain

$$\frac{\partial\cos\alpha_i}{\partial\theta_i} = -\frac{\kappa^2(\sin\theta_i + \cos\theta_i)(2\kappa + \cos\theta_i - \sin\theta_i)}{((\cos\theta_i + \kappa)^2 + (\sin\theta_i - \kappa)^2)^{1.5}}.$$

Since the result of $\cos\alpha_i \; \forall \; -\frac{1}{4}\pi \leq \theta_i \leq \frac{3}{4}\pi$ is identical to its counterpart $\forall$ $\frac{3}{4}\pi \leq \theta_i \leq \frac{7}{4}\pi$, thus we only consider the case of $-\frac{1}{4}\pi \leq \theta_i \leq \frac{3}{4}\pi$. Making

$\frac{\partial \cos \alpha_i}{\partial \theta_i} = 0$, we can show that $\cos \alpha_i$ is minimized when

$$2\kappa + \cos \theta_i - \sin \theta_i = 0. \tag{R.3}$$

Solving (R.3), we obtain

$$\begin{aligned} \cos \theta_i &= \frac{-2\kappa + \sqrt{2 - 4\kappa^2}}{2}, \\ \sin \theta_i &= \frac{2\kappa + \sqrt{2 - 4\kappa^2}}{2}. \end{aligned} \tag{R.4}$$

This concludes the proof of step 4.

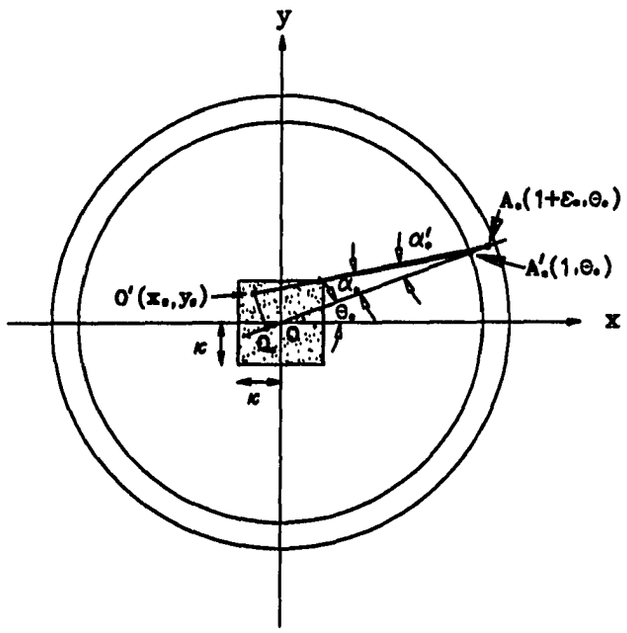

Figure R.1: Diagram of (x_c, y_c) and (x_*, y_*) when $\cos\alpha^*$ occurs – Example 1.

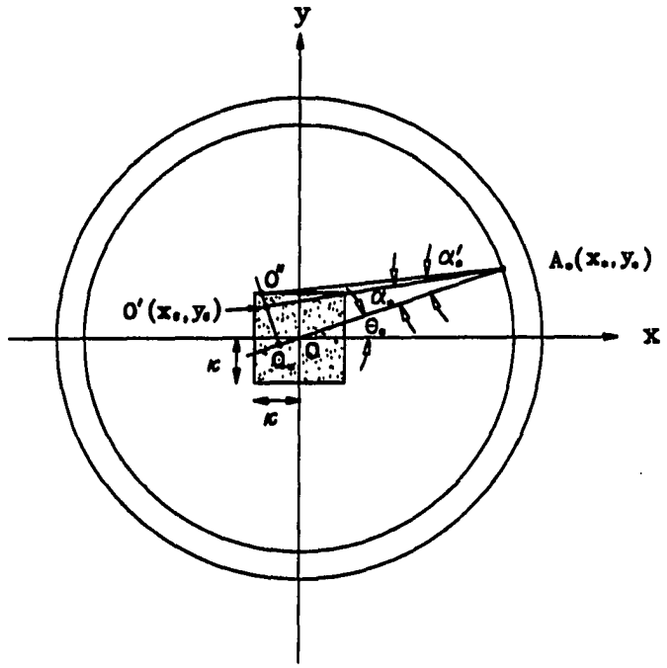

Figure R.2: Layout of (x_c, y_c) and (x_*, y_*) when $\cos\alpha^*$ occurs – Example 2.

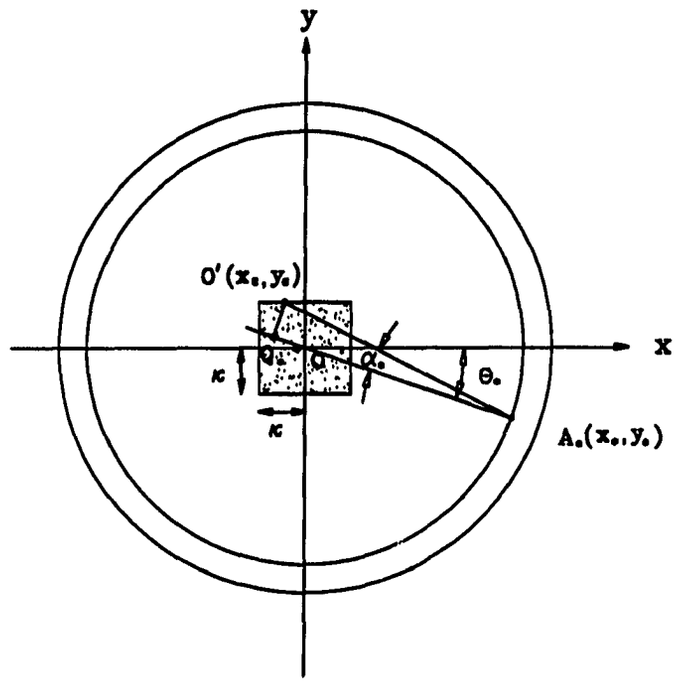

Figure R.3: Representation of (x_c, y_c) and (x_*, y_*) when $\cos\alpha^*$ occurs – Example 3.

APPENDIX S. $f(Bdry(G_n)) > f(0,0)$

Proof:

1. For $(x_c, y_c) \in G_n$, it is clear that

$$f(x_c, y_c) \leq f(0,0).$$

If (x_c, y_c) only occurs at $(0,0)$, then we have

$$f(Bdry(G_n)) > f(0,0). \tag{S.1}$$

Otherwise, if $(x_c, y_c) \neq (0,0)$, then

$$\sum_{i=1}^{n} \Delta_i > 0. \tag{S.2}$$

Following the same procedure as in chapter 4.1.1, we obtain

$$\delta_* > -\sqrt{n-1}\kappa. \tag{S.3}$$

Thus we know that if $(x_c, y_c) \neq (0,0)$, then (x_c, y_c) is restricted to be in $Int(G_n)$. As a result, we obtain

$$f(Bdry(G_n)) > f(0,0). \tag{S.4}$$

This concludes the proof.

APPENDIX T. THE LIMIT OF s_n

Proof:

1. Let circle CA1 be a circle with center at point A_1 with a polar coordinate of $(1, 0)$ and a radius of $1 - \sqrt{n-1}\kappa$, and circle CA2 be a circle with center at point A_2 with a polar coordinate of $(1, \frac{2\pi}{n})$ and a radius of $1 - \sqrt{n-1}\kappa$ as shown in Figure T.1. The circle CA1 intersects the x axis at point L. We draw a circle, say circle CA0, with center at point L and a radius of $1 - \sqrt{n-1}\kappa$. It is clear that point A_2 will be outside the circle CA0. Therefore, we obtain

$$\overline{A_1L} < \overline{A_2L}. \tag{T.1}$$

Thus we know that the circles CA1 and CA2 will not intersect at point L, otherwise $\overline{A_1L} = \overline{A_2L}$, which contradicts (T.1). Let point M be the intersection of two circles of CA1 and CA2. As a result, the x coordinate of point M, s_n, is greater than $\overline{OL}$. i.e.,

$$\begin{aligned} s_n &> \overline{OL} \\ \Rightarrow s_n &> 1 - (1 - \sqrt{n-1}\kappa) \\ \Rightarrow s_n &> \sqrt{n-1}\kappa. \end{aligned}$$

This concludes the proof.

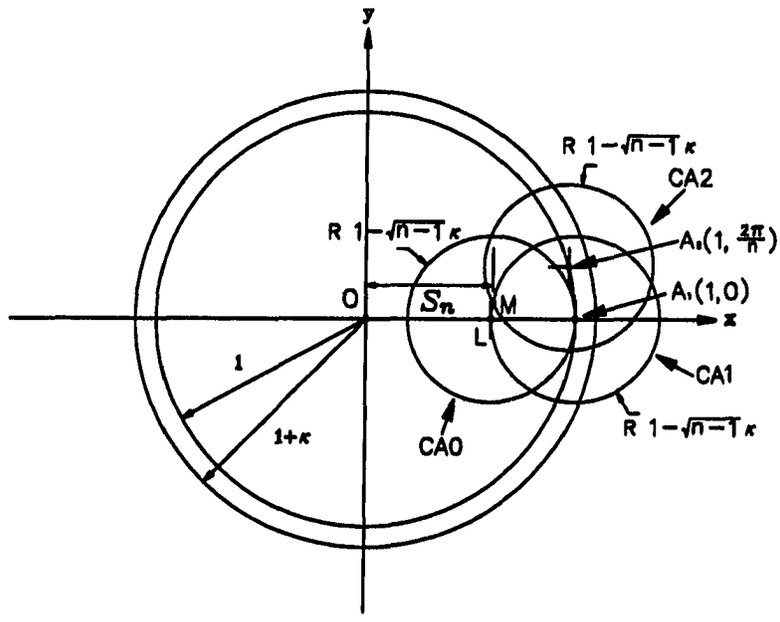

Figure T.1: An Illustration of s_n as the x Coordinate of the Intersection of Two Circles CA1 and CA2.

APPENDIX U. MEASUREMENTS OF WORN-OUT BUSHING

Table U.1: Measurements of Worn-Out Bushing.

level	order of data	x	y	z
1	1	0.36559	0.05095	0.23454
	2	0.35227	0.10884	0.23445
	3	0.32819	0.16128	0.23434
	4	0.30055	0.21177	0.23425
	5	0.26280	0.25477	0.23434
	6	0.22161	0.29570	0.23448
	7	0.17180	0.32272	0.23458
	8	0.11895	0.34481	0.23478
	9	0.06417	0.36202	0.23484
	10	0.00635	0.36613	0.23484
	11	-0.05319	0.36126	0.23486
	12	-0.10834	0.34863	0.23491
	13	-0.16229	0.32757	0.23491
	14	-0.21053	0.29926	0.23491
	15	-0.25548	0.26247	0.23493
	16	-0.29335	0.22008	0.23497
	17	-0.32448	0.17160	0.23500
	18	-0.34754	0.11891	0.23502
	19	-0.36201	0.06384	0.23505
	20	-0.36806	0.00586	0.23510
	21	-0.36433	-0.05419	0.23517
	22	-0.35178	-0.10980	0.23508
	23	-0.33029	-0.16367	0.23506
	24	-0.30138	-0.21256	0.23502
	25	-0.26417	-0.25696	0.23499

Table U.1 (Continued)

level	order of data	x	y	z
1	26	-0.22064	-0.29588	0.23487
	27	-0.17196	-0.32569	0.23474
	28	-0.11955	-0.34811	0.23480
	29	-0.06408	-0.36229	0.23479
	30	-0.00594	-0.36747	0.23473
	31	0.05426	-0.36304	0.23464
	32	0.10917	-0.34966	0.23461
	33	0.16143	-0.32878	0.23468
	34	0.21086	-0.29942	0.23468
	35	0.25501	-0.26291	0.23456
	36	0.29297	-0.21985	0.23454
	37	0.32287	-0.17174	0.23453
	38	0.34952	-0.11982	0.23453
	39	0.36442	-0.06475	0.23448
	40	0.36135	-0.00675	0.23440
2	1	0.36596	0.01356	1.11275
	2	0.35923	0.07162	1.11265
	3	0.34395	0.12697	1.11273
	4	0.31999	0.17852	1.11308
	5	0.28763	0.22650	1.11349
	6	0.24933	0.26810	1.11358
	7	0.20413	0.30373	1.11372
	8	0.15508	0.33156	1.11376
	9	0.10104	0.35197	1.11380
	10	0.04450	0.36335	1.11382
	11	-0.01469	0.36579	1.11384
	12	-0.07191	0.35896	1.11386
	13	-0.12661	0.34343	1.11390
	14	-0.17862	0.31952	1.11389
	15	-0.22627	0.28768	1.11388
	16	-0.26842	0.24869	1.11402
	17	-0.30383	0.20391	1.11401
	18	-0.33161	0.15409	1.11403
	19	-0.35148	0.10055	1.11404

Table U.1 (Continued)

level	order of data	x	y	z
2	20	-0.36304	0.04418	1.11407
	21	-0.36550	-0.01430	1.11413
	22	-0.35855	-0.07206	1.11405
	23	-0.34302	-0.12689	1.11398
	24	-0.31919	-0.17828	1.11393
	25	-0.28721	-0.22626	1.11392
	26	-0.24852	-0.26813	1.11379
	27	-0.20301	-0.30411	1.11375
	28	-0.15356	-0.33183	1.11377
	29	-0.10122	-0.35145	1.11371
	30	-0.04469	-0.36295	1.11369
	31	0.01506	-0.36532	1.11368
	32	0.07240	-0.35829	1.11370
	33	0.12733	-0.34247	1.11365
	34	0.17856	-0.31968	1.11356
	35	0.22650	-0.28747	1.11355
	36	0.26876	-0.24892	1.11354
	37	0.30454	-0.20403	1.11353
	38	0.33265	-0.15458	1.11354
	39	0.35192	-0.10086	1.11351
	40	0.36336	-0.04483	1.11345
3	1	0.36755	0.03249	1.99229
	2	0.36050	0.09235	1.99208
	3	0.33969	0.14634	1.99198
	4	0.31220	0.19640	1.99186
	5	0.27786	0.24265	1.99211
	6	0.23661	0.28265	1.99226
	7	0.18991	0.31612	1.99251
	8	0.13886	0.34148	1.99269
	9	0.08366	0.35886	1.99275
	10	0.02623	0.36724	1.99277
	11	-0.03380	0.36583	1.99276
	12	-0.09028	0.35585	1.99282
	13	-0.14398	0.33732	1.99286
	14	-0.19465	0.31027	1.99290
	15	-0.24033	0.27578	1.99289

Table U.1 (Continued)

level	order of data	x	y	z
3	16	-0.27997	0.23468	1.99291
	17	-0.31248	0.18786	1.99293
	18	-0.33762	0.13659	1.99295
	19	-0.35434	0.08206	1.99299
	20	-0.36280	0.02578	1.99303
	21	-0.36196	-0.03390	1.99309
	22	-0.35217	-0.08969	1.99304
	23	-0.33383	-0.14323	1.99296
	24	-0.30722	-0.19365	1.99297
	25	-0.27349	-0.23890	1.99288
	26	-0.23210	-0.27949	1.99279
	27	-0.18572	-0.31243	1.99273
	28	-0.13553	-0.33748	1.99271
	29	-0.08129	-0.35479	1.99267
	30	-0.02441	-0.36353	1.99261
	31	0.03528	-0.36294	1.99266
	32	0.09128	-0.35325	1.99265
	33	0.14453	-0.33505	1.99259
	34	0.19599	-0.30946	1.99258
	35	0.24194	-0.27544	1.99257
	36	0.28140	-0.23378	1.99249
	37	0.31417	-0.18726	1.99243
	38	0.33918	-0.13577	1.99243
	39	0.35624	-0.08183	1.99235
	40	0.36755	-0.02527	1.99230